

UNIVERSITY OF THE WITWATERSRAND

# GEOL 7048

A Research Report submitted to the Faculty of Science, University of the Witwatersrand, in partial fulfilment of the requirements for the degree of Master of Science.



**WITS**  
UNIVERSITY

Musiwa Trudy Mudau

11/2020

***Manganese genesis, analysis and future demand: A case study from the United Manganese of Kalahari (UMK), Hotazel, South Africa***

Supervisors: Prof. Judith Kinnaird and Co-Supervisor Prof. Paul Nex

## DECLARATION

I, Trudy Musiwa Mudau declare that this research report is my own work except where proper referencing and acknowledgement is made. This work has not previously been submitted for a degree requirement to any other University. I, therefore, submit it for the examination and award of the Degree of Master of Science (Geology) at the University of the Witwatersrand.

**Signature**

A handwritten signature in black ink, consisting of a large loop on the left and several vertical strokes on the right, ending in a small flourish.

**Musiwa Trudy Mudau**

**Date: 11 November 2020**

## **ACKNOWLEDGMENTS**

I would first like to thank my thesis supervisor Prof. Judith Kinnaird and co-supervisor Prof. Paul Nex of the Department of Geology at Wits University and Stephan Laubscher of United Manganese of Kalahari. They pointed me in the right the direction whenever I needed it.

I would also like to thank the following experts, and colleagues who were involved during the research project: Khathutshelo Tshikovhi from the United Manganese of Kalahari, Hannes van der Merwe from the African Geomine Services, Dudu Kgware from ABC labs and Abram Bodiba from South32, without their fervent involvement and input, the research and experimental work would not have been successful.

I must express my very deep appreciation to my siblings; Mulisa, Mulondi and Maano, for their non-stop motivation, parents; Tumelo Errol Mudau and Tshamano Gloria Mudau for providing me with constant support and continuous inspiration throughout the years of study and through the researching and writing process of this thesis. My daughter Anesu has been a continuous source of encouragement, not just for my academic endeavours, but also other aspects of my life. This accomplishment would not have been possible without them.

Lastly, I would like to acknowledge my circle of friends for the various roles they played in my studies, thank you.

## ABSTRACT

*The origin of the biggest manganese deposit in the world has been extensively researched and discussed for years with no consensus on the origin, due to its complex mineral associations. The Kalahari manganese field occurs within the 2.5Ga Proterozoic Transvaal Supergroup, it is restricted to the Hotazel Formation of the Postmasburg Group in the Griqualand West basin and is at least 1100km<sup>2</sup> in extent. The Kalahari Formation, comprising sand, calcrete, clay and pebble beds covers the ore-bearing Hotazel Formation, while the Mooidraai Formation, comprising dolomites locally underlies the Kalahari Formation. The ore bearing Hotazel Formation is composed of alternating layers of banded iron formations and braunite lutites. The difference in mineral distribution and ore composition has given rise to three types of ore; the slightly altered Mamatwan-type low-grade, the hydrothermally altered Wessels-type high-grade ore and the supergene enriched ore. The predominant minerals of the Kalahari basin are bixbyite, braunite, cryptomelane, hausmannite, jacobsite, kutnahorite and todorokite.*

*United Manganese of Kalahari mine extracts the economic lower ore body, that has an average of 20m in thickness. The mine hosts two types of manganese ore; the low-grade mamatwan-type and the supergene altered ore. The chemical composition of these types of manganese ore is determined using different analytical methods, titration and X-ray fluorescence are the most suitable for analysing oxides. In most cases, however, these methods have given quite significant differences of up to 2.5% in manganese content. As 2.5% manganese is a significant amount, re-analysis is required.*

*Due to the globally competitive market, manganese ore is directly impacted by the demand in the steel industry. The amount of manganese used in the steel industry per quantity of steel produced has declined over time, due to improvements in technology since the 1950s. However, the worldwide increase in demand for steel will increase the demand for manganese. With the imminent 4<sup>th</sup> industrial revolution, the future for demand of manganese ore will be impacted.*

*This research supports some of the previous studies on the genesis of manganese, with regard to a sedimentary origin and addressing the question of differences in assay values of the above mentioned analytical methods. The study ultimately looks into the economics of manganese, with focus on the future demand.*

## LIST OF ABBREVIATIONS

**BIF** → Banded Iron Formation

**KMF** → Kalahari Manganese Field

**MBOD** → Middle Manganese Body

**LBOD** → Lower Manganese Body

**UBOD** → Upper Manganese Body

**XRD** → X-Ray Diffraction

**XRF** → X-Ray Fluorescence

## TABLE OF CONTENTS

<b>DECLARATION</b> .....	<b>1</b>
<b>ACKNOWLEDGMENTS</b> .....	<b>2</b>
<b>ABSTRACT</b> .....	<b>3</b>
<b>LIST OF ABBREVIATIONS</b> .....	<b>4</b>
<b>TABLE OF CONTENTS</b> .....	<b>5</b>
<b>LIST OF TABLES AND FIGURES</b> .....	<b>7</b>
<b>CHAPTER 1</b> .....	<b>10</b>
<b>INTRODUCTION</b> .....	<b>10</b>
1.1 MANGANESE PRODUCTION AND THE ECONOMY .....	10
1.2 HISTORICAL BACKGROUND .....	12
1.3 AIMS AND OBJECTIVES .....	14
1.4 FIELD WORK .....	15
<b>CHAPTER 2</b> .....	<b>16</b>
<b>STRATIGRAPHY</b> .....	<b>16</b>
2.1 INTRODUCTION .....	16
2.2 KALAHARI FORMATION .....	18
2.2.1 KALAHARI DEPOSIT .....	21
2.2.2 CALCRETE SEQUENCE .....	21
2.2.2.1 CALCRETE.....	21
2.2.2.2 RED CLAY BED.....	25
2.2.2.3 PEBBLE BED (FIG 2.11).....	26
2.3 MOOIDRAAI FORMATION (MDF).....	26
2.4 HOTAZEL FORMATION .....	26
2.4.8 ONGELUK FORMATION .....	32
2.4.9 CONCLUSION.....	32
<b>CHAPTER 3</b> .....	<b>33</b>
<b>THE LOWER MANGANESE BODY</b> .....	<b>33</b>
3.1 INTRODUCTION .....	33
3.2 ORE TYPES .....	33
3.3 LOWER BODY ZONES.....	37
3.5 ORE GENESIS DISCUSSION .....	50
3.6 CONCLUSION.....	52
<b>CHAPTER 4</b> .....	<b>53</b>
<b>ANALYTICAL METHODS</b> .....	<b>53</b>
4.1 INTRODUCTION .....	53

4.2 QUANTITATIVE ANALYTICAL METHODS .....	54
4.3 WET METHODS .....	54
i. Titration of manganese from manganese ore .....	54
ii. Titration of Iron from manganese ore .....	55
4.4 DRY METHODS.....	60
4.5 SAMPLE ANALYSIS .....	62
4.6 RESULTS AND DISCUSSIONS .....	65
4.7 CONCLUSIONS.....	70
<b>CHAPTER 5.....</b>	<b>71</b>
<b>MANGANESE ECONOMICS AND THE FUTURE.....</b>	<b>71</b>
5.1 INTRODUCTION .....	71
5.2 MANGANESE USES AND APPLICATIONS .....	72
5.3 THE FOURTH INDUSTRIAL REVOLUTION.....	73
5.4 DEMAND AND SUPPLY .....	76
5.5 CONCLUSION.....	82
<b>CHAPTER 6.....</b>	<b>83</b>
<b>SUMMARY AND CONCLUSIONS .....</b>	<b>83</b>
<b>REFERENCES.....</b>	<b>85</b>

## LIST OF FIGURES

Figure 1.1 South African map showing the locality of UMK (internal paper) .....	11
Figure 1.2 South African Manganese production and sales, adapted from the Chamber of Mines 2017. 12	
Figure 2.1 Geology of the Transvaal and Griqualand West basin A. A small-scale geological map showing the Griqualand West Basin and the Transvaal Basin on the Kaapvaal Craton, B. Geological map of the Transvaal Supergroup in Griqualand West showing distribution of major stratigraphic units, the location of the Kalahari Manganese Field and the N-S trending Black Ridge thrust (from Beukes, 1983.) .....	17
Figure 2.2 Geological map of the Griqualand West basin (Bengtson, et.al. 2017).....	18
Figure 2.3 Stratigraphic section of the Griqualand West sub-basin (Bengtson et.al. 2017).....	19
Figure 2.4 Map showing the location of selected boreholes in the area of the study.....	20
Figure 2.5 The Kalahari deposit displayed in chips from drilling and in a face from mining (a) Percussion drilling samples from borehole logging and (b) the freely dug bench of the aeolian unlithified Kalahari sand.....	21
Figure 2.6 Top lime (a) dry top lime sample (b) wet disintegrated top lime sample .....	22
Figure 2.7 Example of a rock found after the middle lime blast.....	23
Figure 2.9 Example of lower lime specimen .....	24
Figure 2.8 Bottom lime calcrete samples .....	24
Figure 2.10 Calcrete benches showing different types of calcretes .....	25
Figure 2.11. Pebble bed with pebbles as little as 2cm to 10cm in a Calcrete matrix .....	26
Figure 2.12 Cross-section showing the manganese horizons within the Hotazel Iron Formation and farms where UMK holds a mining license (Van der Merwe, 2015) .....	27
Figure 2.13 Percussion borehole log for S_RC38 .....	31
Figure 3.1 Different types of ore, with and without carbonates (a) Supergene altered ore, with clear absence of carbonates, (b) Primary unaltered ore with carbonates.....	34
Figure 3.2 Percussion borehole log for R_RC58.....	36
Figure 3.3 Diamond borehole log for UEE034 showing lithology, subzones and grades from the right to the left respectively. ....	48
Figure 3.4 Different sub-zones that occur in the Lower Body of the Manganese ore. (a) V-Zone, banded braunite-lutite with small and large brown and white ooids. (b) W-Zone, banded braunite-lutite containing dominant irregularly shaped brown widely scattered carbonate ooids. (c) X-Zone, banded braunite-lutite with carbonate ooids of various sizes. The ooids are small, widely scattered at the top and closely spaced towards the base. (d) Y-Zone, braunite-lutite containing white and abundant brown laminae, thick lentils and small oxide rich ooids. (e) Z-Zone, braunite-lutite containing white carbonate stringers and fine white and pink ooids. (f) M-zone, braunite-lutite displaying ellipsoidal and irregularly shaped brownish oxide dominated ooids of various sizes. (g) C-Zone, braunite-lutite containing white and brownish oxidised ooids and very thin laminae. (h) N-Zone, braunite-lutite with microbands, fine pink ooids and stringers. (i) B-Zone, laminated brownish-black jacobsonite braunite-lutite containing brown carbonate laminae.....	49
Figure 3.5 The Kalahari Manganese Field with all deposits (a) Structural map of the Kalahari Manganese Field in South Africa, illustrating the distribution of the various manganese mines in the area, including	

the low-grade Mamatwan mine in the south and the high-grade (after Vafeas et.al., 2018). (b)

Lithostratigraphic profile of the Hotazel Formation indicating the three cycles of manganese deposition (Cairncross and Beukes, 2013)..... 51

Figure 4.1 Manganese sample with zinc oxide emulsion ..... 55

Figure 4.2 The endpoint of the Manganese Titration..... 55

Figure 4.3 Graphical presentation of the round robin results for manganese and iron. .... 59

Figure 4.2 Sample preparation for analysis through the fusion process (internal paper)..... 60

Figure 4.5 Fused bead specimen before going into the XRF machine (left) and the view of chemical compounds after the fusion process (right). All elements are converted to oxides. (internal paper)..... 61

Figure 4.6 Pressed pellets in rings (left) and an enlarged view of the surface texture after pulverising (internal paper) ..... 61

Figure 4.7 Schematic diagram of a wavelength dispersive X-ray fluorescence spectrometer (Wegrzynek, 2004) ..... 63

Figure 4.8 Comparison of Mn between wet chemistry and RXF method correlation ..... 69

Figure 4.9 Comparison of Mn between wet chemistry and RXF method correlation ..... 70

Figure 5.1 Manganese ore and the consuming sectors (Clarke and Upson 2017) ..... 73

Figure 5.2 Highlights of industrial revolutions indicating the different characteristics and achievements. .... 74

Figure 5.3 Elements required for green energy technologies as indicated by the Minerals Council South Africa. Manganese is relevant in the 4<sup>th</sup> industrial revolution and will be used in wind technology, electric vehicles and energy storage. .... 75

Figure 5.4 Mass distribution of the lumpy product screen tests for ARD1-69 ..... 78

Figure 5.5 Mass distribution of the fines product screen tests for CV02 ..... 79

APPENDIX..... 89

Figure I – Pictures taken at ABC labs for wet chemistry analysis..... 89

..... 89

## LIST OF TABLES

Table 1.1 Employment and earnings in South African mines, adapted from the Chamber of Mines 2017 .....	11
<a href="#">Table 3.1 List of minerals and their chemical formula</a> .....	34
<a href="#">Table 3.2 Average thicknesses of the different sub-zones in the Lower Body Manganese ore as observed from drill core of UEE034</a> .....	36
<a href="#">Table 4.1 Kalahari Round robin results</a> .....	57
<a href="#">Table 4.2 The below listed participants contributed to the round-robin: the labs are listed in alphabetical order</a> .....	57
<a href="#">Table 4.3 The table below shows the different techniques used by the participants</a> .....	58
<a href="#">Table 4.4 Comparison of sample preparation techniques (Krusberski, 2010 – SA institute of mining and Metallurgy – Analytical Challenges in Metallurgy)</a> .....	64
<a href="#">Table 4.5 Certified Reference Material (CRM) test</a> .....	65
<a href="#">Table 4.6 Mn t-Test: Paired two sample for Means</a> .....	66
<a href="#">Table 4.7 Fe t-Test: Paired two sample for Means</a> .....	66
<a href="#">Table 4.8 Accuracy test results using 10 replicates of CRM (AMIS 407) samples for both Mn and Fe</a> .....	67
<a href="#">Table 4.9 Mn regression statistics showing relationship between the variables</a> .....	68
<a href="#">Table 4.10 Fe regression statistics showing relationship between the variables</a> .....	69
<a href="#">Table 5.1 Different revolutions showing the periods of revolution and major the changes (World Economic Forum)</a> .....	73
<a href="#">Table 5.2 depicts the typical UMK grade specifications of the saleable product (lower limit and upper unit). Samples with high Mn content typically produce more fines than the sample with lower Mn content</a> .....	76
<a href="#">Table 5.3 Cumulative % of a lumpy product screen test. ARD 1-69</a> .....	77
<a href="#">Table 5.4 Size determination work sheet for a lumpy product (15x75mm)</a> .....	78
<a href="#">Table 5.6 Size determination work sheet for a fines product (0x6mm) for CV02</a> .....	80
<a href="#">Table 5.5 A6 Cumulative % of a fines product screen tests for CV02</a> .....	80

## CHAPTER 1

### INTRODUCTION

#### 1.1 Manganese production and the economy

Manganese is the 12<sup>th</sup> most abundant of the elements in the Earth's crust, and depicted as Mn, a transition metal in the periodic table. Manganese is a chemical element with an atomic mass of 25 and constitutes 0.1% (1000 ppm) of the Earth's crust. Manganese does not exist as a free element in nature but is usually associated with iron (Fe) and other Fe-related compounds. For the purpose of the study, it will be discussed in its ore form. The element was discovered by a Swedish chemist, Johan Gottlieb Gahn, by heating pyrolusite (MnO<sub>2</sub>). It was proposed to be an element by Carl Wilhelm Scheele in 1774.

Manganese has a variety of uses in the industry, spanning from steel manufacturing and industrial to biological applications. Its major use in the steel industry is when it is added to steel to increase ductility to counter steel structure brittleness; it is also used in manganese phosphating, in order to reduce rust and corrosion in steel. It is believed that, of general phosphate coatings, manganese phosphate coating has the highest hardness and superior corrosion and wear resistances. Other industrial applications either in its ionised, permanganate and dioxide state, include pigmentation of various colours, as a powerful oxidising agent in alkali and alkaline earth metals and it acts as a cathode material in different industrial batteries e.g. zinc-carbon and alkaline batteries. Biological applications of manganese are also numerous; however, in this study, the focus will be based mainly on steel production.

The mine, United Manganese of Kalahari (UMK) started in 2005 (Fig. 1.1), with the aim of exploring manganese ore covered by the Cenozoic Kalahari Formation and other formations found in the Kuruman area, Northern Cape Province of South Africa. An exploration campaign in the form of diamond drilling was carried out, as a way of evaluating the ore deposit, and other geological features that could possibly hinder future extraction.

Manganese mining is essential as there are currently no suitable substitutes for its applicability to metallurgy (Caruthers, 2009). One of the largest uses of manganese ore, as mentioned above, is in the steel industry, where China has emerged as the largest producer in steel as a result of its continuing expansion in infrastructure. Within the 10 years between 2005 and 2015 China increased its output from 31.0% of global steel production to half the world production with 49.6%.

In South Africa, mining is one of the major contributors to the country's GDP. Different commodities, manganese being one of them, have seen the total employee earnings rise by a huge margin since 2004. The growth of the manganese industry has also seen a concomitant rise in its employment rate which

increased from just above 3,000 to 9,971 in 2014, although the employment number declined to 7,240 in 2016 (Chamber of Mines, 2017).

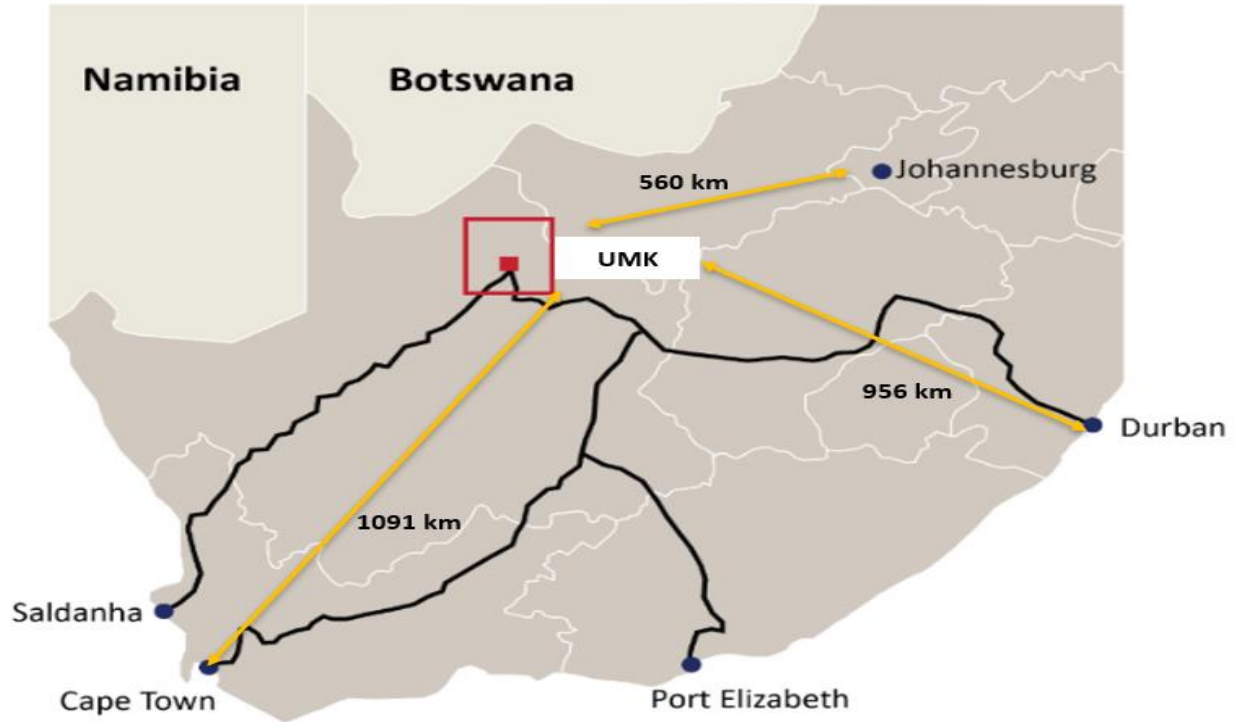


Figure 1.1 South African map showing the locality of UMK (internal paper)

Manganese production and sales have also experienced turbulence in 2009, 2011 and 2015, (Table 1.1) as a result of the global financial crises which hugely impacted the metal prices. It has however managed to recover from all of these for the time being (Fig. 1.2).

Table 1.1 Employment and earnings in South African mines, adapted from the Chamber of Mines 2017

Year	Production tonnes	Local sales		Export sales		Total sales	
		Mass 1,000t	Value R'000	Mass 1,000t	Value R'000	Mass 1,000t	Value R'000
2004	4,206,746	–	642,414	2,403	1,082,285	–	1,724,699
2005	4,611,683	–	681,861	2,119	1,518,965	–	2,200,826
2006	5,213,338	–	727,182	2,846	1,518,653	–	2,245,835
2007	5,996,086	–	934,901	3,691	2,636,526	–	3,571,427
2008	6,807,059	–	1,761,849	4,689	15,581,560	–	17,343,408
2009	4,578,770	–	583,602	3,976	5,003,011	–	5,586,613
2010	7,171,745	–	1,320,564	5,986	9,340,026	–	10,660,590
2011	8,651,842	–	1,325,214	6,773	8,569,854	–	9,895,067
2012	8,943,415	–	1,134,842	7,498	9,685,812	–	10,820,654
2013	10,957,133	–	1,506,434	–	12,969,545	–	14,475,979
2014	14,051,244	–	1,641,633	–	14,734,415	–	16,376,049
2015	15,952,416	–	860,474	–	12,657,775	–	13,518,249
2016	13,735,509	–	879,774	–	18,861,301	–	19,741,075

Besides the global financial crises that manganese faces, there are other specific local challenges, including;

- Transport and logistics – Manganese mines are situated far in-land and this poses a challenge because ore needs to be transported to the ports which are about 900km from the mines. The local consumers are also located in areas just over 700km from the mines. This has made the transport and logistics cost to be higher than the ore extraction cost. The other challenge is the transport capacity, which is supplied by the state-owned entity Transnet Freight Rails (TFR), as they are only capable of moving 5.5Mt per year of ore to the harbours, which is way below what the mines in the area are producing.
- Power supply – due to ineffective management of the state-owned power utility, the country has experienced power cuts, leading to mines resorting and heavily relying on fuel as another source of power, which comes at a huge cost. Not only have there been power cuts, but also a sharp price increase per unit from Eskom.

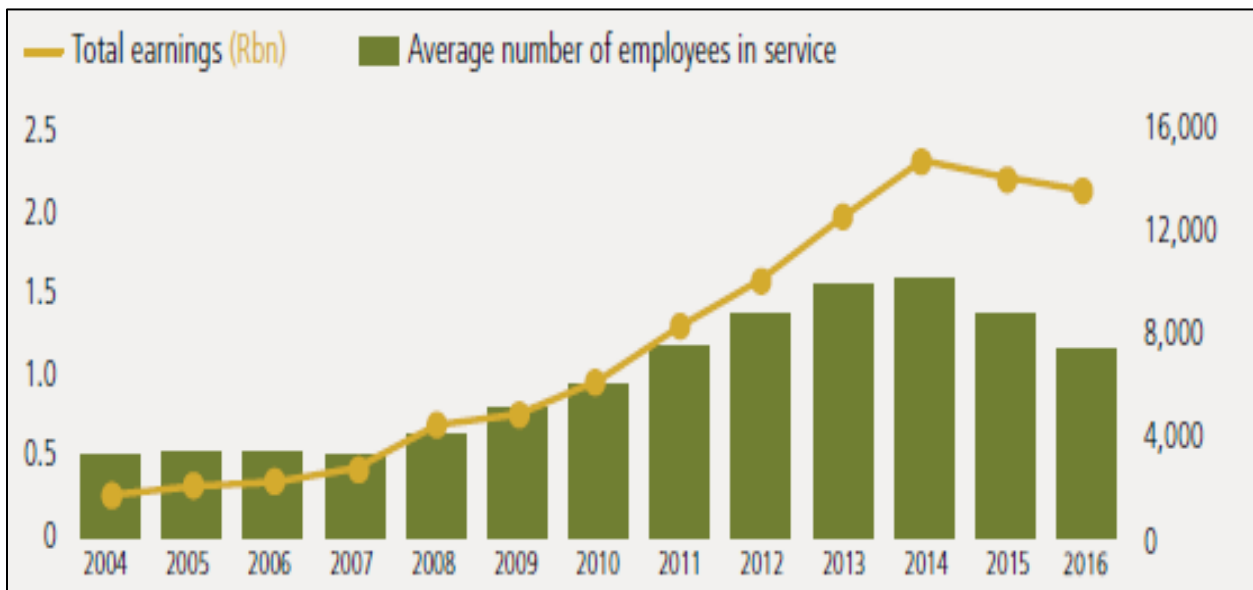


Figure 1.2 South African Manganese production and sales, adapted from the Chamber of Mines 2017.

## 1.2 Historical background

The manganese deposits in the area were discovered in the early 1900s, when the manganese-bearing Black Rock outcrop was discovered. The Black Rock outcrop was described in detail by Boardman in 1922 but was not of interest until 1941 when it was acquired by Samancor. However Black Rock is now known as the Associated Manganese Mines of South Africa (ASSMANG) which at that stage owned a vast portion of the manganese bearing property. Since then the area has been studied in great detail, which led to more ore extracting operations opening and the Kalahari deposit has been exploited since. Some of the biggest producing companies were Assmang and BHP; these companies owned most of the farms where the ore was discovered. With the new legislation however, the above-mentioned organisations lost parts

of their properties to the young miners like UMK, Kudumane Manganese Resources, Kalagadi Manganese, Tshipi Ntle and Sebilo Resources. To date, prospecting in some areas is still taking place.

The manganese deposit in the Kalahari has been studied and researched. Kuleshov (2012), argues that in spite of the research done to appreciate the manganese ores and their chemical composition, many aspects of the way in which ore was formed remain insufficiently studied. He believes that the development of models should consider the following aspects;

- Sources of ore forming substance (metallic and non-metallic),
- Formation environment, both exogenic and endogenic, i.e. (climate, paleogeography, paleobasin type, physiochemical conditions, pH, Eh, temperature, pressure and other aspects),
- The temporal evolution of ore formation,

Clearly, not all of these have been considered.

Since the 1980s, De Villiers (1983), focused on the genetic relationship between the Kalahari deposit and the Postmasburg deposit as precipitated by the hypogene fluids resulting in the suggestion that the deposits were of magmatic hydrothermal origin. In 1982, Beukes noted 3 chemo-sedimentary cycles of BIF and braunite lutite in the Hotazel Formation. Kleyenstuber identified new minerals in 1984 and also sub-divided the ores into Mamatwan-type and Wessels-type ores and an uneconomic jacobsonite ore. In 1986, Nel et.al. were the first to detail the mineralogical zones discussed in this report in Chapter 3. In 1986, Jennings discussed the general geology in Middelplaats, a farm which is one the largest farms within the Kalahari manganese basin. Further in 1993, Kleyenstüber gave an update on manganese ore characteristics and other minerals found in the KMF, which suggested that the origin of the manganese was volcano-sedimentary. Mineralogical identification, mineral paragenesis and the role of structural features in metasomatic alteration and ore upgrading in the northern parts were also discussed by Burger, (1994) Gutzmer, (1996) and Gutzmer and Beukes (1995 and 1997).

The genetic models for Kalahari ores have been grouped into three camps (Tsikos and Moore, 1998) and are:

- Large scale epigenetic replacement, whereby Kalahari manganese ores are thought to have formed as a result of younger hypogene replacement at the expense of a suitable protolith, i.e. during a younger hypogene hydrothermal event (De Villiers, 1983).
- Submarine volcanogenic exhalative activity involving interaction between mid ocean ridge-type submarine volcanism and rapid precipitation of Mn and Fe-rich compounds (Cornel and Schütte, 1995).
- Pure chemical precipitation which places particular emphasis on various environmental parameters (sea-level fluctuations, climate change) involved in the deposition of iron and manganese minerals with volcanism acting either as a nearest (Beukes, 1983; Nel et al., 1986) or a remote (Tsikos and Moore, 1997) metalliferous source. The latter seems to have gained popularity amongst many authors.

In contrast, Kuleshov (2012) mentions four genetic types of deposits that were defined: (1) Sedimentary (sedimentary proper and volcanosedimentary); (2) Magmatogenic (hydrothermal and contact-metasomatic); (3) Meta-morphogenetic (related to regional and contact metamorphism of sedimentary and magmatogenic ore accumulations); and (4) Weathering crust deposits (residual, infiltrational, and karst cavern filling).

In 1998, Tsikos and Moore suggested that most commercial deposits were sedimentary in origin, but with additional factors and processes, while Kuleshov (2012) mentions some processes such as sea-floor volcanic activity, sea level fluctuations, climate changes, and biological productivity as being critical in the development of large accumulations of manganiferous sediment in depositional environments of various ages (Frakes and Bolton, 1992). Most manganese ore reserve in the world are concentrated in deposits confined to sedimentary basins (Kuleshov, 2010). This however depends on the composition of the sediments and the source of manganese, knowing this, will enable one to divide and categorise the type of deposit into sedimentary or volcano sedimentary. Based on the detailed analysis of Oligocene manganiferous sediments, five factors that controlled manganese accumulation in sedimentary basins were defined (Strakhov et al., 1968; Kuleshov, 2010): (1) intensity of ore component precipitation from bottom waters; (2) hydrodynamic regime and paleogeography of the ore formation area; (3) dilution of manganiferous sediment with terrigenous material; (4) Mn redistribution during diagenetic sediment transformation; and (5) reworking of the ore bed with the removal of finely dispersed terrigenous material from the bed. To add to this, it is without a doubt that most commercial deposits are of sedimentary origin.

This study focused on stratigraphy, mineralogy and structural controls of all manganese ore zones in the UMK mining lease area on the farms: Rissik, Smartt, Botha, Middleplaats, Roldraai, Mooidraai and Heuningdraai.

### **1.3 Aims and objectives**

The purpose of this study is to give more insight to gain a better understanding of the genetic model and the distinguishing features of the ore packages with regard to the chemical compositions and other physical characteristics.

Different analytical methods are applied to determine the chemical characteristics and concentrations of the mineral-forming compounds during exploration programs. The analyses help in categorising the different ore packages and defining the mining horizons. These further lead to informed decisions in marketing. The reliability of these analyses however is wholly dependent on a lot of processes that take place before the sample is analysed. Sampling and sample preparation processes as defined in the ISO standards will be defined, and will be compared to the current practises, to see if they give rise to any prejudices which have a negative impact on the outcome of the results. Analytical results from the different methods applied in analysing manganese samples will be compared to see if they give rise to

significant differences in percentages, and the causes of the differences with the possibility of suggesting the best analytical method to apply to manganese and other related elements.

Lastly, the study also aims to shed some light into the economics of the manganese industry as a whole, the impact of the 4<sup>th</sup> industrial revolution (4IR) and attempt to predict the future demand of manganese ore.

#### **1.4 Field work**

Fieldwork investigations involved the use of handheld GPS for siting and drilling of boreholes. Percussion drilling and PVC casing was applied to the Kalahari Formation due to its unstable nature. Casing stabilises the Kalahari by preventing the Kalahari Sand from falling in during drilling and stops clay from swelling and eventually resulting in the caving in of the borehole. Diamond drilling was then applied at the depth of competent material, i.e. Moidraai dolomites. One borehole was selected from the diamond drilling campaign that was carried out to investigate the possibilities of underground mining, the two additional boreholes were selected from the historical infill reverse circulation (RC) drilling campaign that took place to increase open pit life of mine. Thus, four boreholes in total were analysed in this study.

Selected boreholes from both drilling campaigns were logged by the author. Core was then taken off-site for relative density (RD tests) and sampling, and then transported to the lab for chemical analysis through the XRF and wet chemistry titration methods. The data were then logged on Sable database warehouse software, capturing lithology (local and major stratigraphy) RD logs and sampling logs. Assay results were also imported as and when they were reported from the analytical lab. Quality checks are done in the database to check any out-of-range data before data was handed over for modelling. Lithology, assay, RD logs and QA/QC reports have been provided in this report.

Two samples were also taken from the lumpy and fines stockpiles to determine size distributions, this was done to show the calculations used to ensure quality sizes.

## CHAPTER 2

### STRATIGRAPHY

#### 2.1 Introduction

The Kalahari Manganese Field occurs in the Griqualand West basin of the Transvaal Supergroup (Fig. 2.1). The Transvaal Supergroup is a late-Archaeon earliest Proterozoic platform succession developed on the Kaapvaal craton, spanning the approximate period of 2.65-2.05Ga (Moore et.al, 2001). The basin is thought to have developed in response to intracratonic extension on the stabilised Kaapvaal-Limpopo-Zimbabwe block and comprises nearly 15, 000m of relatively low metamorphosed volcanic, clastic and chemical sedimentary rocks (Thomas et.al., 1993; Eriksson et.al., 1993). The Transvaal Supergroup (Fig. 2.1) has three major subdivisions ranging from the lower, middle to the upper sequence and are: the Chuniespoort Group and Western Ghaap Group, which are the lowermost sequences, followed by the middle sequence which is represented by two groups; one in the Transvaal which is the Pretoria Group and the other in Griqualand West which is the Postmasburg Group (Beukes, 1983). The uppermost sequence mainly comprises volcanic rocks of the Rooiberg Group. The deposition of the Transvaal sequence in the Griqualand West according to Beukes et.al., (1987) took place on a continental margin and was controlled by three major tectonic sedimentary elements;

- A shallow water platform on the Kaapvaal craton
- A platform edge (shelf margin) located parallel to the Griqualand fault zone (a growth fault across which there are a number of facies changes)
- A deep basin along the western margin of the Kaapvaal craton.

For the purpose of this report, the focus is mainly on the middle sequence, specifically the Postmasburg Group which hosts the largest land-based manganese deposit.

The deposit occurs in the form of three discrete, chemical sedimentary units interbedded with iron formations (Tsikos and Moore, 1997; Tsikos et.al 2003), forming the Hotazel Formation, within the Transvaal Supergroup that is 2.56 Ga in age (Beukes, 1983). The basal part of the Transvaal comprises the basaltic andesites of the 2.2 Ga Ongeluk Formation. Above the Hotazel Formation there is the Moidraai Formation which is observed mostly towards the south and western parts, as a result, it is absent to the east where manganese ore is accessed at shallower depths. The Postmasburg Group is made up of the Moidraai Formation, Hotazel Formation and the Makganyenye Formation (Fig. 2.4). These Formations are covered by the Tertiary-aged Kalahari Formation comprising Kalahari sand, calcrete sequence, red clay beds and pebble/gravel beds.

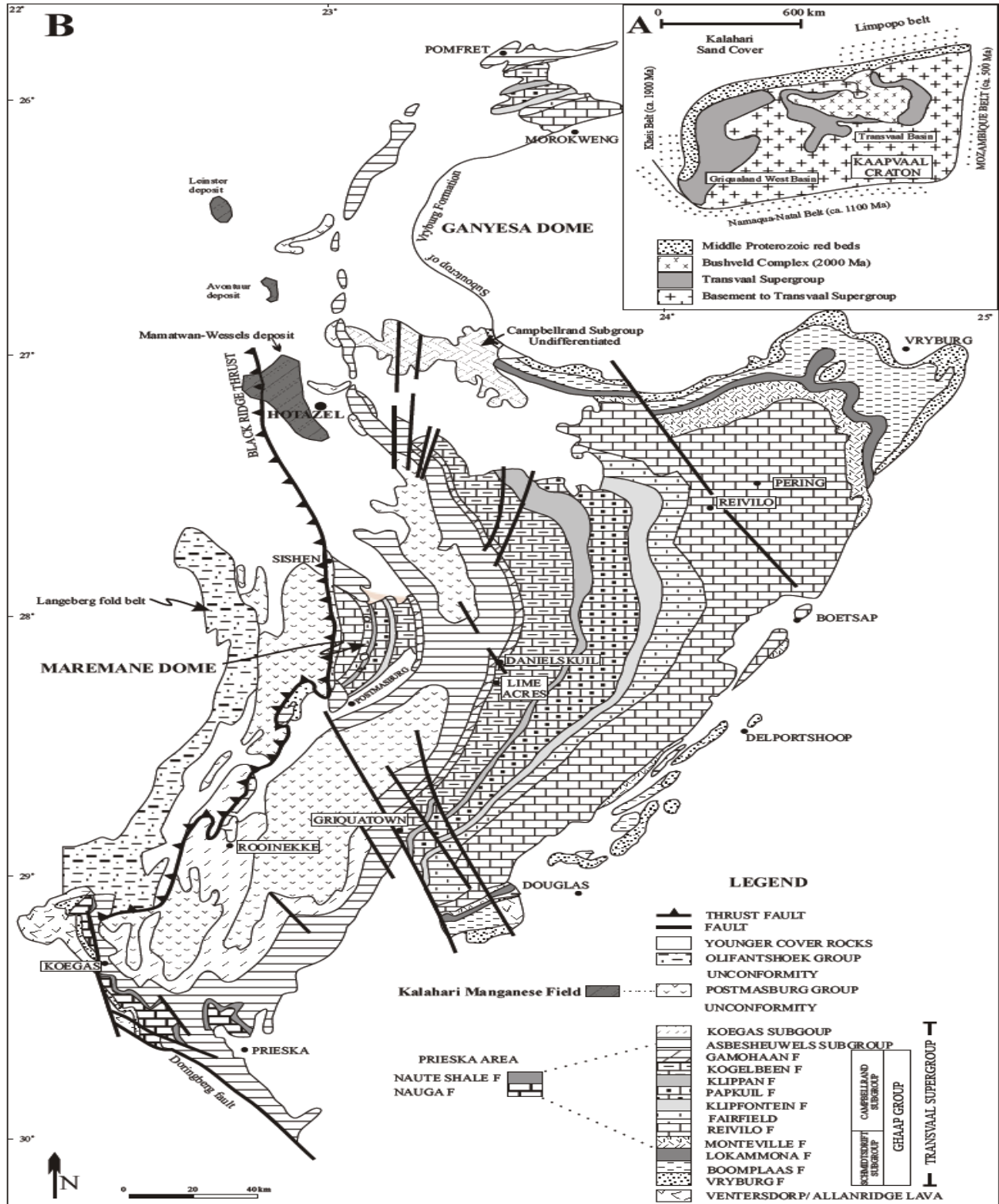


Figure 2.1 Geology of the Transvaal and Griqualand West basin. A. A small-scale geological map showing the Griqualand West Basin and the Transvaal Basin on the Kaapvaal Craton, B. Geological map of the Transvaal Supergroup in Griqualand West showing distribution of major stratigraphic units, the location of the Kalahari Manganese Field and the N-S trending Black Ridge thrust (from Beukes, 1983.)

## 2.2 Kalahari Formation

The Kalahari Formation is Cenozoic in age (Puchner, 2002) and thus the youngest of the stratigraphic units. In South Africa, it covers the North West and the area of interest, which is the Northern Cape Province (Puchner, 2002). Thomas and Shaw, (1990), have analysed records of 320 boreholes of the Kalahari region and revealed a wide range of stratigraphic associations between the different lithological units, and they state that a typical stratigraphic description of the sediments on a regional scale is not possible. Kalahari sand covers a wide area up to 2.5 million km<sup>2</sup> of South Africa and varies in thickness over the surface due to the undulating palaeosurface (Haddon, 2005). The sand overlays the Calcrete sequence which displays different characteristics and, as a result, has locally been divided into top lime, middle lime, bottom lime and lower lime. The Calcrete sequence overlies the Red clay bed, which is underlain by a pebble bed.

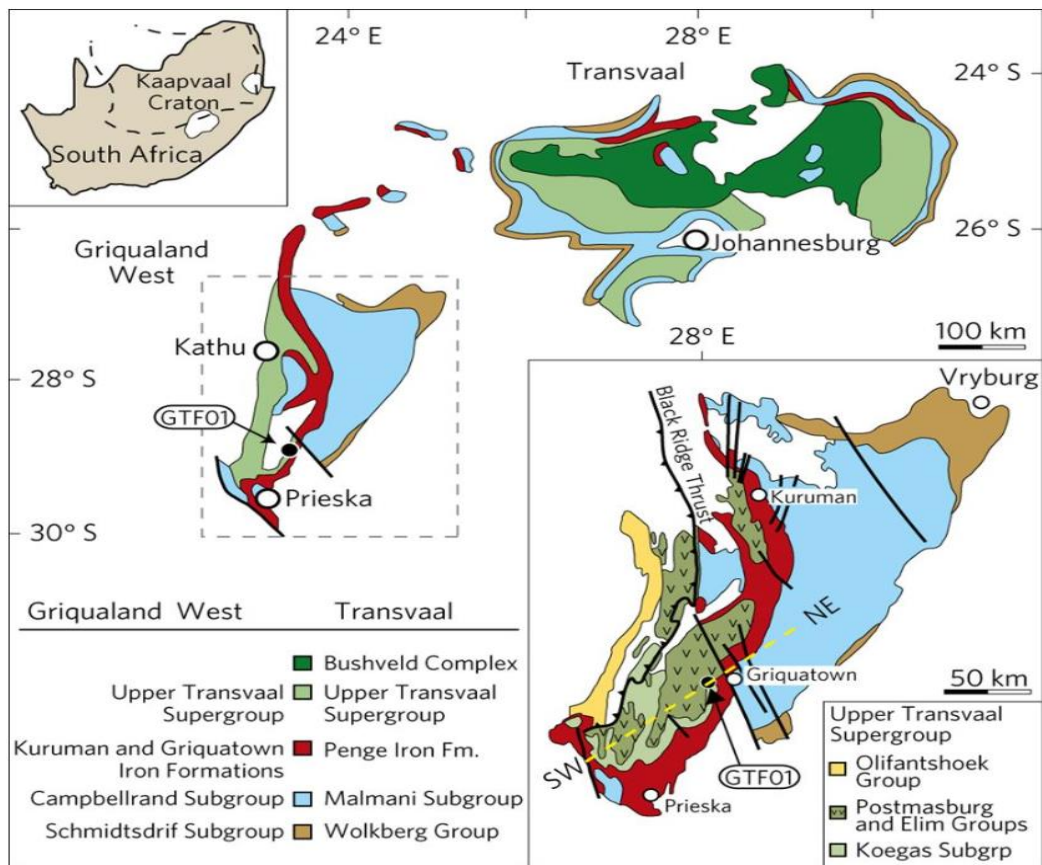


Figure 2.2 Geological map of the Griqualand West basin (Bengtson, et.al. 2017)

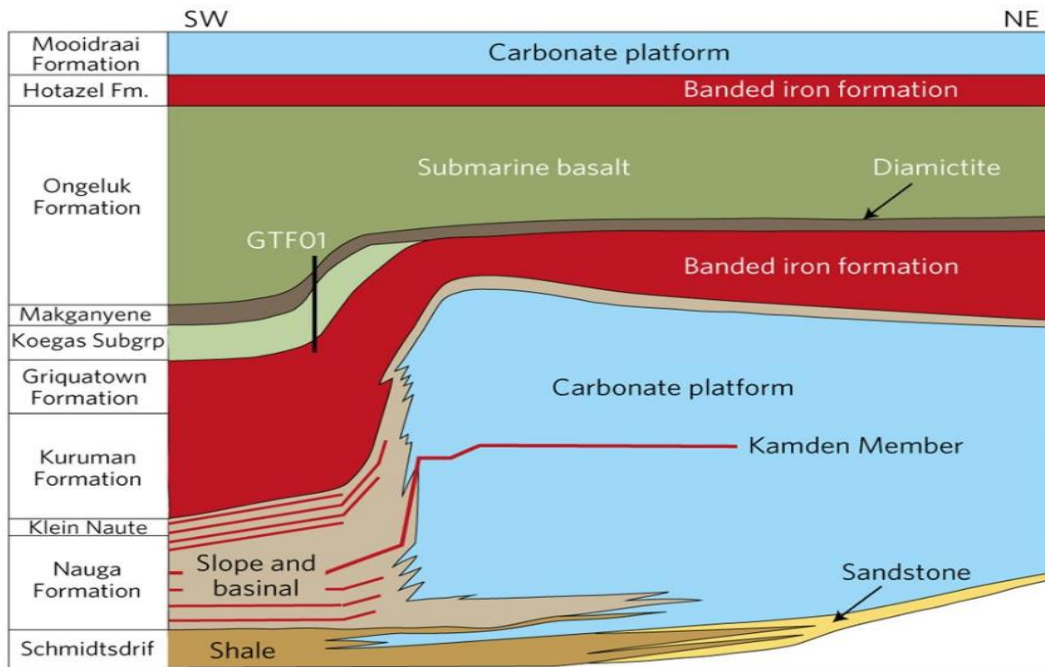


Figure 2.3 Stratigraphic section of the Griqualand West sub-basin (Bengtson et.al. 2017)

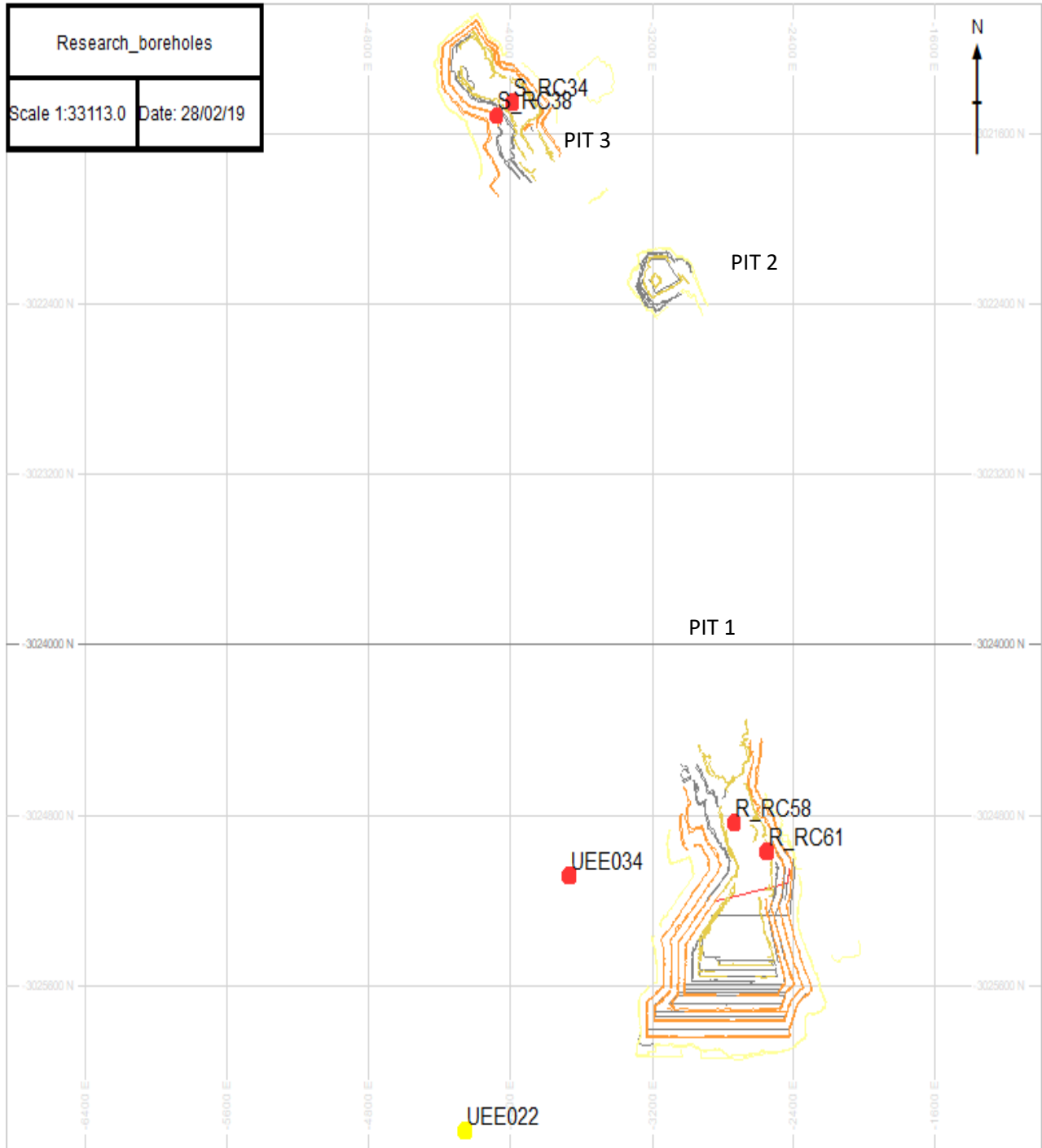


Figure 2.4 Map showing the location of selected boreholes in the area of the study

### 2.2.1 Kalahari deposit

The aeolian unlithified Kalahari sand in the area is reddish brown and has a gradational increase in reddening with depth, ranging from 2m in the northeast to 9m towards the southwest of the mining lease area. It covers the whole mining lease area and increases in thickness towards the southwest where the South32 Mamatwan open pit mining operation is taking place. The Kalahari sand is very fine-grained with grains of <1mm in size. It overlies a thick unit of red clay with an irregular topographic contact. Due to its unconsolidated character, it collapses during drilling and as a result boreholes need to be cased to stabilise the borehole and prevent material from falling back into the hole. The other advantage for mining as a result of its unlithified character, is that it is a free dig, meaning there is no need for drilling and blasting to expose the underlying material. The first 2m of the Kalahari cover has been categorised as the top soil due to the fact that it has got living organisms. The top soil is mined and stockpiled separately for rehabilitation purposes. It has got different plant species, some of them being protected trees, namely the Kameel and Vaal Kameeldoring trees.

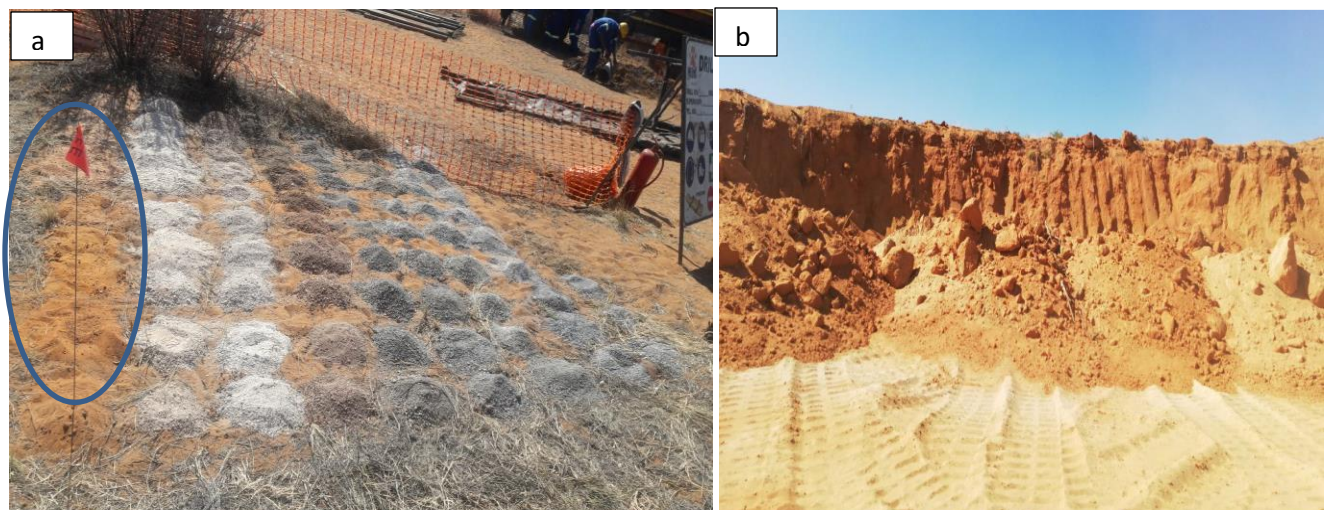


Figure 2.5 The Kalahari deposit displayed in chips from drilling and in a face from mining (a) Percussion drilling samples from borehole logging and (b) the freely dug bench of the aeolian unlithified Kalahari sand

### 2.2.2 Calcrete sequence

#### 2.2.2.1 Calcrete

Calcrete is defined as a rock that is composed of calcium carbonate, that formed when calcium-rich solutions moved through the sediments and over time became concentrated until they precipitated as low-magnesium calcite crystals. Ion effect, CO<sub>2</sub> degassing and evapotranspiration are the main factors that trigger precipitation of calcium carbonate. Calcrete forms through pedogenesis (soil forming process) or groundwater processes or the combination of both soil-forming and groundwater processes. Carbonate sources vary from aeolian dust, rain water, plants, sheet wash or shells (Vermak, 1984; Dhir et.al., 2004). Calcium carbonate cemented crusts, often referred to as calcretes, form an important component of many

contemporary dryland landscapes and can act as a key paleoenvironmental indicator where they are found in Quaternary or older contexts (Goudie, 1983; Nash et.al., 2003). Locally, where mining activities are taking place, the calcrete sequence is thicker than the required 15m maximum bench height and also has varying properties, as a result it has been subdivided into the following units;

- i) **Top lime (Fig. 2.6)** – the first calcrete unit below the Kalahari sand, can be as shallow as 5m below the Kalahari sand. The layer is red in colour, resembling that of the Kalahari sand. The

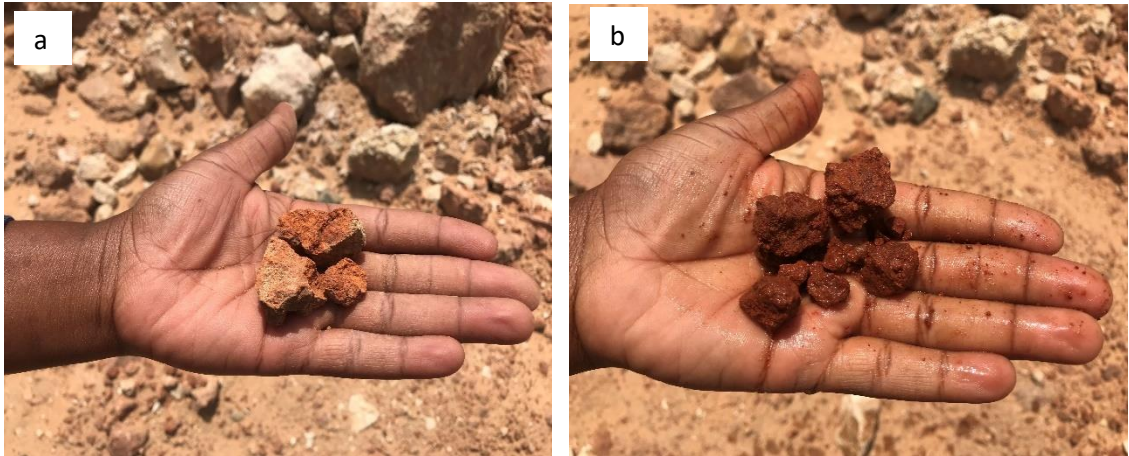


Figure 2.6 Top lime (a) dry top lime sample (b) wet disintegrated top lime sample

only differentiating factor between top lime and the red Kalahari sand is the texture of the grains. The top lime is very brittle and unstable for mining. This is a layer of calcrete that has an average thickness of 10m, it has more sand and increases in clay content towards the west, it poses a lot of challenges during drilling because as the air pressure blows down the hole, there are cavities created at the bottom of the holes, which usually result in a collapsing borehole and ultimately delays production. When cavities are created, there is a lot of room for explosives during charging, as a result, more explosives are pumped down the hole and this increases the cost of mining from drilling to blasting. Top lime holes are usually cased using PVC pipes to avoid a collapse and ultimately overcharging them with explosives. Without proper care of this material during drilling and blasting, the resultant face is usually very uneven and the profile has cavities and bulges, posing a risk to the loading personnel. To mitigate any risks associated with potential instability, a safety berm is maintained at least 5.0m from the toe of the highwall, it is at least 1.5m in height and is constructed of loose material. The bench height is limited to 10.0m to reduce the potential for uncontrolled rock falls related to the weak rock mass.

- ii) **Middle lime (Fig. 2.7)** – this layer of calcrete is composed of a thin hard white calcrete with a layer of pebble bed which is the most dominant. The pebble bed comprises pebbles and cobbles which range from 2mm to over 10cm in size in a hard white matrix. The pebbles in the matrix are sub-rounded, rounded to well-rounded dolerite, chert and sometimes jaspilite.

These pebbles are evidence of transportation over distance. On the eastern portion of the lease area where current mining activities are taking place, the layer lies immediately on top of the supergene altered manganese layer. This manganese layer yields high-grades, further details of why the ore is termed supergene are given in the chapter that follows. Other characteristics of this top lime calcrete layer are that it fines upwards, with the bottom having thicker fragments that reduce in size up the stratigraphic column. The presence of conglomerate pebbles and cobbles in the calcrete is evidence that there was reworking of the sediments through a river flow. There is usually a sharp contact from top lime to middle lime, bottom lime and lower lime. The division of the calcrete or limes as they are locally referred to, was purely based on physical properties which vary with depth and thickness which ultimately have a direct impact to slope stability.



Figure 2.7 Example of a rock found after the middle lime blast

- iii) **Bottom lime (Fig. 2.8)** – is similar to the middle lime with less pebbles, and is whiter in colour than the middle lime. This layer is more stable and poses no threat to drilling and blasting. It yields a more stable highwall than the layers that overlie it. Due to its lack of clay content, this calcrete is deemed competent for road construction on the mine and is used for such. Small calcite veins, less than 1mm in thickness are observed in this layer. These veins may be a result of upwelling of carbonate-rich fluids that were leached from the manganese ore, which ultimately resulted in supergene enrichment.



Figure 2.8 Bottom lime calcrete samples



Figure 2.9 Example of lower lime specimen

- iv) **Lower lime (Fig. 2.9)** – This is the bottom most layer of the calcrete sequence that overlies the banded iron stone of the Hotazel Formation. It is very hard and competent. It is light red in colour, resembling a quartzite. The difference is noted by using an acid to test the presence of carbonates.



Figure 2.10 Calcrete benches showing different types of calcretes

A red clay bed lies below the calcrete sequence and sometimes patches of red clay are found in the calcrete, especially the top lime. These clays have been described by authors like Smit in SACS, (1980) and Jennings (1986) as marls. Locally at UMK it is simply referred to as the Red clay bed (RCB). It is red in colour, hence the name RCB, displaying its ferruginous nature, that is somewhat silty and sometimes with pebbles. The clay is expansive, problematic and hygroscopic. Water tables are usually intersected at the RCB, however, drilling exploration boreholes has proved difficult over the past years in the area when such material is intersected, because it swells up and results in the boreholes collapsing. Polyvinyl chloride (PVC) casing has failed in some instances to stabilise the hole, which intersected water at the RCB, as a result, steel/metal casing was introduced in holes where water is intersected at the depth of the RCB.

Due to its delicate nature, RCB also poses a risk in blasting, an RCB explosive charged block has a lot of cavities from production drilling and takes up a lot of explosives due the fact that during drilling, cavities are created even as sleeves are used to prevent them from caving. When charging, explosives seep through the cavities.

UMK has recorded the thickness of 30m maximum so far for the RCB. It doesn't only have risks during drilling, maintaining a clay waste dump is also a challenge, the required dumping methods differ from those of other waste materials.

### 2.2.2.3 Pebble bed (Fig 2.11)

Pebble beds are also locally categorised as part of the calcrete sequence in the Kalahari Formation. Calcrete matrix-supported pebbles of weathered lava, jaspilite, and quartz range from 2cm to 10cm in size. This layer gives rise to challenges similar to those experienced when drilling and blasting the RCB. The pebble bed is also another good conduit of groundwater.



Figure 2.11. Pebble bed with pebbles as little as 2cm to 10cm in a Calcrete matrix

## 2.3 Mooidraai Formation (MDF)

The Mooidraai Formation is the top-most layer of the Griqualand West basin in the Transvaal Supergroup. It is composed of dolomites and sometimes a cherty algal microbanded sequences. This Formation lies below the Kalahari Formation. It is only observed towards the southwest of the lease area, which is the direction that the manganese basin dips towards. The Mooidraai Formation comprises dolomites in various colours such as yellow, brown, white, black and red. This succession of marine carbonate rocks conformably overlies the manganese-bearing formation. The different colours of these dolomites reflect different environments and/or different stages of deposition. Sulphides like disseminated pyrite are very common in black cherty dolomites.

## 2.4 Hotazel Formation

The Hotazel Formation is a layer in the Griqualand West Basin Group below the Mooidraai Formation and it immediately overlies the Ongeluk Formation (Fig. 2.12). It comprises alternating layers of banded iron formations (BIF) and manganese ores; the upper BIF (UBIF), upper Manganese body (UBOD), middle upper

BIF (MBU), middle manganese body (MBOD) middle lower BIF (MBL), lower manganese body (LBOD) and the lower BIF respectively. It is quite evident that these layers were deposited in a basin-like structure that dips towards the southwest of the lease area. What is observed during drilling is that not all of the above-mentioned layers of the Hotazel Formation appear in the east and sometimes the north part, rather they start appearing at depth towards the west (Fig. 2.12).

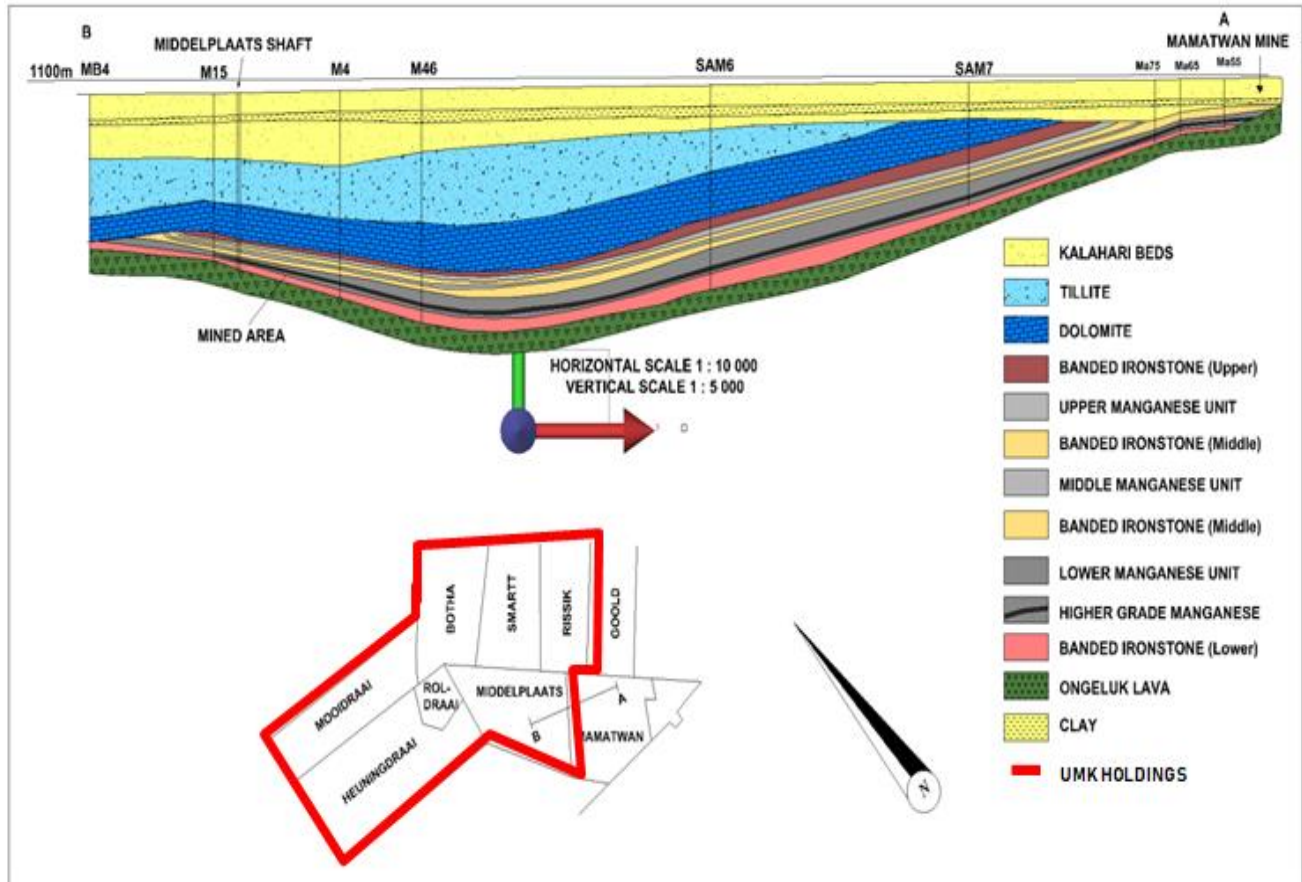


Figure 2.12 Cross-section showing the manganese horizons within the Hotazel Iron Formation and farms where UMK holds a mining license (Van der Merwe, 2015)

### 2.4.1 Upper BIF

The Upper BIF is the top most layer of the Hotazel Formation, lying below the Kalahari Formation and it is quite shallow in the northeast, if present at all, and this reduces the stripping ratio and ultimately the mining cost (Fig. 2.12). Its thickness ranges from 0m to 20m and this thickness increases from the northeast to the southwest of the lease area (Fig. 2.12), where it is found under the Moiddraai dolomites. It covers the upper manganese body (UBOD), and is characterised by different types of BIFs, those that are not banded and BIFs that have disrupted meso- microband and have been locally been termed the rhythmites; e.g.

1. Hematite-magnetite-carbonate-chert rhythmite (RFeMCCa);
2. Greenalite-magnetite-carbonate-chert rhythmite (RGMCCa) and
3. Hematite-carbonate-chert rhythmite (RFeCCa).

The non-banded BIFs have the same composition and are prefixed with B e.g. BFeMCCa (Hematite-magnetite-carbonate-chert BIF). Chert is present as pods and billows and pillows. From these BIFs, it is quite clear that magnetite does not co-exist with hematite, and that hematite, when not present, has been replaced by greenalite, this is evidence of low temperature depositional environments.

#### **2.4.2 Upper body**

The upper body which lies under the upper BIF, was always thought to have an average thickness of about 6m throughout the Kalahari Manganese basin. However, recent drilling proved the upper body thickness to be highly variable, ranging from between 6 and 26m thick. Historically, the Hotazel mine extracted it at a thickness of 7m with only a 13m parting between the UBOD and the LBOD compared to the 50m found in the southwest of the basin.

Toward the southern parts of the lease area, the upper body contains disrupted carbonate flow bands, similar to the Upper BIF and Upper Middle BIF. The carbonate structures have been manganised, suggesting carbonate replacement by manganese. Manganese values are commonly less than 20wt% Mn over a 5-6m thickness that is fairly constant in the southern and northern parts, however in other parts, the manganese values are above 30%, often with individual values >40%. Carbonate bedding is absent and the ore appears more massive.

High-grade Wessels-type ore was intersected between a fault and a dyke in the northeast of the lease area. Immediately toward the northwest of this area, the upper body thickness varies quite considerably from 6.5m to 15m, closely following an antiformal structure, thickening on the flanks and thinning over the crest. Similarly, Mn grades drop toward the flanks and increase over the dome. The above-mentioned event suggests that the sill in this area is older than the upper body and that the bulging caused a positive topography, which was in place when the upper body was precipitated.

Further north, the sill is not present and the upper body reaches thicknesses of up to 26m comprising alternating cycles dominated by either carbonate ooids or carbonate microbands and stringers. The ooids are coarse, especially near the top, resembling small concretions. Manganese values vary from the mid-20% to low 30%, with the best values generally confined to the bottom 10m. This layer is considered to be economical.

#### **2.4.3 Middle upper BIF**

This layer is situated under the upper body and lies above a very thin middle manganese body, the middle upper BIF resembles the middle lower BIF, the two middle BIFs (upper and lower) have been separated by the thin manganese middle body. This is poorly developed in the northeast, and very shallow. The three layers, i.e. Middle upper BIF, Middle Body and Middle lower BIF, are not apparent in the northeast, and the present BIF is just called the Middle BIF without the distinguishing 'upper and lower'. As the strata dips and thickens to the southwest, the two middle BIFs are observed with the middle manganese body as the separator. Boreholes situated on the north are shallow and the two middle BIFs are not present. This is not the case for boreholes that are on the south of the lease area, however for the purpose of not

confusing the database and inclusion of the very thin uneconomical middle manganese body, the three layers are captured as one middle BIF.

#### **2.4.4 Middle body**

The middle body varies its stratigraphic position within the Middle BIF, while the lower body and the upper body define the base and the top, respectively. The middle body is for the most part not developed within the area drilled. In most borehole intersections the middle body comprises a 3.3-4m thick, hematite lutite containing carbonate stringers and ooids. The distance between the base of the middle body and the top of the lower body increases toward the north from 16.86m to 47.07m. Further north the parting again decreases to 22.15m. It is currently uneconomical.

#### **2.4.5 Middle lower BIF**

This unit is almost the mirror image of the Middle upper BIF. It is locally captured as one package with the Middle upper BIF and the MBOD. This layer, like the middle upper BIF, is also poorly developed in the northeast, and is also very shallow. In the southwest, where it gets intersected, it is characterised by a thin Fe and Mn lutite layer. This layer is a transition from the BIF to the lower body.

#### **2.4.6 Lower Body**

The Lower manganese body (LBOD), is the most sought-after economic zone. United Manganese of Kalahari is mining the LBOD thickness of 20m, observed in drillhole S\_RC38 (Fig. 2.13). Its thickness is maximal (45m) at the southern boundary of the Kalahari field (Mamatwan deposit) and decreases northward to 5m at a distance of 35km (Wessels deposit).



# UNITED MANGANESE OF KALAHARI



Farm: SMARTT 314  
Borehole: S\_RC38

X: -3021520  
Y: -4073.95  
Z: 1050.77  
LO23\_WGS84

End Drill Date:

Scale: 1:100

## Geological Description

## Sample Details

Mn Fe SiO2 Al2O3 CaO MgO Na2O K2O P2O5 LOI Mn/Fe RD

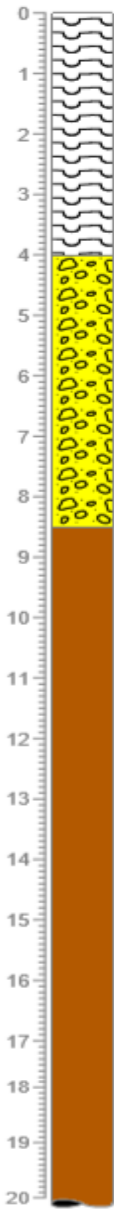
0.00 - 4.00 m Calcrete

### 0.00 - 8.50 :Kalahari Formation

4.00 - 8.50 m Pebbly sand

### 8.50 - 28.50 :Hotazel FM - Middle BIF (Upper and Lower)

8.50 - 28.50 m Banded Iron Formation



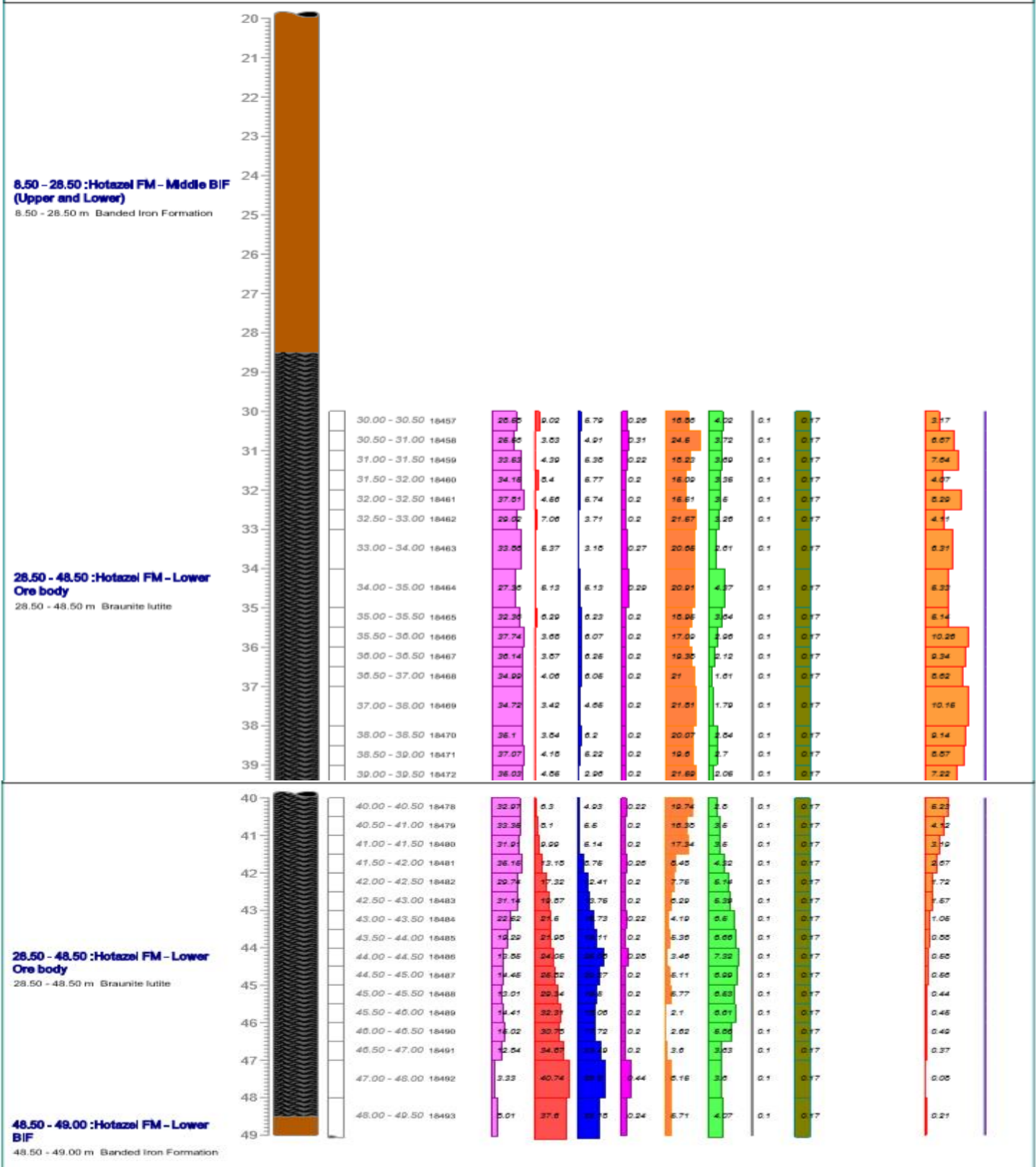


Figure 2.13 Percussion borehole log for S\_RC38

#### **2.4.7 Lower BIF**

The thickness of this unit varies very little, (18-20m), all the way through Rissik farm and through the southern parts of Smartt farm (Fig. 2.12). However, toward the northern parts of Smartt the thickness drops drastically to just under 5m in places. The lower contact of the lower body with the upper part of the lower BIF unit is gradational as it changes to the Fe/Mn lutite (L-zone).

#### **2.4.8 Ongeluk Formation**

The Ongeluk Formation conformably overlies the Makganyenye diamictites in the Kuruman area, a laterally extensive sequence of tholeiitic basaltic andesites which were extruded under water in a marginal basin within a continental setting of the Kaapvaal craton (Schutte, 1992). Schutte sub-divided the lava types into two, namely the Regional Ongeluk lava, which is grey-green to bluish grey and the Kalahari Ongeluk lava, which is bright maroon in colour and occurs towards the edge of the Kalahari Basin.

#### **2.4.9 Conclusion**

The Hotazel deposit is covered by Cenozoic mostly unconsolidated sediments of the Kalahari Formation. These form a layer on the easternmost parts of the Kalahari basin, where the Hotazel Formation is intersected immediately below the Kalahari Formation. The Kalahari Formation seems to have impacted the east where the sub-outcrop exists, to be of economic importance, in that its porous nature aided the movement of groundwater that leached carbonates out of the manganese layer and resulted in elevated economic grades. It is also important to mention that there is no evidence of a high temperature environment for the movement of this groundwater, this is just a pure chemical reaction. The Kalahari Formation is also important in groundwater exploration. The Kalahari Formation must be well understood especially the geotechnical aspects of it due to its unconsolidated and unstable nature. This is important for the development of both underground mining, especially shaft sinking and open cast mining where slope stability is key to maintaining safety standards.

South-westwards, in the direction of dip of the basin, other formations are intersected, i.e. the Mooidraai Formation. The dolomites are carbonate rocks that precipitated in the marine environments. The formation is characterised by disseminated pyrite in some areas, giving evidence of upwelling high temperature fluids. These fluids mostly moved through the displaced faults after structural events like the Black Ridge thrust, leading to the alteration that upgraded manganese to the now Wessels-type ore (discussed in the next chapter).

## CHAPTER 3

### THE LOWER MANGANESE BODY

#### 3.1 Introduction

Previously, various authors proposed that the manganese in the Kalahari deposit is a representation of consolidated sediments that resulted from volcanogenic exhalative processes in the ocean environment (Beukes, 1983; Kleyenstuber, 1984, 1985; Nel et al., 1986; Schutte, 1992; Cornell and Schutte, 1995, 1996; Tsikos et al., 1997). To date, there is no one definitive model that is generally accepted for the genesis of the huge deposits, however, there are models that have gained popularity and these models indicate a sedimentary origin (Kuleshov, 2012).

Based on the structural, mineralogical and chemical properties, the body is divided into 11 subzones (from the bottom to top): B, L, N, H, C, M, Z, Y, X, W and V (Nel et al., 1986; Gutzmer et al., 1997; Kuleshov, 2012). The initial accumulation of manganese in the primary stages did not reach economic values (Kuleshov, 2011), until later processes like metamorphism, retrograde diagenesis and metasomatism led to its upgrade. Most boreholes drilled close to geological structures like dykes and faults have yielded very good grade manganese, this just shows that there is structural influence on the grade and, thus, supports the suggestions of Kuleshov (2012).

Gutzmer and Beukes (1995), have indicated that there is generally no observable severe deformation and metamorphism defined in the entire Kalahari deposit except for the hydrothermal Wessels event. This event is restricted to the faulted northern part, an area affected by east-verging thrust duplication and north-northeast-trending normal faulting (Tsikos et al., 2003), namely the Black Ridge thrust fault (BRTF), (Fig. 1.2). Beukes et al. (2016), allude that the structure of the main Kalahari deposit is that of a double plunging syncline that was peneplaned by erosion prior to deposition of the overlying ~2.0 Ga Mapedi/Gamagara red bed succession of the Elim Group. The syncline, together with the Mapedi/Gamagara red beds, were tilted to the northwest prior to, or during, development of the Black Ridge thrust fault that duplicates strata along the western margin of the synclinal structure (Beukes et al., 2016). This resulted in the manganese ore being shallow on the south-eastern margin of the basin, making it favourable for open pit mining and getting deeper towards the western side of the basin where ore access is through underground mining.

#### 3.2 Ore types

The Kalahari manganese deposit bears 3 types of ore, namely;

- **The hydrothermally altered Wessels-type ore** – This type of ore has been upgraded by the Black Ridge thrust fault (BRTF), event which according to Van Niekerk (2006), is attributed to the tectonic collision of the Kheis Terrane in the west. Gnos et al. (2003), have indicated that the structural event resulted in infiltration of compression-related fluids in the stratigraphy as a fluid-

front prior to thrusting at around 1 048.1 Ma +/- 5.9 Ma. These fluids utilised the pre-existing extension-related normal faults (Fig. 2.1) in the area as conduits, resulting in the manganese-enriched, carbonate depleted 'Wessels-type' ore in the northern KMF below the Black Ridge thrust fault (Gutzmer, 1996). The typical composition of the Wessels-type ore is  $Mn_3O_4$ . United Manganese of Kalahari is situated further south from the Wessels-type ore zone, (Fig. 3.1a), thus there is no borehole in this study depicting this type of ore. Minerals typically found in the Wessels-type ore are hausmannite, bixbyite and braunite II (Table 3.1).

**Table 3.1 List of minerals and their chemical formula**

Bixbyite	$Mn^{3+}_{1.5}Fe^{3+}_{0.5}O_3$
Braunite II	$Mn^{2+}Mn_6^{3+}SiO_{12}$
Cryptomelane	$KMn_8O_{16}$
Hausmannite	$Mn_3O_4$
Kutnahorite	$Ca(Mn,Mg)(CO_3)_2$
Todorokite	$Mn^{4+}, Mn^{2+}_8(O, OH)_{16} + 2H_2O$

- Supergene enriched** - Supergene enrichment is only found underneath the Cenozoic Kalahari unconformity in the most eastern parts of the property comprising mainly of cryptomelane and todorokite (Table 3.1). Ore was intersected at very shallow depth, 4m below the Kalahari sand of the Kalahari Formation. The supergene enrichment resulted from the circulation of oxygenated groundwater that penetrated the ore and leached out carbonate minerals whilst upgrading the manganese content. The process seems to have been aided by a thin Kalahari cover, fractures, faults and dykes. Strongly supergene altered ore appears massive, dark black in colour with no microscopical detectable carbonates (Fig. 3.1a) Supergene alteration is best achieved within zones containing carbonate ooids rather than laminae. Generally, it appears that the thinner the ore horizon preserved underneath the Kalahari unconformity the better the upgrading. The supergene altered ore is porous and has a density of 2.0-3.4 g/cm<sup>3</sup>, which requires less explosive energy during blasting. This ore breaks up easily and results in a high percentage of fines after blasting.

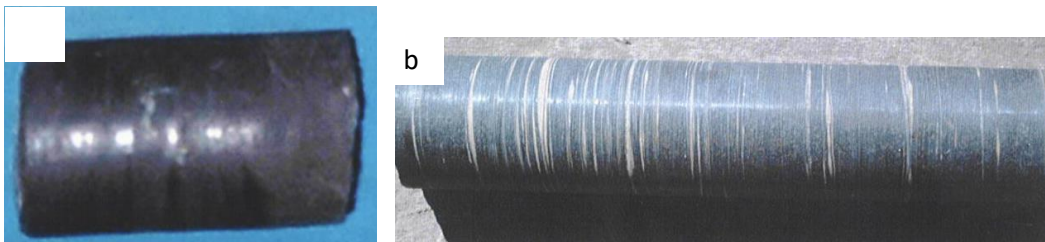


**Figure 3.1 Different types of ore, with and without carbonates (a) Supergene altered ore, with clear absence of carbonates, (b) Primary unaltered ore with carbonates**

- The primary low-grade Mamatwan-type ore** (Fig. 3.1b and Fig. 3.2) is the most dominant ore type of the Kalahari basin. The ore is dark brown to dull greyish black in colour. It is finely laminated and very



# UNITED MANGANESE OF KALAHARI



Farm: RISSIK 330  
Borehole: R\_RC58

X: -3024841.931  
Y: -2732.596  
Z: 1053.787  
LO23\_WGS84

End Drill Date:

Scale: 1:100

## Geological Description

## Sample Details

Mn Fe SiO2 Al2O3 CaO MgO Na2O K2O P2O5 LOI Mn/Fe RD

Depth (m)	Sample ID	Mn	Fe	SiO2	Al2O3	CaO	MgO	Na2O	K2O	P2O5	LOI	Mn/Fe	RD
0.00 - 4.50													
5.50 - 6.00	18287	26.6	7.3	2.4	1.02	2.33	6.37	0.49	1.76	0.046	12.85	3.83	
6.00 - 6.50	18288	27	9.42	2.1	2.37	4.44	2.21	0.25	2.26	0.04	13.24	2.57	
6.50 - 7.00	18289	20.1	7.45	1.5	1.02	14.1	6.74	0.15	1.79	0.025	22.52	2.59	
7.00 - 7.50	18290	26.5	7.53	1.14	0.3	13.5	7.27	0.15	2.43	0.05	22.74	3.42	
7.50 - 8.00	18291	25.6	12.3	2.1	0.15	10.5	7.07	0.17	1	0.067	20.85	2.33	
8.00 - 8.50	18292	34.1	13.1	5.16	0.19	9.45	2.24	0.19	0.14	0.059	13.03	2.50	
8.50 - 9.00	18293	29.7	5.53	4.63	0.2	17.3	1.75	0.05	0.05	0.045	20.90	3.44	
9.00 - 9.50	18294	30.5	6.46	5.04	0.25	17.5	4.47	0.15	0.05	0.042	20.82	6.01	
9.50 - 10.00	18295												
10.00 - 10.50	18296	30	4.14	4.51	0.17	21.7	2.51	0.01	0.05	0.037	21.81	7.28	
10.50 - 11.00	18297	25.4	3.45	4.14	0.19	25.2	2.35	0.02	0.05	0.031	25.03	7.49	
11.00 - 11.50	18298	30	4.24	5.23	0.3	19.5	4.3	0.01	0.05	0.035	21.71	7.05	
11.50 - 12.00	18299	30.5	4.1	5.05	0.22	19.1	4.75	0.01	0.05	0.036	21.52	7.51	
12.00 - 12.50	18300	22.9	5.1	3.73	0.15	25.6	4.25	0.02	0.04	0.035	25.30	4.49	
12.50 - 13.00	18301	26.2	7.03	4.3	0.19	21.3	4.43	0.02	0.04	0.045	23.73	3.55	
13.00 - 13.50	18306	31.4	6.55	5.57	0.2	15.4	4.42	0.01	0.04	0.037	20.43	5.65	
13.50 - 14.00	18307	34.1	6.74	5.29	0.15	14.7	4.23	0.01	0.04	0.042	15.52	5.94	
14.00 - 14.50	18308	34	10.3	5.47	0.21	12.3	3.51	0.01	0.03	0.043	15.55	3.30	
14.50 - 15.00	18309	35.3	7.11	5.53	0.21	12.7	3.23	0.01	0.02	0.042	15.75	5.11	
15.00 - 15.50	18310	35.1	3.26	5.55	0.11	15	4.47	0.01	0.03	0.039	15.34	9.14	
15.50 - 16.00	18311	35.5	4.23	5.21	0.05	17.2	2.4	0.04	0.02	0.032	17.43	5.70	
16.00 - 16.50	18312	35.7	4.05	4.67	0.05	17.4	2.3	0.04	0.02	0.03	17.59	5.51	
16.50 - 17.00	18313	35.9	3.94	5.29	0.1	15.6	1.29	0.01	0.02	0.042	15.72	9.37	
17.00 - 17.50	18314	35.4	3.17	5.25	0.14	15.1	2.05	0.01	0.02	0.032	17.91	11.45	
17.50 - 18.00	18315	35.5	3.25	5.31	0.12	20.3	1.32	0.03	0.03	0.031	17.92	10.95	
17.50 - 18.00	18315	35.5	3.25	5.31	0.12	20.3	1.32	0.03	0.03	0.031	17.92	10.95	
18.00 - 18.50	18316	35.5	3.71	5.4	0.12	15.7	1.49	0.01	0.03	0.035	15.77	9.22	
18.50 - 19.00	18317	35.6	3.9	5.27	0.12	19.1	1.52	0.01	0.03	0.034	17.97	9.10	
19.00 - 19.50	18318	41.2	4.33	4.77	0.12	15.1	1.54	0.02	0.04	0.039	14.40	9.52	
19.50 - 20.00	18319	35.5	4.79	5.42	0.15	15.3	2.74	0.01	0.05	0.037	17.45	7.43	

Geologist: Trudy Mudau

Page: 1 of 2



### **3.3 Lower body zones**

#### **V – Zone**

The V-Zone (Fig. .4a) is characterised by grey massive braunite lutite which contains fine white carbonate microbands, stringers and fine pink ooids. Intergrowths are usually located near the top while the bottom comprises fine pink ooids.

#### **W – Zone**

Mined together with the V-Zone is the W-Zone. The W-Zone is also a massive braunite lutite containing occasional carbonate microbands and stringers (Fig. 3.4b)

#### **X – Zone**

The X-zone was described by Nel et al. (1986) at Mamatwan mine as, “dark grey ore with large concentrically banded white carbonate ovoids and brown to white carbonate nodules.” Preston (2001) further divided it into three subzones, X1, X2 and X3, the description is very close to what is observed at the United Manganese of Kalahari mine. In the study area, this zone is a massive grey to brown lutite with an average thickness of 2.56m. It contains white carbonate microbands, stringers and fine white and pink ooids, with white ooids present towards the base. The manganese content is slightly elevated compared to the V and W zones (Fig. 3.4c).

#### **Y – Zone**

This zone is classified as a parting for mining purposes. The grades are not viable and need blending to achieve the required sales. The zone has an average thickness of 1.5m as observed in the drill core. The manganese content of this zone is between 28.30% and 32.90% (Fig. 3.4d). Although these grades are intersected at shallower depth than expected, they do correlate with the ones observed in the Kalagadi mine, as described by Rasmeni (2012). The carbonates of the Y-Zone are white mesobands, microbands, stringers and pink ooids (Fig. 3.4d)

#### **Z – Zone**

Locally classified together with the Y-Zone as the parting, the observed average thickness from UEE034 is 0.7m. The manganese content ranges above 35% while the iron content decreases, and it contains white carbonate stringers and fine white and pink ooids (Fig. 3.4e).

#### **M – Zone**

The M-Zone (Fig3.4f) is a dark grey and massive braunite lutite, which contains carbonates that are present mostly as coarse ooids and occasional microbands and stringers. The M-Zone has an average of 1.14m in borehole - UEE034 (Fig. 3.3) and the grades are elevated to just over 36.4% Mn. This is one of the most economic zones in the LBOD.

### **C – Zone**

The C zone is grey and contains carbonates in a form of laminae fashioned ooids. Very thin hausmannite layers are observed within massive braunite. Mesobands and microbands, although they occur, are not very visible. This zone is thicker than the M-zone with an average of 2.6m, the grades are however similar to those of the M-Zone (Fig. 3.4g)

### **N – Zone**

This layer (Fig. 3.4h) is the thickest of all the zones as observed in the drill core used for this study (Fig. 3.3). At 3.14m thickness, it hosts carbonates ranging from microbands, fine pink ooids and stringers. The grades have peaked at 36.8% in the studied drill core.

### **M-C-N Zone**

In mining, the **M**, **C**, and **N** zones are consolidated and described as one package (the **MCN** zone) due to their elevated grades and sometimes resemblance in their carbonate structures. The **MCN** zone is the most sought-after layer as it hosts the highest grades and is the thickest of all the zones. This is referred to as the bottom cut in mining terms.

### **B – Zone**

The B-zone in UEE034 is characterised by an elevated Fe content and low carbonate (CaO) content (Fig. 3.3). It also is characterised by its magnetism, which is the best distinguishing feature from the N-Zone. The magnetism marks the start of transition from the LBOD to the LBIF. This zone has an average thickness of 1.12m in the sampled drilled core. It attains a maximum of 29% Mn content and 16.2% Fe maximum. Also called the Fe/Mn lutite, it has visible layers of hematite with those of hausmannite, it also has pink microbands, sometimes mesobands, stringers and faded ooids. This is considered to be the footwall in mining terms. This footwall sometimes yields up to 32% of Mn with an elevated Fe content. If its thickness reaches and/or exceeds 2m, it is selected for mining and it is locally called the high metal content (HMC), a new horizon discovered and named in the UMK mine.

The **B** is categorised with the **L** zone (found in the Lower BIF) in terms of mining. These layers are basically the transition zones from the LBOD to the Lower BIF.

### **L – Zone**

This is the base that informs the drilling to stop, the grey manganese colour totally diminishes and red is more visible. Often, it is drilled for 2m to confirm the transition from the LBOD to the LBIF. Also magnetic at depth, the Fe content for the first 0.5m sampled reaches 19.7% and manganese content drops to below 22%. The L-zone sometimes comprises a non-magnetic, maroon coloured mudstone, containing stacked sedimentary sets, each about 5cm thick and bounded at the top and bottom by about 3mm thick, faint green to white carbonate laminae containing fine carbonate stringers in between. The L-zone grades downward into a brick red, crinkly carbonate microbanded, non-magnetic hematite lutite. Flat ooids are common. This horizon grades downward into a massive brick red, non-magnetic hematite lutite, containing carbonates mostly as disseminations. Jaspelite – Sishen-type ore are not quantified in the study area

### **3.4 Mining terminology**

At UMK Mine, the LBOD was divided in 6 units for mining purposes based on grade and thickness

- Top Cut (Zones V and W): Normally ferruginous with Mn content of less than 30%
- Upper Cut (Zone X): Normally more than 38% Mn close to the sub-outcrop, otherwise it is generally 35% Mn down-dip (towards the inner part of the basin, which dips to the west)
- Parting (Zones Y and Z): Normally less than 33% Mn content and sometimes not found in the east, which is the sub-outcrop where there is supergene enriched ore.
- Bottom Cut (Zones M, C and N): Main economical horizon normally with grades greater than 35% Mn.
- High Metal Content/HMC (Zone B): Normally 35% Mn and metal/iron content more than 10%, this product is only mineable if its thickness is 2m or more and is saleable.
- Footwall (Zone L): part of the Lower BIF in the lithostratigraphy, it has Mn content less than 33% Mn and Fe of more than 10%.



# UNITED MANGANESE OF THE KALAHARI

## Detailed Assay Log

**Borehole: UEE034**

Farm: Rissik 330

Scale: 1:100  
Projection: Lo23  
Datum: Wgs84

X Surveyed: -3664.83

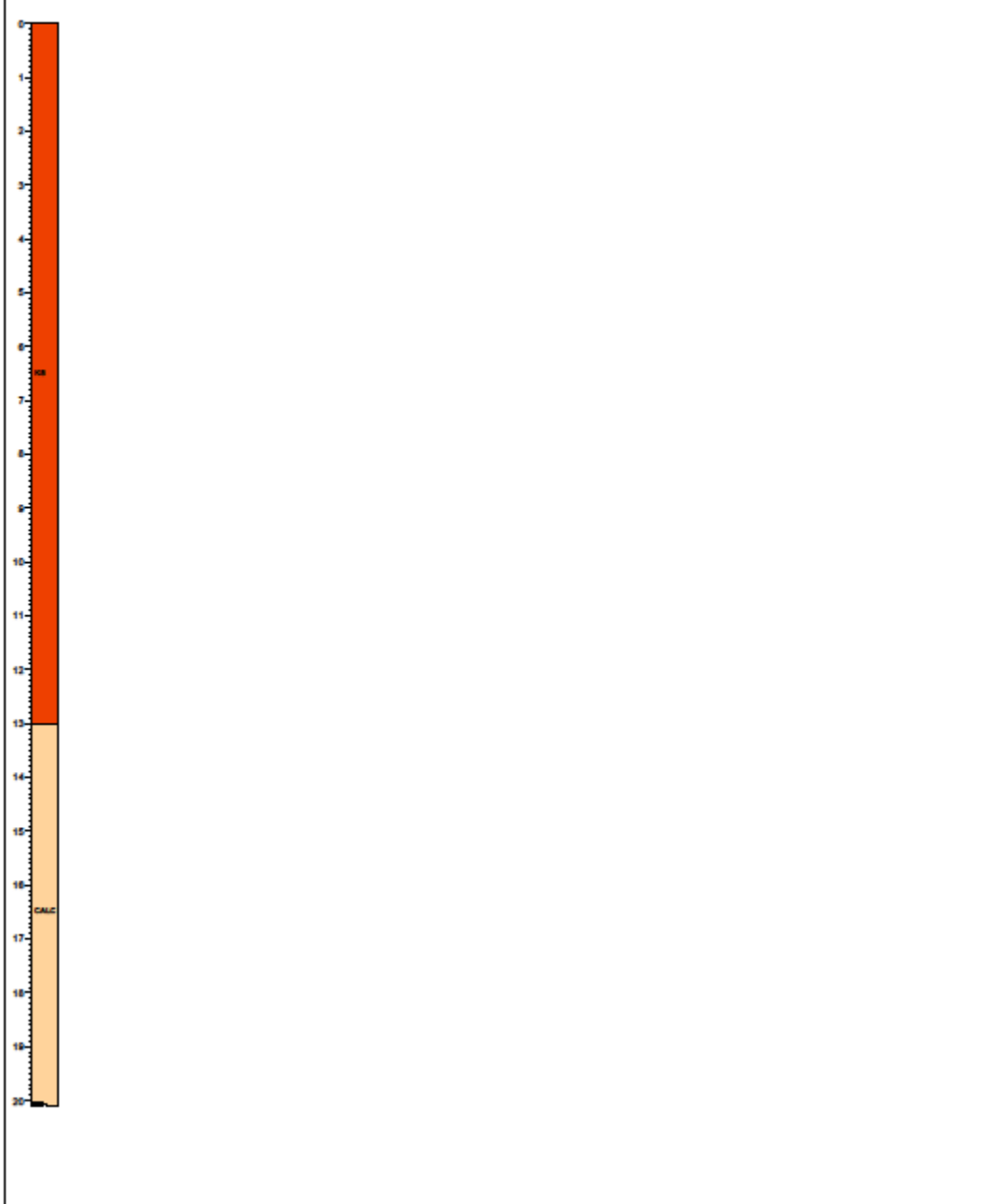
Y Surveyed: -3025089.66

Z Surveyed: 1082.017

Final depth: 153.40

End date: 2017/10/14

Geology		Minecut Sample Details				Fusion Assay Results										
Stratigraphy	Subzone	From	To	Sample	Mn (%)	Fe (%)	SiO2 (%)	Al2O3 (%)	CaO (%)	MgO (%)	Na2O (%)	K2O (%)	P2O5 (%)	LOI (%)	MnFe	RD



Geologist: Trudy Mudau

Page 1 of 8



# UNITED MANGANESE OF THE KALAHARI

## Detailed Assay Log

**Borehole: UEE034**

Farm: Rissik 330

Scale: 1:100  
Projection: Lo23  
Datum: Wgs84

X Surveyed: -3664.83

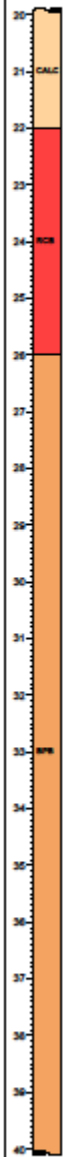
Y Surveyed: -3025089.66

Z Surveyed: 1082.017

Final depth: 153.40

End date: 2017/10/14

Geology		Minecut Sample Details				Fusion Assay Results										
Stratigraphy	Subzone	From	To	Sample	Mn (%)	Fe (%)	SiO <sub>2</sub> (%)	Al <sub>2</sub> O <sub>3</sub> (%)	CaO (%)	MgO (%)	Na <sub>2</sub> O (%)	K <sub>2</sub> O (%)	P <sub>2</sub> O <sub>5</sub> (%)	LOI (%)	MnFe	RD



Geologist: Trudy Mudau

Page 2 of 8



# UNITED MANGANESE OF THE KALAHARI

## Detailed Assay Log

**Borehole: UEE034**

Farm: Rissik 330

Scale: 1:100  
Projection: Lo23  
Datum: Wgs84

X Surveyed: -3664.83

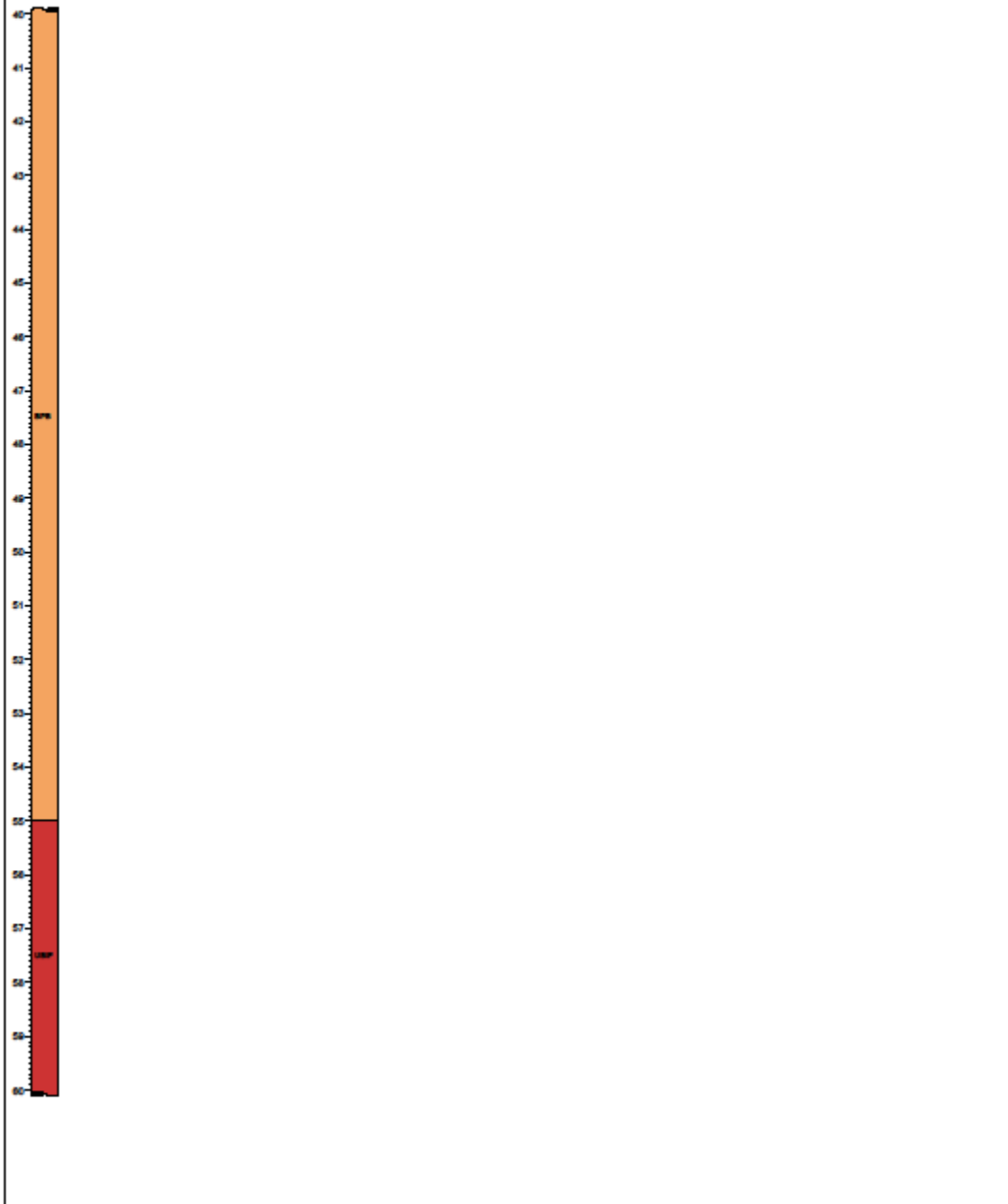
Y Surveyed: -3025089.66

Z Surveyed: 1082.017

Final depth: 153.40

End date: 2017/10/14

Geology		Minecut Sample Details				Fusion Assay Results										
Stratigraphy	Subzone	From	To	Sample	Mn (%)	Fe (%)	SiO <sub>2</sub> (%)	Al <sub>2</sub> O <sub>3</sub> (%)	CaO (%)	MgO (%)	Na <sub>2</sub> O (%)	K <sub>2</sub> O (%)	P <sub>2</sub> O <sub>5</sub> (%)	LOI (%)	MnFe	RD



Geologist: Trudy Mudau

Page 3 of 8



# UNITED MANGANESE OF THE KALAHARI

## Detailed Assay Log

**Borehole: UEE034**

Farm: Rissik 330

Scale: 1:100  
Projection: Lo23  
Datum: Wgs84

X Surveyed: -3664.83

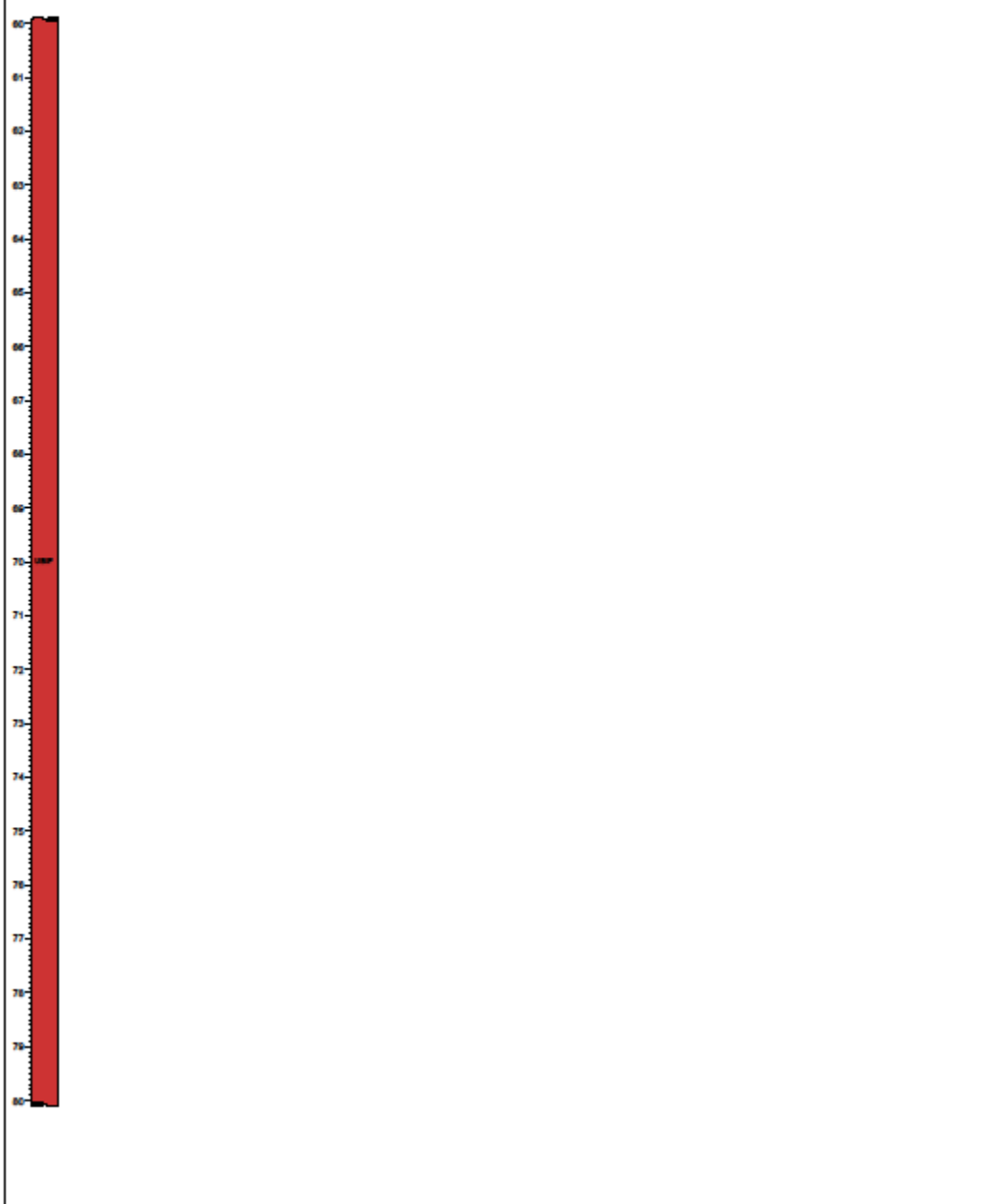
Y Surveyed: -3025089.66

Z Surveyed: 1082.017

Final depth: 153.40

End date: 2017/10/14

Geology	Minecut Sample Details	Fusion Assay Results
Stratigraphy Subzone	From To Sample Mn (%) Fe (%) SiO2 (%) Al2O3 (%) CaO (%) MgO (%) Na2O (%) K2O (%) P2O5 (%) LOI (%) MeFe RD	



Geologist: Trudy Mudau

Page 4 of 8



# UNITED MANGANESE OF THE KALAHARI

## Detailed Assay Log

**Borehole: UEE034**

Farm: Rissik 330

Scale: 1:100  
Projection: Lo23  
Datum: Wgs84

X Surveyed: -3664.83

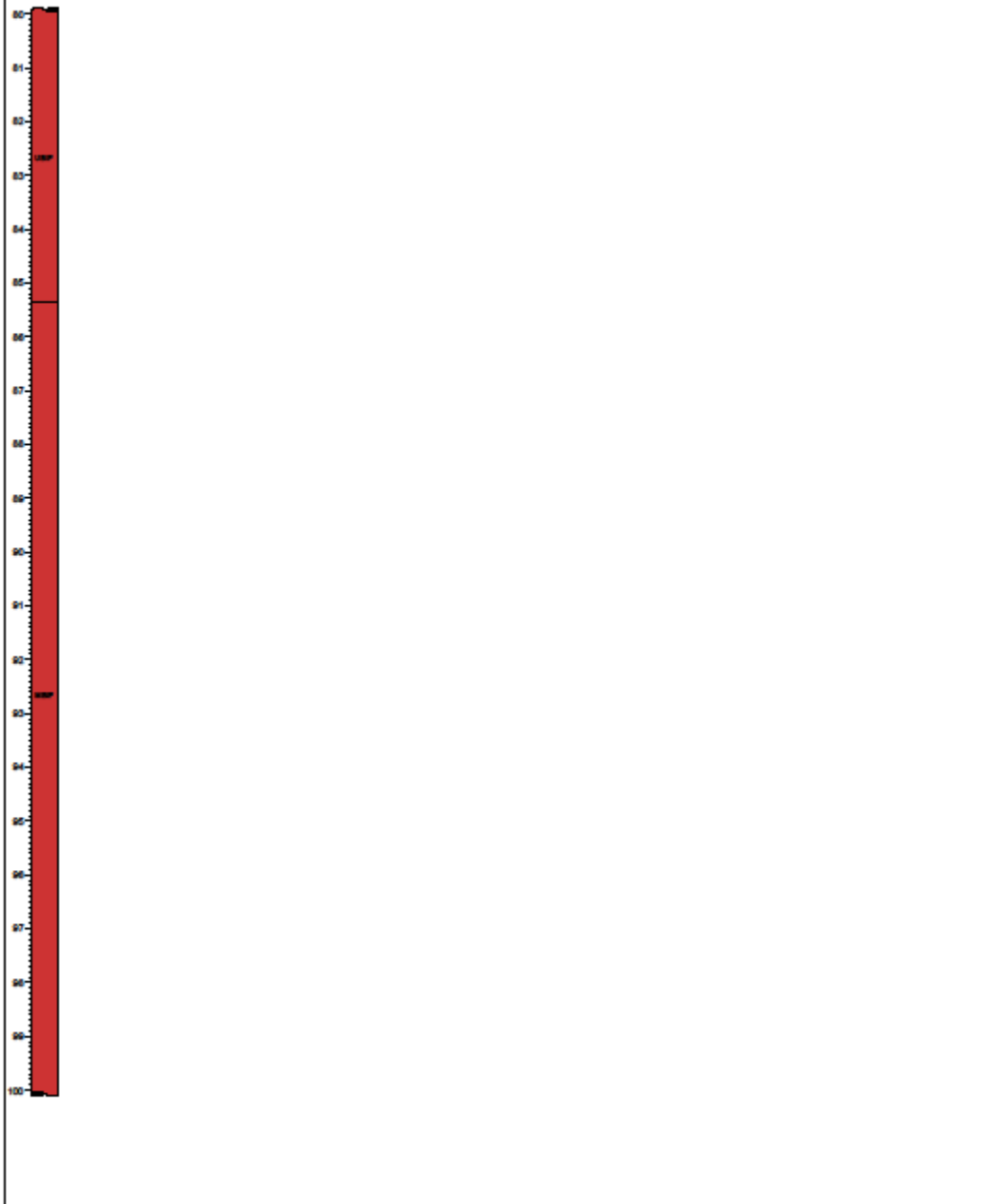
Y Surveyed: -3025089.66

Z Surveyed: 1082.017

Final depth: 153.40

End date: 2017/10/14

Geology		Minecut Sample Details				Fusion Assay Results										
Stratigraphy	Subzone	From	To	Sample	Mn (%)	Fe (%)	SiO <sub>2</sub> (%)	Al <sub>2</sub> O <sub>3</sub> (%)	CaO (%)	MgO (%)	Na <sub>2</sub> O (%)	K <sub>2</sub> O (%)	P <sub>2</sub> O <sub>5</sub> (%)	LOI (%)	MnFe	RD



Geologist: Trudy Mudau

Page 5 of 8



# UNITED MANGANESE OF THE KALAHARI

## Detailed Assay Log

**Borehole: UEE034**

Farm: Rissik 330

Scale: 1:100  
Projection: Lo23  
Datum: Wgs84

X Surveyed: -3664.83

Y Surveyed: -3025089.66

Z Surveyed: 1082.017

Final depth: 153.40

End date: 2017/10/14

Geology		Minecut Sample Details				Fusion Assay Results										
Stratigraphy	Subzone	From	To	Sample	Mn (%)	Fe (%)	SiO <sub>2</sub> (%)	Al <sub>2</sub> O <sub>3</sub> (%)	CaO (%)	MgO (%)	Na <sub>2</sub> O (%)	K <sub>2</sub> O (%)	P <sub>2</sub> O <sub>5</sub> (%)	LOI (%)	MnFe	RD



Geologist: Trudy Mudau

Page 6 of 8



# UNITED MANGANESE OF THE KALAHARI

## Detailed Assay Log

**Borehole: UEE034**

Farm: Rissik 330

Scale: 1:100  
Projection: Lo23  
Datum: Wgs84

X Surveyed: -3664.83

Y Surveyed: -3025089.66

Z Surveyed: 1082.017

Final depth: 153.40

End date: 2017/10/14

Geology		Minecut Sample Details				Fusion Assay Results										
Stratigraphy	Subzone	From	To	Sample	Mn (%)	Fe (%)	SiO <sub>2</sub> (%)	Al <sub>2</sub> O <sub>3</sub> (%)	CaO (%)	MgO (%)	Na <sub>2</sub> O (%)	K <sub>2</sub> O (%)	P <sub>2</sub> O <sub>5</sub> (%)	LOI (%)	MnFe	RD



Geologist: Trudy Mudau

Page 6 of 8





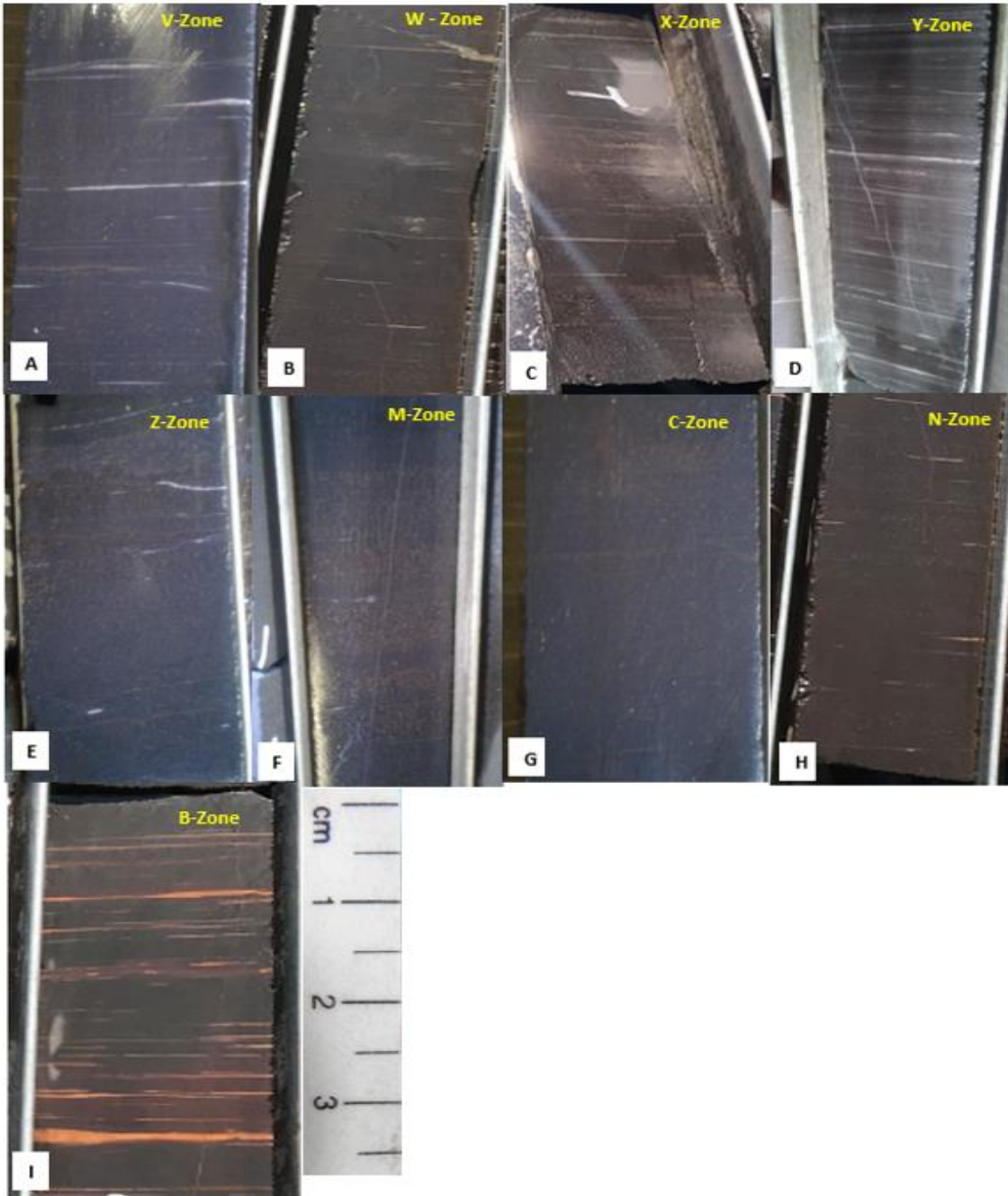


Figure 3.4 Different sub-zones that occur in the Lower Body of the Manganese ore. (a) V-Zone, banded braunite-lutite with small and large brown and white ooids. (b) W-Zone, banded braunite-lutite containing dominant irregularly shaped brown widely scattered carbonate ooids. (c) X-Zone, banded braunite-lutite with carbonate ooids of various sizes. The ooids are small, widely scattered at the top and closely spaced towards the base. (d) Y-Zone, braunite-lutite containing white and abundant brown laminae, thick lenticles and small oxide rich ooids. (e) Z-Zone, braunite-lutite containing white carbonate stringers and fine white and pink ooids. (f) M-Zone, braunite-lutite displaying ellipsoidal and irregularly shaped brownish oxide dominated ooids of various sizes. (g) C-Zone, braunite-lutite containing white and brownish oxidised ooids and very thin laminae. (h) N-Zone, braunite-lutite with microbands, fine pink ooids and stringers. (i) B-Zone, laminated brownish-black jacobsonite braunite-lutite containing brown carbonate laminae.

### 3.5 Ore genesis discussion

The formation of the Kalahari deposit is said to have taken place in cycles of transgression and regression, Tsikos et.al (1997). Previous studies suggest that this large-scale deposition of banded iron formation was attained by advection of anoxic  $\text{Fe}^{2+}$  saturated waters during the Paleoproterozoic in a layered ocean, through a chemocline zone and subsequent mixing of the water and moderately oxygenated silica-saturated surface waters. Tsikos et.al. (1997) agree with this model but say that it would be applicable to the Hotazel rocks provided that the ascending waters were also  $\text{Mn}^{2+}$  saturated. They further state that manganese was also concentrated given the condition that there were favourable redox conditions that allowed significant build-up of manganese concentrations over a long period. In 1997, Van der Merwe supported this by concluding that the Hotazel iron formation accumulated in a clastic free, stratified water body in which iron and silica were in solution below the redox boundary. His conclusion brings into picture the role played by the Eh and pH balances in precipitating the massive deposit.

Tsikos et.al.(1997) have mentioned the geologic attributes that further cast doubt on the volcanic exhalative origin by stating that;

- The Ongeluk lavas are not typical ophiolites that occur in the mid-ocean ridge, but are basaltic andesite flows of tholeiitic character overlying the continental basement.
- Most volcanogenic sedimentary Mn ores are hosted by radiolarian cherts, jaspers, and jaspilites that do not have much resemblance, both in chemical and mineralogical nature to the Hotazel banded iron formation.
- Volcanogenic sedimentary manganese deposits are naturally siliceous, with Si contents which can reach 40% in some deposits. This differs from the Kalahari ores which contain large amounts of carbonate content in the form of kutnahorite, manganiferous calcite ooids and laminations. The borehole used for this study, UEE034 (Fig. 3.3) has an average Si content in the whole lower body of 5.9% whereas the CaO average content is 17.7%. This is evidence supporting the marine origin of the ore. The abundance of carbonate content can also be seen in the carbonate structures visible to the naked eye that are present throughout the zones of the lower body discussed above.
- Volcanogenic sedimentary manganese deposits are said to occur in a form of small, discontinuous, and frequently uneconomic, lenticular bodies (Roy, 1981; Tsikos et.al., 1997), which is not the case with the voluminous Kalahari Mn ores (Nel et.al., 1986; Tsikos et.al., 1997). This study supports the concept that the Mn ore in the United Manganese of Kalahari is continuous in nature and extends over a huge area, hence the locality of other mining operations in the vicinity (Fig. 3.5a).

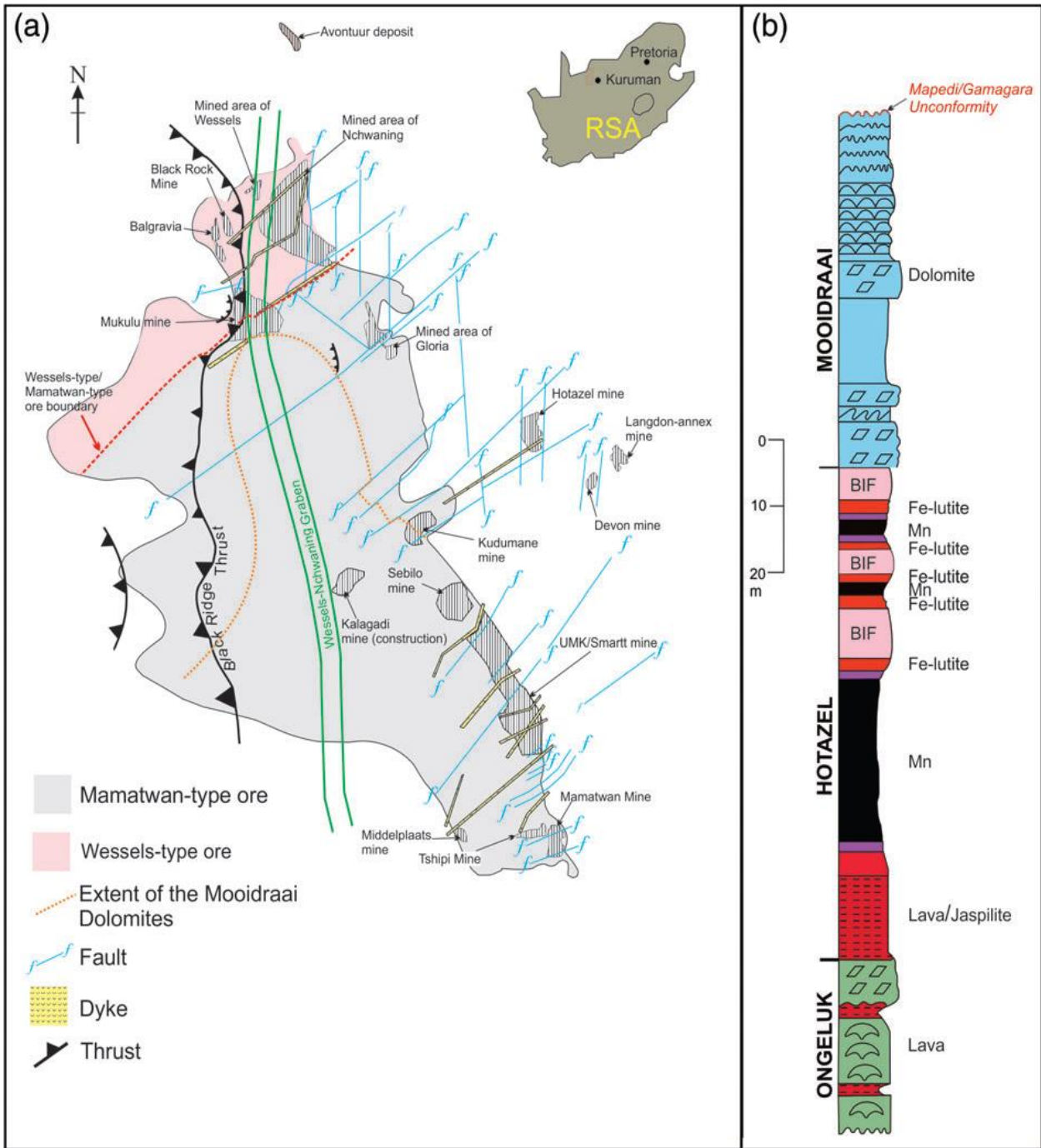


Figure 3.5 The Kalahari Manganese Field with all deposits (a) Structural map of the Kalahari Manganese Field in South Africa, illustrating the distribution of the various manganese mines in the area, including the low-grade Mamatwan mine in the south and the high-grade (after Vafeas et.al., 2018). (b) Lithostratigraphic profile of the Hotazel Formation indicating the three cycles of manganese deposition (Cairncross and Beukes, 2013).

### 3.6 Conclusion

The dipping structure and the increase in depth of recovery of the ore from the east to the west is evidence that the manganese ore was deposited in a basin-like structure, hence the term 'Kalahari basin'. The Kalahari Formation unconformably covers the Hotazel Formation in the east, although the Kalahari is independent of the Hotazel Formation and has no bearing on its genesis. These Cenozoic sediments have, however, played a role due to their porous nature that allowed percolation of fluids that leached carbonates out of the Mn ore and led to the supergene enrichment of the Kalahari deposit.

It is also noted that structural events played a crucial role in the upgrading of the primarily uneconomic ore. The Black Ridge thrust fault as discussed in section 3.2 is the major event that resulted in the upgrading of the now Wessels-type ore. The Mamatwan ore was also upgraded, but not to the extent of the Wessels ore. To date, boreholes drilled close to structures, often bear high-grade Mn ore and elevated sulphur content.

The alternating banded layers of manganese and BIF show non-clastic cycles of precipitation and deposition. It was indicated that volcanogenic sedimentary ores usually occur as small, discontinuous and often uneconomic bodies, contrary to the Kalahari deposit, which is massive and continuous over a huge area, making it a non-clastic sea water sedimentary deposit. The low Si and high CaO content observed in the boreholes used for this study, especially UEE034, supports the observations made by Tsikos et.al. (1997), that this deposit is a pure chemical precipitation controlled by various environmental parameters and enhanced by volcanic activities nearby. Thus, the Kalahari deposit originated from upwelling waters that were concentrated in Fe and Mn. The redox boundary increased the concentration and ultimately led to the precipitation iron and manganese rich deposit.

## CHAPTER 4

### ANALYTICAL METHODS

#### 4.1 Introduction

Rock chemistry is key to understanding the concentration of elements/compounds that make up the whole rock. Geochemical analysis is the process through which the economic value of the rock/ore/mineral is revealed. Analytical results thus guide decisions on exploration projects, test work in progress related to beneficiation and ultimately inform marketing decisions in already operating business operations. In Mn smelting operations in South Africa, bulk chemical assays are typically relied on to adhere to specifications of the furnace charge. (Steenkamp et.al, 2020)

Minerals have different chemical associations with unique properties and may be difficult to differentiate especially if they are assembled in one mineral or rock. Manganese ore is one with complex mineral assemblages that need careful consideration in selection of analytical techniques. Different techniques are designed for different element concentrations, whether in percentages (%) or parts per million (PPM).

Historically, chemical reactions were tested in the chemical labs and some of the methods included wet analytical chemistry. Wet analytical chemistry was done through a gravimetric method or volumetric method, also known as titration. With new innovations and technology, instrumental analytical techniques that are now widely used; XRF is used for analysing bulk solid material and trace elements, the ICP-MS technique is applied to trace elements that are measured in ppm, there are also techniques like chromatography and others that do quantitative analysis of water, gas and other volatile material.

The use of these instruments however does not completely make life easy as they require calibration always to eliminate false analytical results. Thus, chemists must always be aware of what they are analysing, the type of method most suited for the analyte and the calibration that goes with it.

Mining is a business and as a result always has to keep clients/manganese ore consumers satisfied through timeous delivery of guaranteed grade and size distribution. For this to occur, the grade and sizing of each product must be known before the product is dispatched to consumers, with the above said, size distribution tests and analytical results turn-around time should be at the rate at which ore is dispatched from the operation.

Analytical methods and preparation processes give different results for the same sample, this chapter aims to highlight the causes for differences in analytical results when using different analytical techniques.

## 4.2 Quantitative analytical methods

Before a sample is analysed, it is first dissolved into or converted into a desired form; soluble or insoluble. The conversion into the desired state is informed by a few factors, e.g. aim of the analysis, method to be used for the analyses, chemical properties of the samples also need to be considered (oxides, carbonates, sulphides, phosphates, sulphates and silicates). The selection of a proper method is important for correct analysis; there are two methods of preparing a sample or breaking it down before analysis, i.e. Wet method (gravimetric, volumetric and colorimetric) and dry method (borate fusion and pressed pellet). The selection of the sample preparation method depends mainly upon the analyte concentration, matrix, instrument operation conditions, costs and the environmental considerations (Badera, et.al, 2012).

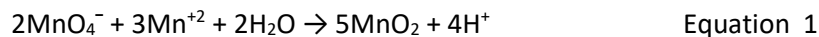
### 4.3 Wet methods

- Volumetric/Titration process

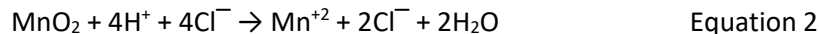
This method is basically the digestion of a sample with acid or acid mixtures to change the complex ore sample to simple chemical compounds. This process is further supplemented by heat and pressure which serve as catalysts to the rate of ore dissolution. There are two popular wet methods; gravimetric method and titrimetric method, also known as volumetric. The volumetric method is most applicable to manganese ore. The traditional titration of manganese is according to the Volhard manganese determination method. Manganese ore undergoes a decomposition reaction in concentrated hydrochloric acid (HCl), which results in a solution that is filtered to remove insoluble siliceous material. With the addition of HCl the solution is then heated until all the ore sample has dissolved. Adding zinc oxide emulsion to the solution increases its pH. After re-heating to about 80°C the solution is titrated against potassium permanganate standard solution. Iron is titrated based on the reduction of iron (III) [Fe<sup>3+</sup>] to iron (II) [Fe<sup>2+</sup>] in an acid medium against potassium dichromate standard solution. A small excess of tin (II) chloride (SnCl<sub>2</sub>) is added for the complete reduction of Fe<sup>3+</sup> to Fe<sup>2+</sup> and to prevent excess of SnCl<sub>2</sub> in the titration, mercury chloride is then added to neutralise the solution.

#### i. Titration of manganese from manganese ore

The stoichiometric reaction for the titration of Mn is as follows:



Concentrated HCl is added to the manganese ore. The solution then undergoes the following reaction:



Zinc oxide emulsion is added and the solution is heated to about 80 °C and titrated against potassium permanganate standard solution.

Procedure – a  $0.3000\text{g} \pm 0.0002$  powdered manganese ore was weighed into a weighing boat. The sample transferred into a clean 1000 ml Erlenmeyer flask. A 30 ml concentrated hydrochloric acid (HCl) was added into the sample. The sample boiled until pieces of manganese ore are no longer visible. A 50 ml of zinc oxide emulsion and 400 ml boiling water was added to the dissolved sample. The flask was placed back on the hotplate to a boiling point. The sample was titrated with standardised potassium permanganate ( $\text{KMnO}_4$ ). The flask mixed vigorously from side to side during titration. The final potassium permanganate was recorded for the calculation of the manganese percentage.



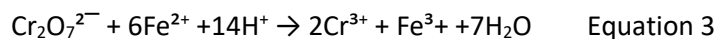
Figure 4.1 Manganese sample with zinc oxide emulsion



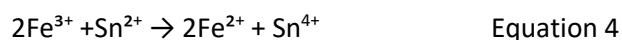
Figure 4.2 The endpoint of the Manganese Titration

## ii. Titration of Iron from manganese ore

The stoichiometric reaction for the titration of Fe against Potassium Dichromate ( $\text{K}_2\text{Cr}_2\text{O}_7$ ) occurs as follows:



The reduction of  $\text{Fe}^{3+}$  to  $\text{Fe}^{2+}$  with  $\text{SnCl}_2$ , which is represented as follows:



$\text{SnCl}_2$  is then neutralised with mercury chloride and the reaction is as follows:



Procedure -  $0.3000\text{g} \pm 0.0002\text{g}$  sample was accurately weighed into a 500 ml Erlenmeyer flask and 30 ml concentrated hydrochloric acid (HCl) was added to the sample and heated until the sample was dissolved. Stannous chloride was added to the solution drop by drop until the solution was decolourised. A 5 ml of mercuric chloride solution was added to the sample after cooling. The sample was stirred and left to stand for 2-3 minutes. The solution was diluted with cold water to  $\pm 200$  ml, 25 ml sulphuric acid was added and a few drops of Fe indicator. The sample was titrated with 0.04N potassium dichromate solution until the

purple colour becomes stable and the titration value recorded. The total iron content was calculated as follows: % Fe = titre value x 0.666666.

After analysis, it is mandatory for the method to be validated to ensure accuracy and precision. This ensures that the analyte is not over- or underestimated. There are statistical procedures used, which are done internally using single laboratory techniques, and there are also techniques applied using the inter-laboratory comparison. The final goal of the validation of an analytical method is to ensure that every future measurement in routine analysis will be close enough to the unknown true value for the content of the analyte in the sample. Accordingly, the objectives of validation are not simply to obtain estimates of trueness or bias and precision, but also to evaluate those risks that can be expressed by the measurement uncertainty associated with the result (González et.al, 2007). One of the techniques used internally by a single lab include accuracy – a certified reference material (CRM) is analysed and compared to the certificate true value. Another technique of validating the method is by inter-laboratory comparisons. The Kalahari inter-laboratory comparison scheme, also known as the round robin (Table 4.1 and 4.2), is used where 21 chemical laboratories participate. The Samples were prepared according to the prescribed sample preparation. The variation in the samples due to homogeneity was tested before distribution to the participating laboratory. The particle size was tested to determine the pulp of the samples and the sample pass the pulp criteria of 90% of the sample passing 75 µm sieve on the wet screen. The Analysis of Variance (ANOVA) was used to evaluate the parameters an analytical method during this validation phase, The ANOVA was computed using the Microsoft excel 2010 function. The participating laboratories used the test method that they believe was technically appropriate. Participating laboratory treated the samples in the same way as they would treat a routine sample. All laboratories stated the method used on the reporting templates. The results of the inter-laboratory test were compiled in the predetermined calculation sheet agreed by the scheme participants.

The z-scores represent a measure of how far a result is from the (consensus) assigned value. The statistics of a normal distribution means that 95 % of data points will lie between a z-score of –2 and +2. The z score is calculated using the following formula

Equation 6: The z-score calculation

$$z = \frac{x - \mu}{\sigma} \text{ Equation 6}$$

$x$  = sample score (actual value of analysis)

$\mu$  = the sample mean

$\sigma$  = the sample standard deviation

The basic performance categories

$|Z| \leq 2$  Satisfactory

$2 \leq |Z| \leq 3$  Questionable

$|Z| \geq 3$  Unsatisfactory

Table 4.1 Kalahari Round robin results

## Kalahari Manganese Round Robin Scheme



Manganese Ore Round Robin without outliers									Outliers - Calculated Z-Values							
SAMPLE M1L-8									Sep-19							
LAB ID	%Mn	%Fe	%SiO <sub>2</sub>	%CaO	%MgO	%Al <sub>2</sub> O <sub>3</sub>	%P	%LOI	LAB ID	%Mn	%Fe	%SiO <sub>2</sub>	%CaO	%MgO	%Al <sub>2</sub> O <sub>3</sub>	%P
1	38.34	4.57		14.96	3.25	0.190	0.019		1	0.28	0.42	-4.13	1.66	-1.48	-0.19	1.22
2	38.25	4.60	4.60	14.33	3.37	0.214	0.020	16.910	2	-0.20	0.77	0.00	-0.75	-0.03	1.12	2.04
3	38.00	4.43	4.50	14.51	3.26	0.217	0.017	16.430	3	-1.45	-1.22	-0.97	-0.06	-1.36	1.29	-0.41
4									4							
5	38.10	4.50	4.68	14.42	3.42	0.194	0.017	17.210	5	-0.97	-0.42	0.82	-0.42	0.60	0.00	-0.50
6	38.51								6	1.15	3.88					
7		4.71	4.57		3.49	0.180			7	-2.42	2.09	-0.26	3.39	1.43	-0.74	
8	38.32	4.55	4.46		3.37				8	0.20	0.22	-1.39	4.10	-0.03	7.35	7.74
9									9							
10									10							
11									11							
12	38.11	4.43	4.51	14.84	3.37	0.210	0.018	16.250	12	-0.89	-1.26	-0.87	1.20	-0.03	0.90	0.41
13									13							
14	37.98	4.46	4.72	15.14		0.186		16.632	14	-1.57	-0.90	1.29	2.37	3.10	-0.38	-3.78
15	38.27								15	-0.08	7.11					
16	38.39	4.54	4.70	14.54	3.44	0.180	0.017		16	0.54	0.06	1.07	0.05	0.82	-0.74	-0.41
17	38.60	4.60	4.66	14.73	3.49	0.190	0.019	16.970	17	1.61	0.77	0.66	0.78	1.43	-0.19	1.22
18	38.51	4.53	4.44	14.50		0.231			18	1.16	-0.06	-1.54	-0.11	4.89	2.02	-6.11
19	38.29	4.45	4.63	14.51	3.37	0.225	0.017	17.116	19	0.00	-1.08	0.31	-0.05	0.03	1.72	-0.53
20									20							
21									21							
Average:									Z  ≤ 2 Satisfactory							
Median:									2 ≤  Z  ≤ 3 Questionable							
Standard Deviation:									Z  ≥ 3 Unsatisfactory							
Upper Outlier Limit:									No results							
Lower Outlier Limit:																

Table 4.2 The below listed participants contributed to the round-robin: the labs are listed in alphabetical order

Lab name	%Mn	%Fe	%SiO <sub>2</sub>	%CaO	%MgO	%Al <sub>2</sub> O <sub>3</sub>	%P	%LOI
ABC Laboratories	WT-MT	WT-MT						
Alfred H. Knight South Africa	F-XRF	F-XRF	F-XRF	F-XRF	F-XRF	F-XRF	F-XRF	
Assmang Blackrock	WT-MT	WT-AT	PP-XRF	PP-XRF	PP-XRF	PP-XRF	PP-XRF	
Assmang Cato Ridge	WT-AT	WT-MT	PP-XRF	PP-XRF	PP-XRF	PP-XRF		
Intertek Commodities (Minerals Division)	F-XRF	F-XRF	F-XRF	F-XRF	F-XRF	F-XRF	F-XRF	IF
Intertek Commodities (Kathu)								
Kudumane	PP-XRF	PP-XRF	PP-XRF	PP-XRF	PP-XRF	PP-XRF	PP-XRF	
Metalloys								
Mineral Testing Company	WT-AT	WT-MT						
Mitra S.K	WT-MT	WT-MT	GRA	WT-MT	WT-MT	WT-MT	WT-MT	IF
SGS - Randfontein	F-XRF	F-XRF	F-XRF	F-XRF	F-XRF	F-XRF	F-XRF	GRA
SGS - UMK	F-XRF	F-XRF	F-XRF	F-XRF	F-XRF	F-XRF	F-XRF	IF
South32 HMM Mamatwan	F-XRF	F-XRF	F-XRF	F-XRF	F-XRF	PP-XRF	F-XRF	IF
South32 HMM Wessels	PP-XRF	PP-XRF	PP-XRF	PP-XRF	F-XRF	PP-XRF	PP-XRF	IF
Transalloys	WT-AT	ICP	GRA	ICP	ICP	ICP	ICP	
UIS	F-XRF	F-XRF	F-XRF	F-XRF	F-XRF	F-XRF	F-XRF	F-XRF

Table 4.3 The table below shows the different techniques used by the participants.

<b>Method Name</b>	<b>Abbreviation</b>
Wet chemical manual titration	WT- MT
Wet chemical autotitrator	WT- AT
Press Pellet X-ray Fluorescence	PP - XRF
Fusion X-ray Fluorescence	F - XRF
Inductive coupled plasma	ICP
Gravimetric	GRA
Ignition in furnace	IF

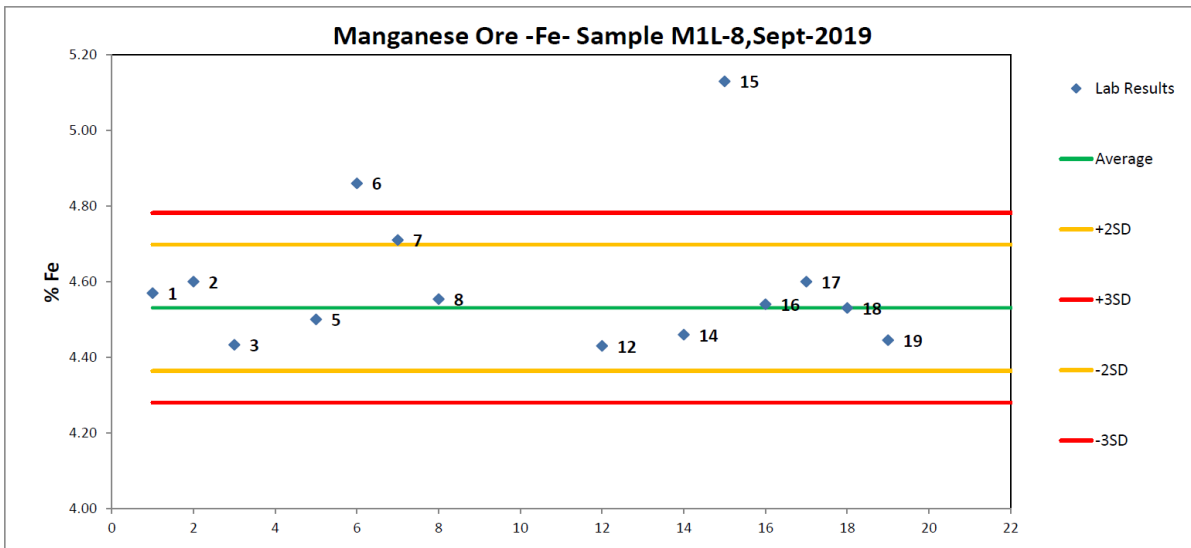
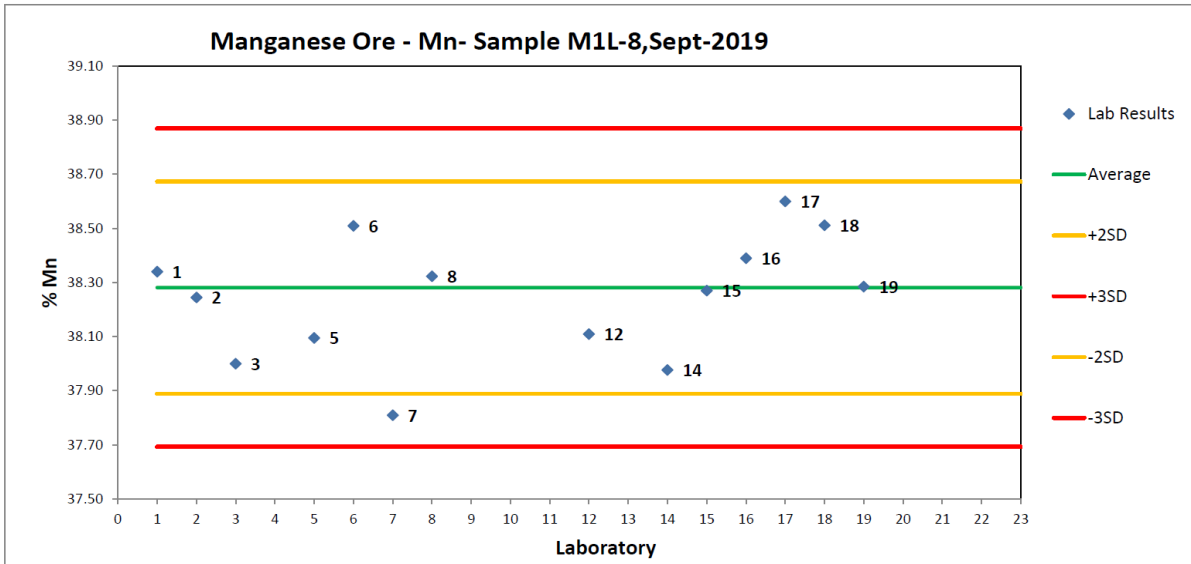


Figure 4.3 Graphical presentation of the round robin results for manganese and iron.

ABC labs is a company that owns a chemical laboratory situated in the Kuruman, this lab uses wet chemistry method for analysing manganese and iron ores. It is the only lab which applies the method in the whole of the Kalahari region in South Africa. They indicate that the downside of this wet analytical chemistry is that it can only determine Mn, Fe and loss on ignition (LOI). They also mention that an advantage to the method is that it achieves more accuracy than other methods that analyses oxides. An exercise to check the above statement was undertaken, results are discussed in section 4.6. The inductively coupled plasma mass spectrometry (ICP/MS) method will need to be applied to determine trace elements. This method makes use of hazardous chemicals and with the change in safety protocol

requirements from the country's Department of Mineral Resources (DMR) and introduction to the new XRF technology, mines have moved to a safer way of analysing samples. It is important to note that there are many quality check points of the product, in and outside the operation, from exploration drilling, grade control during mining through blast hole sampling, plant reconciliation during processing/crushing, consignment when the product is dispatched to the ports. In the ports, there are sampling and analytical processes that are also done, the receiver also does quality checks. The most important steps are at the mine, the port/harbour and the receiver at the final destination, which is the client. Most of the manganese ore is exported to China as the biggest steel industry and also one of the biggest manganese consuming countries. It is important for the three entities to use similar methods of analysis in order to avoid discrepancies in their results and ultimately for the company to incur hefty penalties.

#### 4.4 Dry methods

- Fused bead/Fusion method

The dissolution in dry methods is done through mixing the sample with a fusion mixture, in this case, flux. The most applicable reagent of oxides in dry methods is an acid flux. To achieve a fused bead, 1g of sample and 1g of reagent which is the flux (lithium borate salts) are put together and thoroughly mixed using a glass rod. This mixture is then transferred to a platinum crucible. The crucible is then placed in a furnace where the mixture is molten at 950-1050°C and transferred to platinum containers, forming fused beads. These are left to cool down and are ready to go for XRF analysis (Fig. 4.2)

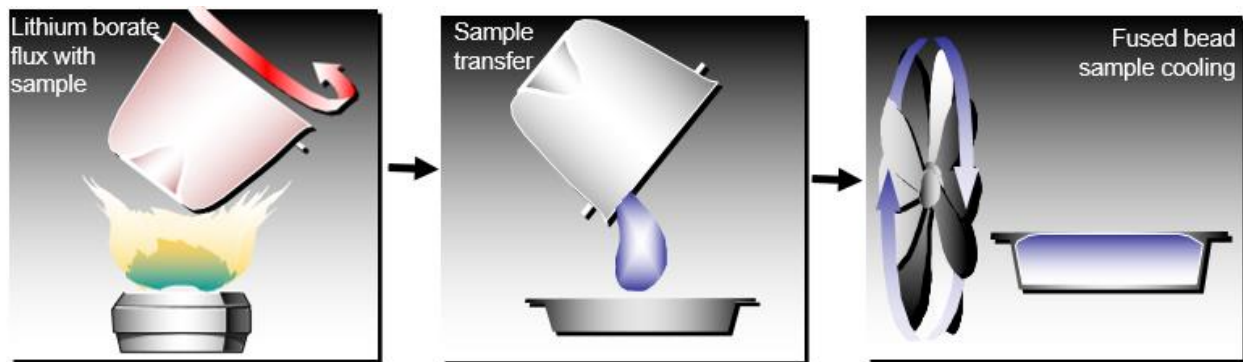


Figure 4.2 Sample preparation for analysis through the fusion process (internal paper)

Through this process, all elements are transformed into oxides and also have the same matrix of the borate glass and the final result is a homogenous and perfectly flat glass specimen, as displayed in Fig. 4.4). The homogeneity of the samples brings about flexibility and ease in using standards. The fusion machine is now automated and as a result, the preparation is quite straight forward, not labour intensive and doesn't require skilled operators. This pre-analysis method is popular in manganese mines because it doesn't expose lab personnel to safety hazards similar to those in wet chemistry, setting up a fusion lab also has a lower cost than that of a wet chemistry analytical lab.

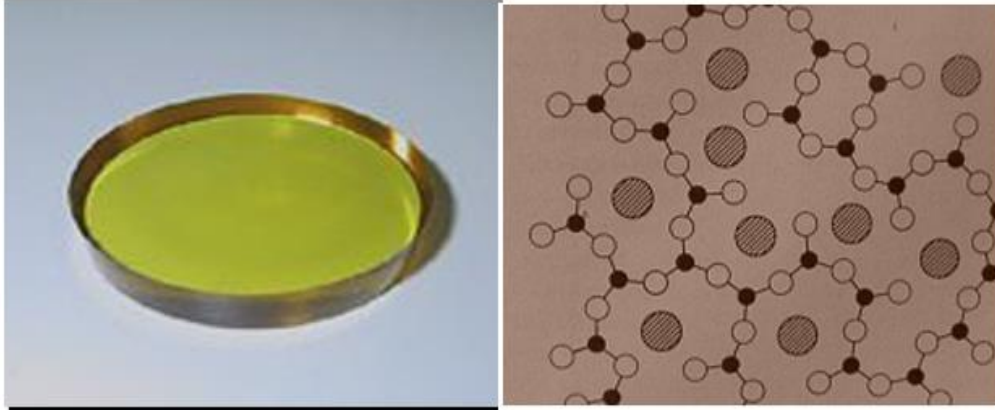


Figure 4.5 Fused bead specimen before going into the XRF machine (left) and the view of chemical compounds after the fusion process (right). All elements are converted to oxides. (internal paper)

- Pressed pellet method

The pressed pellet is achieved through crushing the ore sample to sizes close to 70 $\mu$ m. It is without doubt that the 70 $\mu$ m produces fine dust, this process is called pulverising. The finely crushed sample is then transferred into a ring and pressed to attain one consolidated sample in a mill (Fig. 4.6). Once pressed, the sample is then transferred to an XRF machine for chemical analysis.

The mineralogy in the ore affects the particle size of the minerals in the pressed pellet. Minerals with a higher compressive strength break down slower than softer minerals during pulverising of the sample. Therefore, during the pressing of the pellet, the minerals are not homogeneously distributed throughout because the size and shape of the particles are different, and the flatness of the surface is not guaranteed.

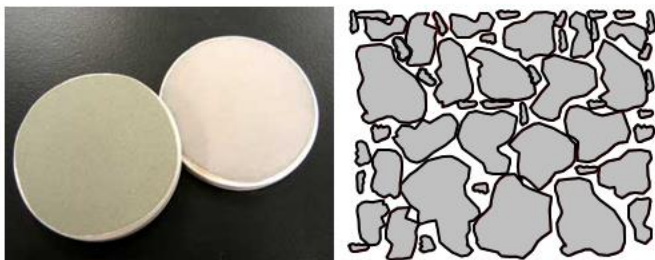


Figure 4.6 Pressed pellets in rings (left) and an enlarged view of the surface texture after pulverising (internal paper)

This problem is effectively eliminated with the fused bead method, as a more homogeneously distributed sample can be created from a liquid.

- Fusion method

The fusion process includes weighing, determination of the moisture content, pulverising and loss on ignition (LOI).

Upon receipt of sample, the sample was placed on a scale to measure the mass, 150g was the desired mass of the sample. The sample was sent for moisture content determination, this was done by weighing the sample on a porcelain crucible to get the wet mass. After getting the wet mass it was placed in the oven to dry for 2hrs at 106°C. The sample was left to cool for 15minutes and later placed on a scale again to determine and record the dry mass. Moisture content determination was done using this formula;

$$\% \text{Moisture content} = \frac{\text{Wet mass} - \text{dry mass}}{\text{Wet mass}} \times 100$$

After moisture content determination, the sample was taken into a mill for pulverisation, this was done by placing the sample in a mill for 5 minutes. Once the sample was pulverised, it was transferred to a clean envelope for safe storage before LOI determination. LOI determination was done to extract all the volatiles by placing the sample in a furnace at 1050°C for 1hr. The sample was mixed with flux after LOI determination, at a 10:1 flux to sample ratio. The mixture is placed in the furnace at 900°C, the furnace process is automated. Once the furnace full cycle is completed, the fusion beads were formed during the cooling process and ready for analysis.

#### 4.5 Sample analysis

- XRF (Fig 4.7)

The first commercial XRF instruments were introduced to the market about 50 years ago. They were the wavelength dispersive X ray fluorescence (WDXRF) spectrometers utilising Bragg's law and reflection on crystal lattices for sequential elemental analysis of sample composition. The advances made in radiation detector technology, especially the introduction of semiconductor detectors, improvements in signal processing electronics, availability and exponential growth of the personal computer market led to invention of the energy dispersive X ray fluorescence (EDXRF) technique (Wegrzynek, 2004). The XRF technique uses high-energy X-ray photons from an X-ray generation analyser to excite secondary fluorescence characteristic X-rays from samples. The characteristic line spectra emitted by the different elements of sample are detected in an analyser. The intensity of each line mirrors the concentration of individual elements, the higher the concentration the higher the intensity.

X-ray fluorescence (XRF) is the emission of characteristic "secondary" (or fluorescent) X-rays from a material that has been excited by bombarding with high-energy X-rays or gamma rays. When materials are exposed to short-wavelength X-rays or to gamma rays, ionisation of their component atoms may take place. Ionisation consists of the ejection of one or more electrons from the atom, and may occur if the atom is exposed to radiation with energy greater than its ionisation potential. X-rays and gamma rays can be energetic enough to expel tightly held electrons from the inner orbitals of the atom. The removal of an

electron in this way makes the electronic structure of the atom unstable, and electrons in higher orbitals "fall" into the lower orbital to fill the hole left behind. In falling, energy is released in the form of a photon, the energy of which is equal to the energy difference of the two orbitals involved. Thus, the material emits radiation, which has energy characteristic of the atoms present. Pressed pellet and fusion prepare samples are analysed using this technique. Krusberski (2010) has compared the two preparation techniques and tabled the advantages and disadvantages of the different preparation techniques (Table 4.4)

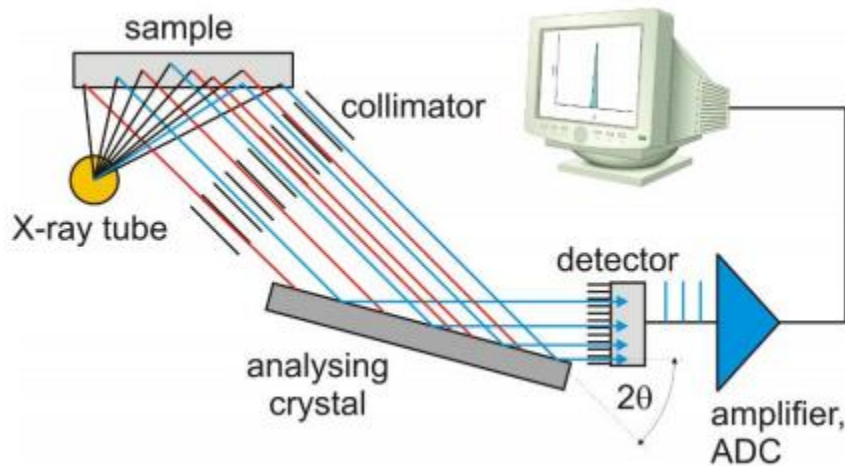


Figure 4.7 Schematic diagram of a wavelength dispersive X-ray fluorescence spectrometer (Wegrzynek, 2004)

The 4<sup>th</sup> industrial revolution (4IR) is fast becoming a reality. Hand held XRF machines, conveyor belt XRF machines and portable in-pit XRF analysers have been introduced. These do not need any sample preparation. The reliability of some of these devices are still being investigated.

Table 4.4 Comparison of sample preparation techniques (Krusberski, 2010 – SA institute of mining and Metallurgy – Analytical Challenges in Metallurgy)

SAMPLE PREPARATION TECHNIQUE	ADVANTAGES	DISADVANTAGES
<b>PRESSED POWDER PELLETT</b>	Short preparation time - <15 minutes per sample	18g of sample required for a 20g pellet
	Suitable for trace element analysis	Particle size effects
	Shorter analysis time than fused bead can be achieved.	Mineralogical matrix effects
	Ideal for production environment	Surface roughness - analytical surface must have mirror surface
	Cost effective - minimal sample preparation equipment, consumables and personnel required	Segregation problems
		Preferential orientation
		Hydration of pellets in humid atmosphere
<b>FUSION BEAD</b>		Cross contamination between pellets from dye set when pelletising or from loading in same cassettes, may occur when using XRF autoloader
	No particle size effects	Longer preparation time required - up to 30 minutes per sample
	No mineralogical effects	Platinum ware (i.e. Crucibles and moulds) expensive
	Homogeneous solid (glass) formed	Presence of metallics or sulphides in sample can damage platinum ware
	In-house standards may be prepared	Analytical surface of bead may be affected by the condition of the mould
	Only 1g of sample required for a bead	Sample: flux ratio critical
		Crystallisation of beads can occur

#### 4.6 Results and discussions

Samples from two boreholes (UEE034 and UEE022) boreholes were taken for analysis. They were analysed using both methods, XRF after fusion preparation and wet chemistry.

The student T test was used to determine if there is any difference between the analysed CRM and the true value of the CRM, the test was to see if the mean of the differences between the CRM analysis and the true value of the CRM deviates significantly from zero or not. Analysis of 3 CRMs was done and the interpretation was done in terms of 95% confidence level. All 3 CRMs were within the acceptable range and hence the method accuracy was acceptable.

Equation 7: T test

$H_0: \mu_d = 0$  null hypothesis

$H_1: \mu_d \neq 0$  alternate hypothesis

Equation 8

$$t_{cal} = \frac{|d-0|}{\frac{s}{\sqrt{n}}}$$

n = degrees of freedom

d = mean of differences within each pair of data

s = standard deviation

Table 4.5 Certified Reference Material (CRM) test

CRM Name	Wet chemistry results		CRM True value		Mean recovery (actual results/CRM true value)	
	%Mn	%Fe	%Mn	%Fe	%Mn	%Fe
<b>SARM 135</b>	43.00	16.10	42.50	16.60	101.18	96.99
<b>SARM 17</b>	38.78	4.28	38.81	4.27	99.92	100.30
<b>AMIS 407</b>	36.18	4.14	36.25	4.22	99.81	98.10

Table 4.6 Mn t-Test: Paired two sample for Means

t-Test: Paired Two Sample for Means		
	Variable 1	Variable 2
Mean	39.31933	47.11765
Variance	11.84788	8.1743
Observations	3	3
Pearson Correlation	0.929933	
Hypothesised Mean Difference	0	
df	2	
t Stat	13.91823	
P(T<=t) one-tail	0.002561	
t Critical one-tail	2.919986	
P(T<=t) two-tail	0.005123	
t Critical two-tail	4.302653	

Table 4.7 Fe t-Test: Paired two sample for Means

t-Test: Paired Two Sample for Means		
	Variable 1	Variable 2
Mean	8.1743	8.363333333
Variance	47.11764547	50.88263333
Observations	3	3
Pearson Correlation	0.999976164	
Hypothesised Mean Difference	0	
df	2	
t Stat	-1.198087989	
P(T<=t) one-tail	0.176801657	
t Critical one-tail	2.91998558	
P(T<=t) two-tail	0.353603314	
t Critical two-tail	4.30265273	

The calculated t values of all elements are lower than the critical value, as indicated in Tables 4.6 and 4.7. The null hypothesis that wet chemistry methods do not differ significantly was accepted. It was concluded that the wet chemistry method does not give significant differences with the results of the CRM true values. The final results obtained are in correlation with the certified values

Accuracy test procedure - 10 replicates of CRM were prepared and analysed using wet chemistry. The mean, standard deviation, RSD were calculated for each sample analysed.

Acceptance criteria – T test was used to determine whether the mean of a set of results obtained from the analysis of a certified reference material (CRM) is significantly different from a certified value of the material.

Table 4.8 Accuracy test results using 10 replicates of CRM (AMIS 407) samples for both Mn and Fe

	Name	Mn	Fe
1	AMIS 407-1	36.11	3.88
2	AMIS 407-2	35.77	4.21
3	AMIS 407-3	36.58	4.66
4	AMIS 407-4	36.68	4.46
5	AMIS 407-5	36.38	3.88
6	AMIS 407-6	36.30	4.13
7	AMIS 407-7	36.21	4.24
8	AMIS 407-8	36.50	4.19
9	AMIS 407-9	36.48	4.28
10	AMIS 407-10	36.50	4.39
	<b>Mean</b>	36.35	4.23
	<b>SD</b>	0.2655	0.2416
	<b>RSD</b>	0.7305	5.7099
	<b>True Value</b>	36.25	4.22
	<b>Tcalc</b>	1.15	0.14
	<b>Tcrit</b>	2.262	2.262
	<b>Comment</b>	Tcalc < Tcrit	Tcalc < Tcrit
	<b>Uncertainty</b>	0.0840	0.0764

The mean of a set of results obtained from the analysis of a certified reference material (CRM) is not significantly different from a certified value of the material therefore the method is accurate. (Table 4.8)

#### Linear regression line

Linearity indicates the ability of a method to produce the test results proportional to the concentration of the analyte within a given working range. The object of regression is to establish the relationship in terms of a mathematical equation;

Equation for a straight line is:  $y = bx + a$

$y$  = intensity (signal output) e.g. absorption intensity;

$b$  = gradient or slope of the line ( $y/x$ )

$x$  = the unknown sample concentration

$a$  = intercept on the  $y$ -axis

Table 4.9 Mn regression statistics showing relationship between the variables

Regression Statistics								
Multiple R	0.99850							
R Square	0.99700							
Adjusted R Square	0.99676							
Standard Error	0.4188							
Observations	15.0000							
ANOVA								
	df	SS	MS	F	Significance F			
Regression	1	756.6	756.6	4313	8.77359E-18			
Residual	13	2.3	0.2					
Total	14	758.9						
	Coefficients	Standard Error	t Stat	P-value	Lower 95%	Upper 95%	Lower 95.0%	Upper 95.0%
Intercept	0.1258	0.4847	0.2596	0.7992	-0.9212	1.1729	-0.9212	1.1729
X Variable 1	0.9945	0.0151	65.6744	0.0000	0.9618	1.0272	0.9618	1.0272

Regression value = 0.9985

Standard error = 0.42

Number of standards analysed = 15

F-test for Significance of linearity

$F_{calc} > 4313$

$F_{crit} = 2.484$

Since  $F_{calc} > F_{crit}$ , linearity/regression is proven to be significant

T-test for Significance of linearity

$H_0$  ( $r = 0$ ) and there's no linear relation between x and y

$H_1$  ( $r > 0$ ) and there's a significant linearity

Two Tailed Test

$t_{calc} = \frac{r}{\sqrt{(1-r^2)}} = 65.674$

$t_{calc} = 65.674$

$t_{crit} = 2.145$

$t_{calc} > t_{crit}$ , therefore reject  $H_0$  and it points out to a significant linearity.

$t_{calc} > t_{crit}$  then there is significant linearity

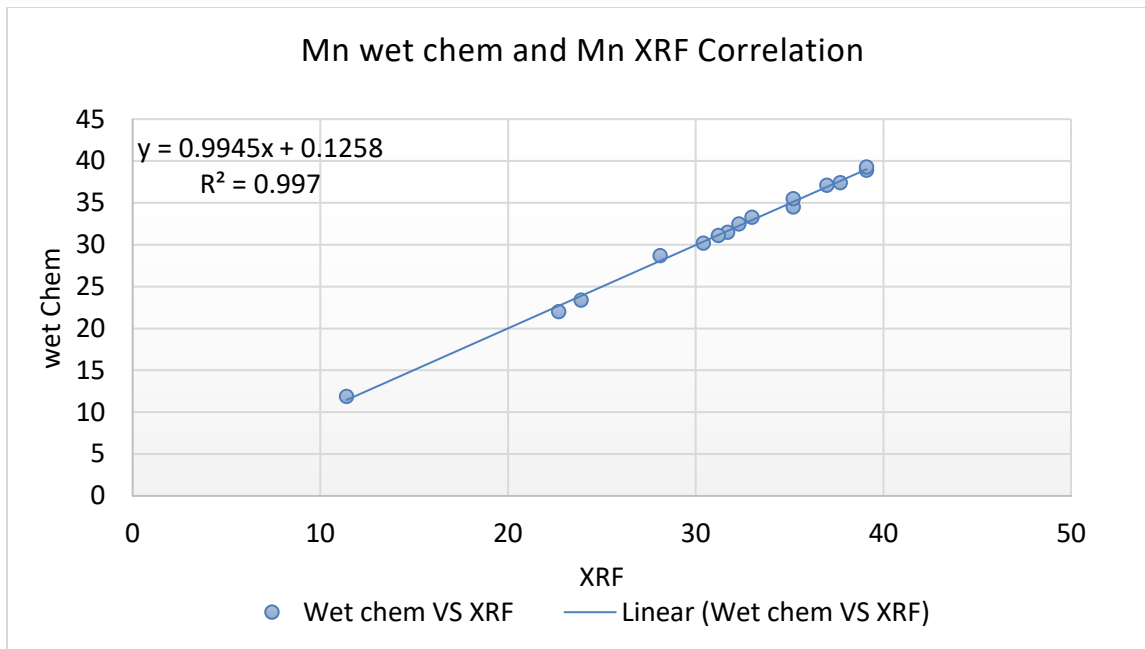


Figure 4.8 Comparison of Mn between wet chemistry and RXF method correlation

Table 4.10 Fe regression statistics showing relationship between the variables

Regression Statistics								
Multiple R	0.9821							
R Square	0.9646							
Adjusted R Square	0.9619							
Standard Error	0.2302							
Observations	15							
ANOVA								
	df	SS	MS	F	Significance F			
Regression	1	18.8	18.8	354.2	8.16588E-11			
Residual	13	0.7	0.1					
Total	14	19.5						
	Coefficients	Standard Error	t Stat	P-value	Lower 95%	Upper 95%	Lower 95.0%	Upper 95.0%
Intercept	-0.062	0.283	-0.220	0.829	-0.674	0.549	-0.674	0.549
X Variable 1	1.030	0.055	18.821	0.000	0.911	1.148	0.911	1.148

Regression value = 0.9821

Random calibration uncertainty = 0.23

Number of standards analysed = 15

F-test for Significance of Linearity

$F_{calc} > 354$

$F_{crit} = 2.484$

Since  $F_{calc} > F_{crit}$ , linearity/regression is proven to be significant

T-test for Significance of linearity

$H_0$  ( $r = 0$ ) and there's no linear relation between x and y

$H_1$  ( $r > 0$ ) and there's a significant linearity

Two Tailed Test

$$t_{\text{calc}} = \frac{r}{\sqrt{\frac{1-r^2}{n-2}}} = 18.821$$

$$t_{\text{calc}} = 18.821$$

$$t_{\text{crit}} = 2.145$$

$t_{\text{calc}} > t_{\text{crit}}$ , therefore reject  $H_0$  and it points out to a significant linearity.

$t_{\text{calc}} > t_{\text{crit}}$  then there is significant linearity

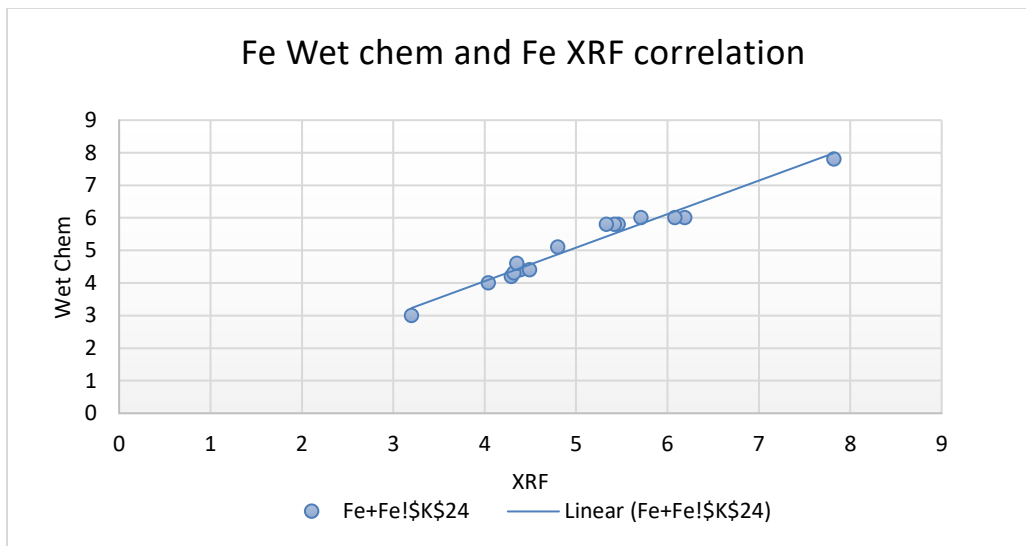


Figure 4.9 Comparison of Mn between wet chemistry and RXF method correlation

#### 4.7 Conclusions

Accurate determination of the chemical concentrations of ore is vital for the mining value chain in that it guarantees confidence from clients, good relationships, reputation and a possibility of higher market share. Accurate analysis depends on the following factors: knowledge of the chemical properties that make up the ore, knowing the reason and the need behind the analyses, preparation technique and choosing the correct method for analysing ore. Looking at the comparison done by Kruberski, (2010), both fusion bead and pressed pellets are unique and both are suitable for analysing manganese. For a low cost and time saving analytical exercise, pressed pellet is the best technique. For accurate results, fusion bead is the best of the two preparation techniques. Wet chemistry is yet another very suitable technique for manganese ore analysis, however it has got safety limitations that makes it unpopular in the mining industry and its stringent safety protocols. Boreholes used in this report were analysed using wet chemistry and XRF (fused bead). The results for both methods correlate. More can be done to enhance the wet chemistry process through automation.

## CHAPTER 5

### MANGANESE ECONOMICS AND THE FUTURE

#### 5.1 Introduction

Manganese ore is a crucial component in modern steelmaking processes as it consumes 94% of the manganese ore produced. As one of the most basic engineering metals, steel has got versatile applications and thus drives the demand for manganese ore. China is the biggest consumer of manganese ore due to its need for manganese processed products. High-grade ore is particularly valuable to producers of alloys, e.g., silico-manganese, ferro-manganese and refined ferro-manganese because it is proportionately more efficient than low-grade ore in the alloying process and there is no practical or satisfactory substitute that currently exists. Overall, it could be argued that, without Mn, the entire steel industry (based on the current physical-chemical properties of steel) would not exist and, as a result, the entire value of the steel industry – an estimated US\$ 964 billion to US\$ 1,446 billion in 2013 – is reliant on the continued supply of Mn (Postle et.al.2015). The market and demand for manganese fines is basically non-existent as steel producers have specific size requirements for products that would meet the requirements of their material handling and feeding systems, as well as process conditions themselves. In SiMn production casting alloy in a double-strand casting machine resulted in much less fines generated compared to layer casting (Bezember, 1995). Size determination tests are required to ensure low fines generation (<10% fines)

China has seen a rapid development since 2003 in the iron and steel industries, which resulted in a significant increase in demand for manganese as China could only supply 70% of its needs from domestic mines. The increase in demand resulted in importing of substantial amounts of ore to meet the new demand. As a result, China is highly dependent on foreign manganese ore supply, most of which is accounted for by South African manganese mines.

Product specifications provide a guideline to the manganese ore producers on required physical and chemical properties for the consumers. These product specifications, especially chemical composition, have changed over the years due to a decline in the ore which has a very high Mn content, especially in South Africa. Sintering was introduced more than 50 years after manganese mining started, to upgrade the low Mn content ore to the sought-after high-grade ore. According to their industrial destination, manganese ores are subdivided into metallurgical, chemical and battery grade. Metallurgical grade ore (chiefly for alloying steel and aluminium) must contain a minimum of 46% Mn. Manganiferous iron ore with 10–25% Mn is alternatively used in iron and steel production. Chemical and battery grade ores should have between 70 and 85% MnO<sub>2</sub> (Pohl, 2011).

The manganese mining industry plays a role in the South African economy and the world as a whole. The mining of Mn ore and production of Mn ferroalloys make significant economic and social contributions to national and regional economies where these activities take place (Postle, et.al.2015), however, with the

imminent 4IR, this will have an impact on required skill sets, mining technology for manganese exploration, mining, and ultimately processing. This chapter looks at the importance and uses of the manganese ore in different sectors, its impact in the manganese mining, processing and consuming communities and how the future for the mineral looks with the looming 4IR.

## 5.2 Manganese uses and applications

Manganese is a very important metal economically as it finds important applications in wide and varied industries (Fig. 5.1). Such importance of manganese contributes significantly to its annual demand and ultimately to the national and global economy. The major uses of manganese include: the steel and alloying industry, rechargeable battery Industry, water treatment, the minor but important use of manganese in the world economy includes: healthcare, electronics, agriculture and health care.

**Steel and alloying industry:** Steel is fundamental to the currently prevailing industrial economy and manganese is essential to steel production. It is the metal's ability to readily combine with sulphur and oxygen, which makes it critical in the production of steel. Manganese is also important as a non-ferrous alloying element. Manganese is used in the ferro alloying industry to produce steel with characteristics such as improved strength, durability and toughness. It is a vital component in steel making with no apparent substitute. It is defined by the United States Geological Survey (USGS) as a 'critical metal'.

**Rechargeable battery technology:** With the renewed focus on renewable energy, battery technology to power everything from electric vehicles to industries, has taken centre stage. The growth of electric vehicle production, for example, Tesla, has seen the demand for the metal rise significantly in recent years. Demand for batteries is growing at an exponential rate as global sales of electric vehicles are forecast to increase from 1.1 million in 2017 to 11 million in 2025. By the end of 2030, the increase in electric vehicles is expected to soar to a fleet of 30 million. While electric vehicles are commonly considered important for increasing battery demand, off grid power storage is also a crucial demand driver. As the increase in efforts to reduce pollution continues, countries are starting to turn to renewable electricity generation, of which the rechargeable battery technology is central.

**Water treatment:** Permanganate is an important chemical derivative of the manganese metal and one of its important applications is in wastewater treatment. It is used as an oxidising agent that removes organic pollutants from the wastewater as part of the treatment process before the water is returned to the environment. Permanganate is a stable solid chemical oxidising agent supplied as a dry powder. It is easy to package handle and store at the user's premises.

Other uses of manganese include the use as a black-brown pigment in paint and a decolouriser for iron-stained glass. Manganese sulphate is used to make a certain fungicide. Manganese (IV) oxide is used as a catalyst. Manganese sulphate is used to make a fungicide. Manganese (II) oxide is a powerful oxidising agent and is used in quantitative analysis.

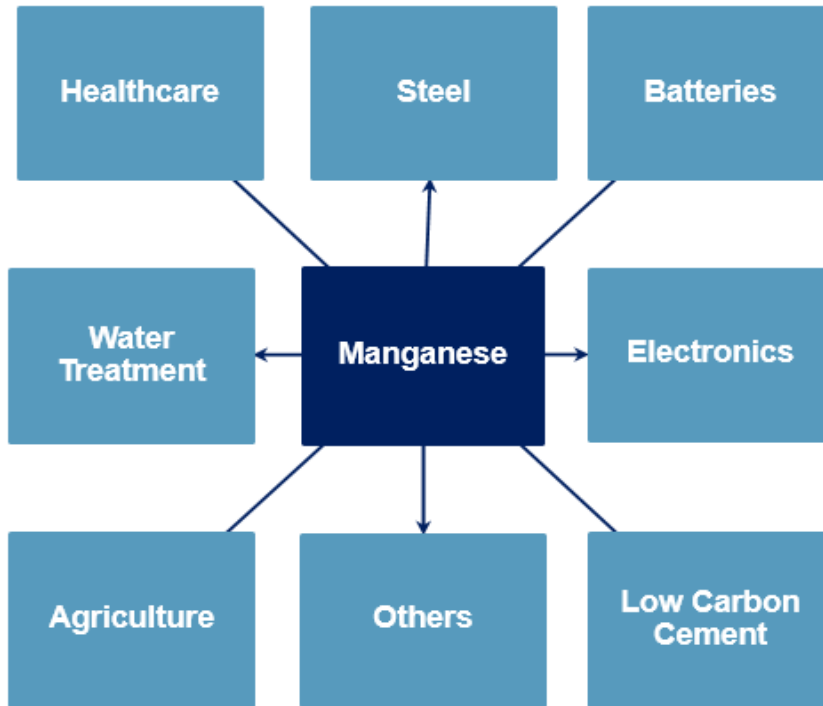


Figure 5.1 Manganese ore and the consuming sectors (Clarke and Upson 2017)

### 5.3 The fourth industrial revolution

The 4IR, a term coined by Klaus Schwab, founder and executive chairman of the World Economic Forum, describes a world where individuals move between digital domains and offline. (Table 5.1)

Table 5.1 Different revolutions showing the periods of revolution and major the changes (World Economic Forum)

## Navigating the next industrial revolution

Revolution	Year	Information
1	1784	Steam, water, mechanical production equipment
2	1870	Division of labour, electricity, mass production
3	1969	Electronics, IT, automated production
4	<b>?</b>	Cyber-physical systems

reality with the use of connected technology to enable and manage their lives (Miller 2015; Xu, et.al. 2018). These revolutions basically change through introducing better and faster ways of processing things.

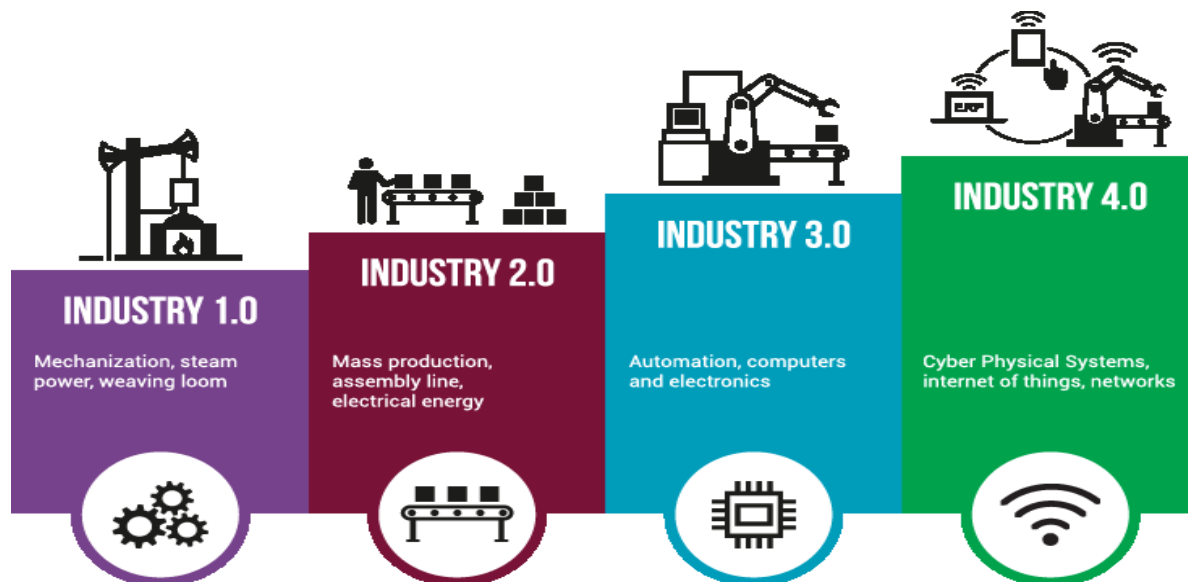


Figure 5.2 Highlights of industrial revolutions indicating the different characteristics and achievements.

Fig. 5.2 shows the main characteristics of the different industrial revolution stages and achievements. The first industrial revolution also known as the age of mechanical production, started in 1760 when the steam engine was invented during a period where life was centred around farming. This shifted the focus and gave way to urbanisation. Coal was the main energy to power trains and steamships as they became the main modes of transport. At this stage manganese was not yet in use, at least not to the extent it is being used currently.

The following second industrial revolution (age of science and mass production) was enabled by gasoline engines, airplanes and chemical fertilisers. These made things easier and faster. It is also in this period where manganese was introduced in the steel industry as an anticorrosion agent. The steel industry has since grown to this day. The third industrial revolution (the digital revolution) is where most processes were automated and functions were carried out by electronics and information technology. Analog devices (a television with antenna) moved to digital (internet connection and streaming live).

In the third industrial revolution, ore bodies are still mapped manually, using manually operated drill rigs for exploration, manual and geophysical wireline logging of samples. Coming to the 4IR which is a revolution that the world is currently transitioning to, the mining industry has been introduced to self-propelled drill rigs, drones which may ultimately be able to do field mapping in the near future, slope monitoring radars, automated and portable XRF geochemical analysers and a lot of other automated machinery. This revolution is characterised by green energy technologies and breakthroughs such as; artificial intelligence (AI), nanotechnology, biotechnology, quantum computing, blockchain, the Internet of Things (IoT) and 3D-printing. Fig. 5.3 depicts sectors in which manganese will be relevant, the required

volumes needed for consumption in these sectors are not known yet. There are advantages and disadvantages to the 4IR.

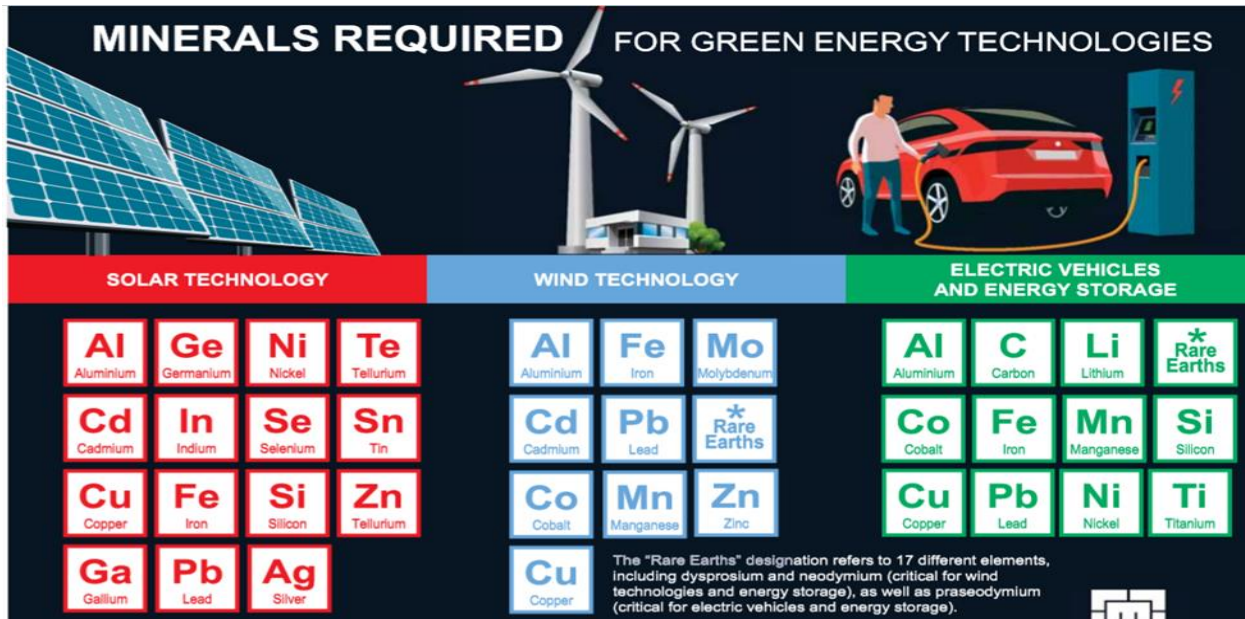


Figure 5.3 Elements required for green energy technologies as indicated by the Minerals Council South Africa. Manganese is relevant in the 4<sup>th</sup> industrial revolution and will be used in wind technology, electric vehicles and energy storage.

Some of the advantages will be: a cleaner environment – this will be due to the use of environmentally friendly processes that will emit less or no gas and less use of petroleum, which will ultimately lead to more hygienic and healthier working environments and reduction of occupational diseases faced in the mining industry today; increased productivity – production will be carried out with use of less resources; new skill sets – remote control and data analytics will be top of the required skill sets for the 4IR; inclusion of more women in the male dominated mining industry and people with disabilities as stated in section 2.4.6.1 of the mining charter – “a minimum of 1.5% employees with disabilities as a percentage of all employees, reflective of national or provincial demographics” (Mining Charter, 2018). Here we see the 4IR aiding in achieving the requirements as set out in the mining charter because the new skill sets will not require lot of physical strength.

There will, however, be disadvantages and these will range from loss of jobs – although there will be new skill sets, not everyone will adapt to the new skills. These skills will not require ordinary labour and capital but mainly new ideas and innovations, this may result in social tensions. Privacy – as it is today, our daily lives are starting to revolve around device connectivity from tracking e.g. body movement while running or exercising, and driving activities. With artificial intelligence, privacy may be a privilege, as a result, organisations will have to tighten up their data security and the government will have to change regulations to ensure safety and privacy of data.

## 5.4 Demand and supply

The main objective for any business is to supply the client with a service or a product. UMK mine is no different, however, the product specifications differ from one mine to the other, this is due to the demand, supply and clients' requirements.

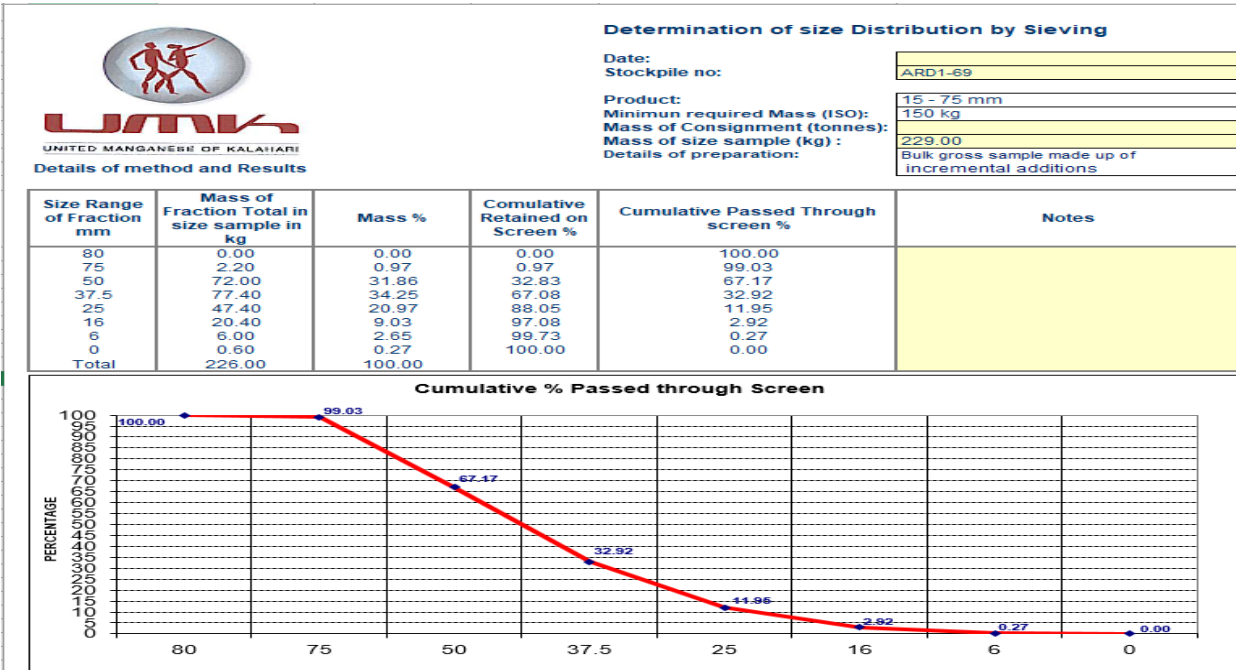
Table 5.2 depicts the typical UMK grade specifications of the saleable product (lower limit and upper unit). Samples with high Mn content typically produce more fines than the sample with lower Mn content

	<u>Mn</u>	<u>Fe</u>	<u>SiO2</u>	<u>CaO</u>	<u>Al2O3</u>	<u>P</u>	<u>MgO</u>
<b>SALES SPECIFICATIONS (LL)</b>	35.5	4.50	5.30	0.99	0.100	0.020	0.20
<b>SALES SPECIFICATIONS (UL)</b>	42.0	10.0	13.0	16.0	0.700	0.050	3.40

Manganese ore grade (Table 5.2) is not the only characteristic that deems the product saleable, sizing is another aspect to consider when marketing. UMK produces 3 different sizes: i.e. Fines - 0 x 6mm, chips - 6 x 15mm and lumpy 15 x 75mm. These sizes can however be changed depending on the client's requirements, by changing the setup of the screens on the processing plant, which is fairly an easy process. Of the 3 products, lumpy is the most saleable. It is important to note that the ore goes through a lot of breaking during the handling process, from blasting to loading, crushing, screening and ultimately dispatch, either by road or rail. By the time it reaches the destination, more fines are created, hence the need to analyse the sizing of the product before dispatch.

Hausmannite ore (Wessels-type ore), which bears higher Mn content is very brittle and easily gets broken during blasting because of its 2.98 t/m<sup>3</sup> in-situ density producing a lot of fines and chips, meaning that most fines and chips stockpile are of good grade. On the other hand, braunite ore, which is the Mamatwan-type ore with an in-situ density of 3.68 t/m<sup>3</sup>, requires more blasting energy to break than the Wessels-type ore and is the primary producer of the most saleable lumpy product, however the Mamatwan-type ore grades are marginal compared to the Wessels-type ore. To achieve good lumpy output, there should be a clear understanding of the different ore types, this may result in changing blast designs and possibly reduction of the amount of explosives used when it comes to the Wessels-type ore. It is also important to note that changing blast designs and reducing explosives will not only eliminate the output of fines, but reduce the fines footprint. Fines do not meet the specifications required by many manufacturers, and as a result, they are processed and agglomerated before they are sent to the market. To achieve a Lumpy saleable grade (required specifications) indicated in Table 5.3, both ores (Mamatwan and Wessels-type ore, and sometime hydrothermally-altered ore) are blended at a ratio. Blending plays an important role in making sure that the saleable product, e.g., lumpy ore is on grade/on spec with a low percentage of fines. Sizing determination or screening tests are done for every consignment that is dispatched to clients, either by rail or by road, to ensure that the shipped product is within required grade and sizing specifications. Lumpy product has a tolerance of about 5% fines and anything beyond that is a reject and may result in hefty penalties, chips and fines products also have a certain percentage of tolerance of the oversize material.

Table 5.3 Cumulative % of a lumpy product screen test. ARD 1-69



Five size determination tests were carried out for this specific sample ARD1-69 (Table 5.3 and 5.4). The sample was weighed and sifted 5 times through the different screen sizes from 0 to 80mm, and results were recorded as shown in Table 5.4. If the masses are accurate and there are no issues with the scale, the total percentage of the masses will add up to 100. There proved to be no errors in this test as all the masses added to 100%. It was found that 1.31% of the mass was lost during the vibration of the screen, this is expected, should there be a negative percentage, it would mean that the size determination test is biased. ARD1-69 test was good in that it did not show any biases and the product is within required size specifications.

Table 5.4 Size determination work sheet for a lumpy product (15x75mm)

Size Determination Work Sheet																
Data fields to be completed																
Size	Sheef Kg Empty	Test 1	Test 1 - Sheef Kg	Test 2	Test 2 - Sheef Kg	Test 3	Test 3 - Sheef Kg	Test 4	Test 4 - Sheef Kg	Test 5	Test 5 - Sheef Kg	Test 6	Test 6 - Sheef Kg	Total Test - Sheef Kg	% of Total	
80	11.00		0.00		0.00		0.00		0.00		0.00		0.00	0.00	0.00%	
75	6.40	7.20	0.80		0.00		0.00	7.80	1.40		0.00		0.00	2.20	0.97%	
50	6.40	19.40	13.00	19.80	13.40	21.20	14.80	17.40	11.00	26.20	19.80		0.00	72.00	31.86%	
37.5	6.60	22.60	16.00	20.40	13.80	21.60	15.00	20.80	14.20	25.00	18.40		0.00	77.40	34.25%	
25	6.80	16.40	9.60	16.80	10.00	16.00	9.20	17.20	10.40	15.00	8.20		0.00	47.40	20.97%	
16	7.20	11.40	4.20	13.00	5.80	9.20	2.00	12.20	5.00	10.60	3.40		0.00	20.40	9.03%	
6	6.80	8.00	1.20	8.80	2.00	7.00	0.20	8.40	1.60	7.80	1.00		0.00	6.00	2.65%	
0	5.60		0.00		0.00		0.00		0.00	6.20	0.60		0.00	0.60	0.27%	
														226.00	100.00%	

Before	229.00
After	226.00
Lost	3.00
% Lost	1.31%

Size	
80+	0.00%
75 - 80mm	0.97%
50 - 75mm	31.86%
37.5 - 50mm	34.25%
25 - 37.5mm	20.97%
16 - 25mm	9.03%
6 - 16mm	2.65%
0 - 6mm	0.27%

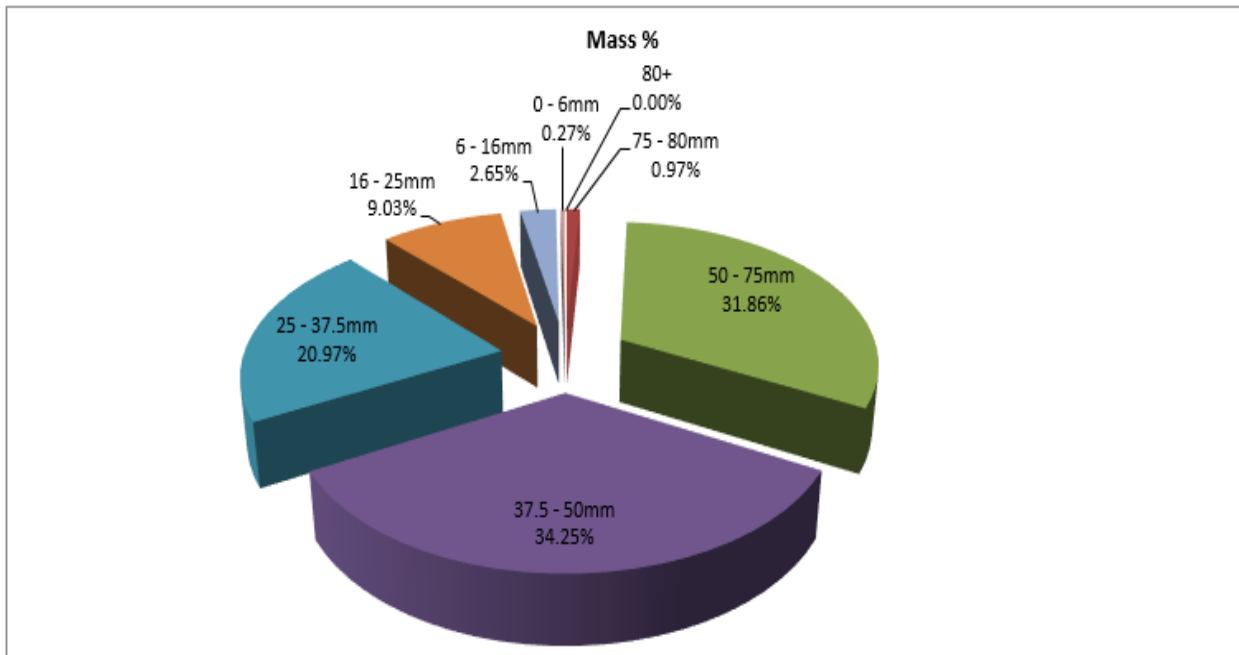


Figure 5.4 Mass distribution of the lumpy product screen tests for ARD1-69

For a fines sample which ranges from 0x6mm, the samples' masses are usually very low as shown in Table 5.5 and 5.6. The CV05 sample is only 7kg, as a result, only one test was carried out for this sample, contrary to lumpy samples. As observed in the lumpy tests, there is also a positive loss of material and the mass percentage adds up to 100%, this only shows that the process did not have any biases.

The screen test also shows that the consignment that the sample was taken from does not have any oversize material, thus the product meets the required specifications.

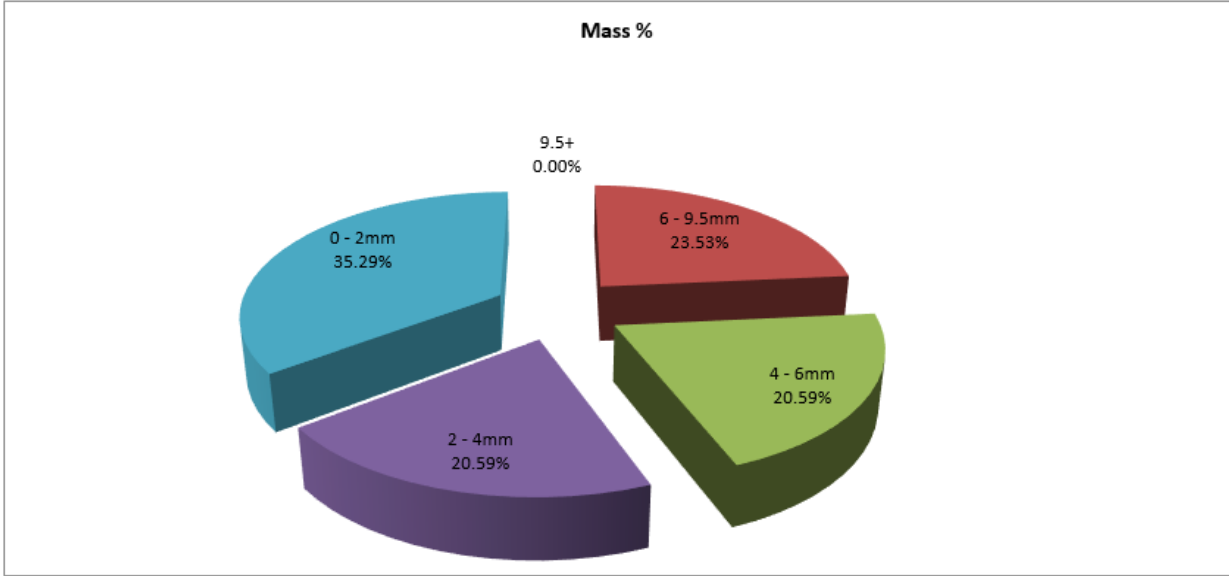


Figure 5.5 Mass distribution of the fines product screen tests for CV02

Table 5.5 A6 Cumulative % of a fines product screen tests for CV02



Details of method and Results

Determination of size Distribution by Sieving

Date:	
Stockpile no:	CV05 04:00-06:00AM
Product:	0 - 6 mm
Minimum required Mass (ISO):	3.72 kg
Mass of Consignment (tonnes):	
Mass of size sample (kg) :	7.00
Details of preparation:	Bulk gross sample made up of incremental additions

Size Range of Fraction mm	Mass of Fraction Total in size sample in kg	Mass %	Comulative Retained on Screen %	Cumulative Passed Through screen %	Notes
9.5	0.00	0.00	0.00	100.00	
6	1.60	23.53	23.53	76.47	
4	1.40	20.59	44.12	55.88	
2	1.40	20.59	64.71	35.29	
0	2.40	35.29	100.00	0.00	
Total	6.80	100.00			

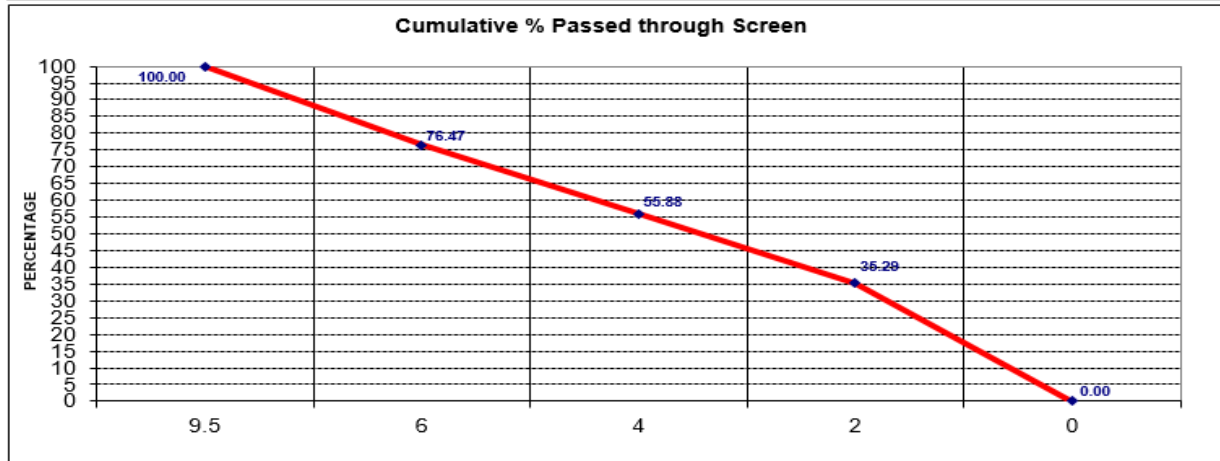


Table 5.6 Size determination work sheet for a fines product (0x6mm) for CV02

Size Determination Work Sheet															
Data fields to be completed															
Size	Sheef Kg Empty	Test 1	Test 1 - Sheef Kg	Test 2	Test 2 - Sheef Kg	Test 3	Test 3 - Sheef Kg	Test 4	Test 4 - Sheef Kg	Test 5	Test 5 - Sheef Kg	Test 6	Test 6 - Sheef Kg	Total Test - Sheef Kg	% of Total
9.5	6.80		0.00		0.00		0.00		0.00		0.00		0.00	0.00	0.00%
6	6.80	8.40	1.60		0.00		0.00		0.00		0.00		0.00	1.60	23.53%
4	7.00	8.40	1.40		0.00		0.00		0.00		0.00		0.00	1.40	20.59%
2	6.60	8.00	1.40		0.00		0.00		0.00		0.00		0.00	1.40	20.59%
0	5.60	8.00	2.40		0.00		0.00		0.00		0.00		0.00	2.40	35.29%
														6.80	100.00%

Before	7.00
After	6.80
Lost	0.20
% Lost	2.86%

Size	
9.5+	0.00%
6 - 9.5mm	23.53%
4 - 6mm	20.59%
2 - 4mm	20.59%
0 - 2mm	35.29%

Clients have different specifications of the manganese ore. There are always adjustments to the screening equipment and the manganese grade (this is achieved by blending different products), to fit the demand of each client.

On the global outlook of manganese, International Manganese Institute (IMnI) statistics for 2019 has indicated that the world's output of manganese ore increased in 2018 for the second consecutive year, on rising demand from manganese alloy smelters, reaching 20.3 million dry metric tonnes up by 6% from 2017, exceeding 2014 production of 19.3 million Mt and marking a new record high. Most of the supply came from South Africa, which has about 80% of the world's manganese reserve. Other countries with substantial reserves are Australia, China, Gabon and Ukraine. The steel industry is the biggest driver for manganese and iron ore production, with over 94% of manganese and 98% of iron ore produced worldwide being used in steel production. As a result, manganese market conditions are closely related to the steel industry. Because there is no suitable substitute for manganese in steel production, the manganese market mirrors the steel market conditions. An increase or growth in the steel industry has a positive impact on manganese demand and vice versa.

Legislation change has enabled fast growth of manganese production in that it created opportunities for new entrants (United Manganese of Kalahari, Kalagadi Manganese Mine, Kudumane Manganese Resources, Tshipi Ntle, Sebilo Resources). There are many other companies undertaking exploration on the same deposit and that is accelerating the local economy and more jobs are being created. Depending on the location of the mine, the product outputs are not entirely uniform. Different blasting, crushing and screening techniques have to be applied to reach the required specifications.

China's drop in domestic supply and increase in imports, has supported the increase in manganese ore prices. The limited rail capacity, rising oil prices and increasing trucking cost have also required the increase in manganese ore prices. The manganese alloy sector is moving towards oversupply, ramping up of manganese supply that is expected, especially in South Africa, and increased stocks in China ports, are some of the factors that put pressure on manganese ore prices. It is without doubt that manganese plays a pivotal role in the steel industry and will maintain similar behaviour to that of steel production. Any oversupply impacts prices and as a result has a negative impact on mining operations whereby production slows down and the whole mine planning process changes. Supply is also affected by transport allocation, the Transnet Freight Rails (TFR) is not so efficient when it comes to train allocations. The ports are operated by Transnet Port Terminals (TPT). Key role players should consider working together in ensuring a balance in ore supply to prevent oversupply, this way they will be able to have more control and flexibility around price fluctuations. Future supply may be a problem in the years to come, mines have to plan now on how they can sustainably supply and for longer periods and manage the price fluctuations. Supplying worldwide demand of metallic raw materials throughout the rest of this century may require 5–10 times the amount of metals contained in known ore deposits, this demand can be met only if mineral deposits containing the required masses of metals, in excess of present-day ore reserves, exist in the Earth's crust (Alberto and Pacino, 2016). Manganese may be exhausted by 2100 and this will be exhausted due to population increases, market conditions, lack of discovery of mega giant deposits and increase in affluence.

## 5.5 Conclusion

It is clear that manganese ore plays a pivotal role in the global society because it is used across a number of industries and at the moment there is no substitute for it. It is important to understand the client's needs and supply accordingly, this builds a good reputation of the organisation. Proper application and compliance to industry good practises in manganese or any other mineral processes (from exploration to load out) will save an organisation and may help the organisation to gain more market share of clients. Manganese ore demand will definitely rise in the near future to cater for the requirements in the growing steel industry. The African continent still has a lot of underdeveloped and developing countries, if the economies grow, there will be a lot of developments across a lot of industries, some of them being steel for construction and automotive industries. The demand for manganese will also grow due to the new 4IR where the mineral will be required in green energy technologies. Although supply will grow due to the number of new entrants that may start mining soon, the quality might not be as good as what is being sold at the moment, sintering will have to be considered to upgrade the ore. The supply will also be affected by the current power issues that South Africa is facing. Unreliable power supply from Eskom has a negative impact on mineral processing, this results in loss of production, train allocations and ultimately demurrage costs from clients, and this is detrimental to the organisation.

Manganese plays a very important role in the global economy, even if the dependence of various industry sectors, products and/or applications on it is not always recognised. It is a critical raw material input for the steel industry but also has a number of other important downstream uses which make a significant economic and social contribution to national and regional economies where these activities take place.

## CHAPTER 6

### SUMMARY AND CONCLUSIONS

Since discovery of manganese and its importance in the steel industry, it does not have a suitable substitute yet. As a result, it is still in demand and thus plays a pivotal role in the global economy. South Africa has the biggest deposit in the world but grapples with sustaining consistent power and transport allocations. The inconsistent power supply from Eskom has resulted in mines resorting to burning diesel as a source of power which in turn is not environmentally friendly and will cost the country heavily in future. Efficient and effective management of the power utility is needed to ensure consistent supply at a stable price.

From the three genetic models discussed in the historical background, this report supports the latest model as defined by Tsikos and Moore (1997) of pure chemical precipitation which places particular emphasis on various environmental parameters (sea-level fluctuations, climate change) involved in the deposition of iron and manganese minerals with volcanism acting either as a nearest (Beukes, 1983; Nel et al., 1986) or a remote (Tsikos and Moore, 1997) metalliferous source. It is significant that manganese was not economic until other factors came to play, and that is the structural events discussed in earlier chapters and the chemical reaction of the Kalahari Formation in the sub-outcrop. Although the Kalahari Formation and its minerals are not indicators of the presence of manganese ore, its porous nature has had a significant economic impact on the ore due to movement of groundwater that leached carbonates out of the manganese layer. Where ore has been intersected at a shallow depth below the Kalahari, it is certain that the ore is of higher-grade. From the boreholes used in this study, it is interpreted that the Kalahari deposit is of sedimentary origin, deposited in shallow marine conditions controlled by different climatic conditions. The initial deposit was not of economic significance until structural events took place. Structures are the main drive behind the economic viability of the Kalahari deposit.

Accuracy tests are an important way of ensuring best outcome results to aid marketing and decision making in the business. Wet chemistry and XRF are best suited for manganese analysis, but more can be done during the 4IR to enhance the way in which the processes are carried out, with XRF having advanced from EDXRF to WDXRF over the years, it can also be done by an older method like wet chemistry to reduce or eliminate the safety and health hazards that come with it.

The use of manganese in the steel industry as an anticorrosion agent has made the growth directly proportional to that steel, with only two big mining companies being the sole producers of manganese ore in South Africa. The change in legislature has opened doors for new entrants and this has spiked the manganese supply. Government has a big role in influencing the mining industry positively or negatively, with that said, more measures must be put in place to ensure proper management of the power utility and rail allocation. We are prone to see an increase in demand of manganese with growth in the steel industry, especially with the need for robotics and green energy technologies in the 4IR. Although supply

will grow due to the number of new entrants that may start mining soon, the quality might not be as good as that currently being sold (35% to 38%), as a result, the cut off grades may need to be lowered to increase the reserve and sintering will have to be considered to upgrade the ore.

## REFERENCES

- Badera, N.R., Zimmermann, B. 2012. Sample preparation for atomic spectroscopic analysis: An overview. *Advances in Applied Science Research*, 3 (3): 1733-1737
- Bengtson, S., Rasmussen, B., Ivarsson, M., Muhling, J., Broman, C., Marone, F., Stampanoni, M., Bekker, A., 2017. Fungus-like mycelial fossils in 2.4-billion-year-old vesicular basalt. *Nature, ecology and evolution*, Vol 1, article number 0141.
- Beukes, N.J., 1983. Paleoenvironmental setting of iron formations in the depositional basin of the Transvaal Super group, South Africa. In: Trendall, A.F., and Morris, R.C. (eds). *Iron formations, facts and problems*, Elsevier, Amsterdam, p. 131-209.
- Beukes, N. J., and Smit, C. A., 1987. New evidence for thrust faulting in Griqualand West, South Africa: implications for stratigraphy and the age of red beds. *South African Journal of Geology*, 90, 378-394.
- Beukes, N.J., Swindell, E.P.W., Wabo, H., 2016. *Manganese Deposits of Africa*. DOI: 10.18814/epiiugs/2016/v39i2/95779
- Bezemer, K. 1995. The silicomanganese production process at Transalloys. *INFACON VII*. Trondheim, Norway, 11-14 June 1995, pp. 573–580.
- Bonga, M. W., 2006. An analysis of the impact of a third player on South Africa's Manganese industry. Directorate: mineral economics
- Caincross, B., Tsikos, H., Harris, C., 2000. Prehnite from the Kalahari manganese field, South Africa, and its possible implications. *South African Journal of Geology*, Vol 103, page 231-236.
- Chamber of Mines of South Africa., 2017. *Facts and Figures 2016*.
- Clarke, C., Upson, S., 2017. A global portrait of the manganese industry—A socioeconomic perspective. *Neurotoxicology*, Vol 58. Pg 173-179.
- Cornell, D.H., and Schütte, P. S.S., 1995. A volcanic-exhalative origin for the world's largest (Kalahari) Manganese field: *Mineral Deposita*, Vol. 30, p. 146-151.
- Cornell, D.H., and Schütte, P. S.S., 1995. The Ongeluk basaltic andesite formation in Griqualand West, South Africa: submarine alteration in a 2222 Ma Proterozoic sea. *Precambrian Research* 79 (1996) 101-123.
- Corathers, L. A., 2009. *Mineral Commodity Summaries 2009: Manganese*. United States Geological Survey
- De Villiers, J.E., 1983. The Manganese Deposits of Griqualand West, South Africa: Some Mineralogic Aspects. *Economic Geology* Vol. 78, p. 1108-1118.
- Douce, A.E.P., 2016. *Metallic Mineral Resources in the Twenty-First Century: II. Constraints on Future Supply*. *Natural Resources Research*, Vol.25, No.1.
- Englinton, B.M., 2006. Evolution of the Namaqua-Natal Belt, southern Africa – A geochronological and isotope geochemical review. *Journal of African earth sciences*, 46, p.93-111.
- Eriksson, P.G., Schweitzer, J.K., Bosch, P.J.A., Schreiber, U.M., Van Deventer, J.L., and Hatton, C.J., 1993. The Transvaal sequence an overview. *Journal of African earth sciences*, v.16, no1/2, p.25-51
- Frakes, L., and Bolton, B. (1992). Effects of ocean chemistry, sea level, and climate on the formation of primary sedimentary manganese ore deposits. *Economic Geology*, Vol. 87, p. 1207-1217.

- Ghazban, F., and Al-Aasm, I. S., 2010. Hydrocarbon-induced diagenetic Dolomite and Pyrite formation associated with the Hormoz Island salt dome, offshore Iran. *Journal of Petroleum Geology*, Vol. 33(2), April 2010, pp. 1 – 14
- Gajigo, O., Mutambatsere, E., Adjei, E., 2011. Manganese Industry Analysis: Implications for Project Finance. Working Paper No. 132.
- Gilbert, M.T., Barinov-Colligon, I., and Miksic, J. R., 1995. Cross-validation of bioanalytical methods between laboratories. *Journal of Pharmaceutical and Biomedical Analysis*, 13(4), 385-394.
- Gnos, E., Armbruster, T., and Villa, I. M., 2003. Norrishite,  $K(\text{Mn}_{23}\text{Li})\text{Si}_4\text{O}_{10}(\text{O})_2$ , an oxymica associated with sugilite from the Wessels Mine, South Africa: Crystal chemistry and  $^{40}\text{Ar}$ - $^{39}\text{Ar}$  dating. *American Mineralogist*, 88, 189–194.
- González, A.G., and Herrador, M. Á. (2007). A practical guide to analytical method validation, including measurement uncertainty and accuracy profiles. *TrAC Trends in Analytical Chemistry*, 26(3), 227-238.
- González, A. G., Herrador, M. Á., and Asuero, A. G. (2010). Intra-laboratory assessment of method accuracy (trueness and precision) by using validation standards. *Talanta*, 82(5), 1995-1998.
- Government Notices. 2018 – Broad based socio- economic empowerment charter for the mining and minerals industry, government gazette, 27 September 2018.
- Gutzmer, J., and Beukes, N. J. 1996. Mineral paragenesis of the Kalahari Manganese Field, South Africa. *Ore Geology Reviews*, 11, 405–428.
- Gutzmer, J., Beukes, N.J., 1997. Effects of mass transfer, compaction and secondary porosity on hydrothermal upgrading of Paleoproterozoic sedimentary manganese ore in the Kalahari Manganese Field, South Africa. *Mineralium Deposita*, Vol. 32, p. 250-256.
- Gutzmer, J., and Beukes, N.J., and Yeh, H.W., 1997. Metasomatic and supergene fault-controlled alteration of Early Proterozoic sedimentary manganese ore at Mamatwan Mine, Kalahari manganese field, South Africa. *South African Journal of Geology*, Vol.100, p. 53-71.
- Haddon, I.G., 2005. The sub-Kalahari geology and tectonic evolution of the Kalahari Basin. Johannesburg: University of the Witwatersrand. (PhD -Thesis) 343 p.
- Hey, M.H., 1972. Mineral analysis and analysts. *Mineralogical magazine*, vol. 39, pp" 4-24
- IMnI Statistics. 2018
- Hunt, A. M., and Speakman, R. J., 2015. Portable XRF analysis of archaeological sediments and ceramics. *Journal of Archaeological Science*, 53(1), 626- 638.
- Johnson, J.E., Webb, S.M., Ma, C., Fischer, W.W., 2015. Manganese mineralogy and diagenesis in the sedimentary rock record. *Geochimica et Cosmochimica Acta*, 173, 210–231.
- Kleyenstüber, A.S.E., 1984. The mineralogy of the manganese bearing Hotazel Formation of the Proterozoic Transvaal Sequence in Griqualand West, South Africa. *Transactions of the Geological Society of South Africa*, Vol. 87, p. 257-272.
- Krusberski, N., 2010. Exploring potential errors in XRF. The Southern African Institute of Mining and Metallurgy Analytical Challenges in Metallurgy
- Kuchera, E., Hafner, O., Drahos, P., 2019. Emerging Technologies for Industry 4.0: OPC Unified Architecture and Virtual / Mixed Reality. Faculty of Electrical Engineering and Information Technology Slovak University of Technology in Bratislava, Slovakia

- Kunzmann, M., Gutzmer, J., Beukes, N.J., Halverson, G.P., 2014. Depositional environment and lithostratigraphy of the paleoproterozoic Mooidraai formation, Kalahari manganese field, South Africa. *South African Journal of Geology*, Vol. 117.2 page 173-192
- Louw, L., 2018. Mining and the fourth revolution. McNeil, J.A., Cecil, E.F., X-ray Fluorescence Measurements of Manganese in Petroglyphs and Graffiti in the Bluff, Utah Area. Department of Physics Colorado School of Mines
- Nash, D.J., McLaren, S.J., 2003. Kalahari valley calcretes: their nature, origins, and environmental significance. *Quaternary International*, 111, 3-22.
- Nel, C.J., Beukes, N.J., and De Villiers., J.E., 1986. The Mamatwan manganese mine of the Kalahari manganese field, in Anhaeuser, C.R., and Maske, S., eds., *Mineral deposits of Southern Africa*: Johannesburg, Geological Society of South Africa, p.963-978.
- Pienaar, P.C., Smith, W.F.P., 1992. A Case Study of the Production of High-grade Manganese Sinter from Low-grade Mamatwan Manganese ore.
- Pohl, W., 2011. *Economic geology principles and practice: metals, minerals, coal and hydrocarbons-introduction to formation and sustainable exploitation of mineral deposits*. Wiley-Blackwell, p.479
- Postle, M., Nwaogu, T., Upson, S., Clark, C., Heinevetter, A., 2015. *Manganese, The Global Picture – A Socio Economic Assessment*, report for the International Manganese Institute, London, Norfolk, UK. RPA.
- Prisecaru, P., 2016. Challenges of the fourth industrial revolution. *Knowledge Horizons – Economics*. Volume 8, No. 1, pp. 57–62
- Puchner, R.A., 2002. *The Geology and Rock Mass Quality of the Cenozoic Kalahari Group, Nchwaning Mine Northern Cape*. Master of Science. School of Geological and Computer Sciences, University of Natal, Durban.
- Ratshomo, K., 2013. *South African Manganese Industry Developments*. Directorate: Mineral Economics
- Rozet, E., Marini, R., Ziemons, E., Boulanger, B., Hubert, P. (2011). Advances in validation, risk and uncertainty assessment of bioanalytical methods. *Journal of Pharmaceutical and Biomedical Analysis*, 55(4), 848-858.
- Schroder, S., Bedorf, D., Beukes, N.J., Gutzmer, J., 2011. From BIF to red beds: Sedimentology and sequence stratigraphy of the Paleoproterozoic Koegas Subgroup (South Africa). *Sedimentary Geology*, 236, p 25-44.
- Schutte, S.S., 1992. Ongeluk volcanism in relation to the Kalahari Manganese deposits.
- Schwab, K., 2016. *The fourth industrial revolution*. Geneva: World Economic Forum. The Transnational Human Rights Review 3
- Shan, H.Z, Zhuo,S.J, Shen,R.X, and Sheng,C. (2008). ). Mineralogical effect correction in wavelength dispersive X-ray florescence analysis of pressed powder pellets. *Spectrochimica Acta Part B: Atomic Spectroscopy*,63(5), 612-616.
- Sorensen, B., Gaal, S., Tangstad, M., Ringdalen, E., Kononov, R., Ostrovski, O. 2010. Properties of manganese ores and their change in the process of calcination. The twelfth international ferroalloys congress sustainable future.

- Steenkamp, J.D., Chetty, D., Singh, A., Hockaday, S.A.C., Denton, G.M. 2020. From ore body to high temperature processing of complex ores: Manganese—A South African Perspective. The Minerals, Metals & Materials Society. DOI 10.1007/s11837-020-04318-x
- Sumner, D.Y., and Beukes, N.J., 2006. Sequence Stratigraphic Development of the Neoproterozoic Transvaal carbonate platform, Kaapvaal Craton, South Africa. *South African Journal of Geology*, Vol. 109, p 11-22.
- Thomas, D.S.G., and Shaw, P.A., 1990. The deposition and the development of the Kalahari Group sediments, central Southern Africa. *Journal of African Earth Sciences*. 10 (1/2), 187-197.
- Thomas, D.S.G., and Shaw, P.A., 1991. *The Kalahari environment*. Cambridge University Press, p.284
- Tsikos, H., 2003. Hydrothermal aegirine from the Palaeoproterozoic Hotazel iron-formation, Kalahari manganese field, South Africa, and its implications: Applied Earth Science. *Transactions Institution of Mining and Metallurgy*, v. 112, no. 2, August, p. 166-167.
- Tsikos, H., and Moore, J.M., 1997. Petrography and geochemistry of the Palaeoproterozoic Hotazel iron-formation, Kalahari Manganese Field, South Africa: Implications for Precambrian manganese metallogenesis. *Economic Geology*, Vol. 92, p.87-97.
- Tsikos, H., and Moore, J.M. (1998). The Kalahari manganese field: an enigmatic association of iron and manganese. *South African Journal of Geology*, Vol. 101 (4), p. 287-290.
- Tsikos, H., Beukes, N.J., Moore, J.M., Harris, C., 2003. Deposition, Diagenesis, and Secondary Enrichment of Metals in the Paleoproterozoic Hotazel Iron Formation, Kalahari Manganese Field, South Africa: in *Econ. Geol.* v98 pp 1449-1462
- Vafeas, N.A., Viljoen, K.S., Blignaut, L.C., 2018. Mineralogical characterization of the thrusting manganese ore above the Blackridge Thrust Fault, Kalahari Manganese Field: The footprint of the Mukulu Enrichment. The Centre of Excellence for Integrated Mineral and Energy Resource Analysis (CIMERA); South African Department of Science and Technology
- Van der Merwe, S.J., 1997. The basin analysis of the Kalahari basin. MSc, University of the Orange Free State.
- Van der Woude, S., 2019. Challenges in mining for the Fourth Industrial Revolution. Minerals Council South Africa. Van Niekerk, H. S., 2006. The origin of the Kheis Terrane and its relationship with the Archean Kaapvaal Craton and the Grenvillian Namaqua Province in southern Africa (Doctoral dissertation). University of Johannesburg, Johannesburg, South Africa.
- Van Zyl, H.J., Bam, W.G., Steenkamp, J.D., 2016. Identifying barriers faced by key role players in the South African Manganese Industry. SAIIIE27 Proceedings, 25th – 27th of October 2016, Stonehenge, South Africa
- Wegrzynek, D. 2004. Commercial applications of x ray spectrometric techniques. IAEA-TM-26430
- Wilson, M.G.C. and Anhaeusser, C.R. (eds), 1988. *The mineral resources of South Africa: Handbook*, Council for Geoscience, 16, 740 pp.
- Xu, M., David, J.M., Kim, S.H., 2018. The Fourth Industrial Revolution: Opportunities and Challenges. *International Journal of Financial Research*. Vol. 9, No. 2; 2018

APPENDIX

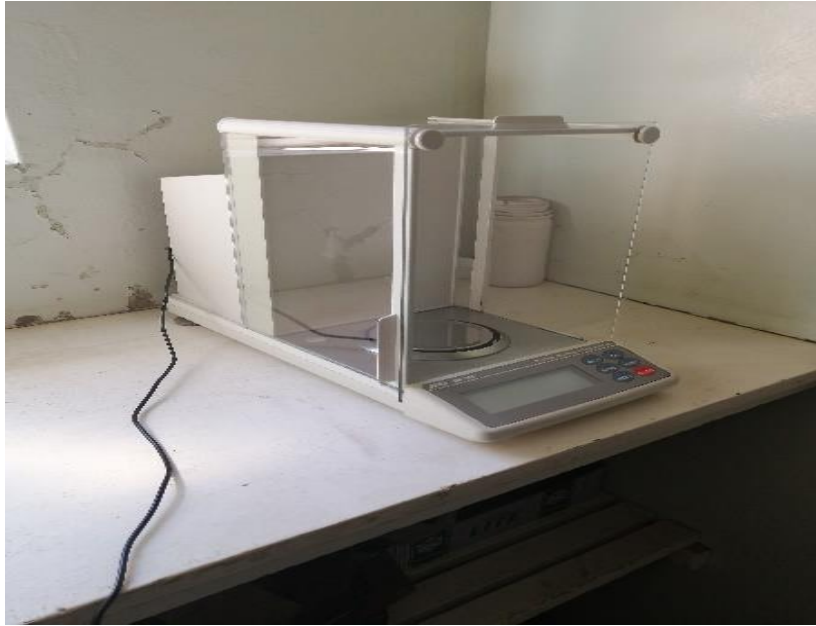


Figure I – Pictures taken at ABC labs for wet chemistry analysis